KUOPION YLIOPISTON JULKAISUJA D. LÄÄKETIEDE 369
KUOPIO UNIVERSITY PUBLICATIONS D. MEDICAL SCIENCES 369

PETRI SIPOLA

Magnetic Resonance Imaging in Hypertrophic Cardiomyopathy

Doctoral dissertation

To be presented by permission of the Faculty of Medicine of the University of Kuopio
for public examination in Auditorium 2, Kuopio University Hospital,
on Friday 28th October 2005, at 12 noon

Departments of Clinical Radiology, Medicine,
Clinical Physiology and Nuclear Medicine
University of Kuopio and
Kuopio University Hospital

KUOPION YLIOPISTO
KUOPIO 2005

Distributor:
Kuopio University Library
P.O. Box 1627
FIN-70211 KUOPIO
FINLAND
Tel. +358 17 163 430
Fax +358 17 163 410
www.uku.fi/kirjasto/julkaisutoiminta/julkmyyn.html

Series Editors:
Professor Esko Alhava, M.D., Ph.D.
Department of Surgery

Professor Raimo Sulkava, M.D., Ph.D.
Department of Public Health and General Practice

Professor Markku Tammi, M.D., Ph.D.
Department of Anatomy

Author´s address:
Department of Clinical Radiology
Kuopio University Hospital
P.O. Box 1777
FIN-70211 KUOPIO
FINLAND
Tel. +358 17 173 311
Fax +358 17 173 341

Supervisors:
Docent Hannu Aronen, M.D., Ph.D.
Helsinki Brain Research Center
Functional Brain Imaging Unit
University of Helsinki

Docent Johanna Kuusisto, M.D., Ph.D.
Department of Medicine
University of Kuopio

Professor Jyrki Kuikka, M.D., Ph.D.
Department of Clinical Physiology and Nuclear Medicine
University of Kuopio

Professor Keijo Peuhkurinen, M.D., Ph.D.
Department of Medicine
University of Kuopio

Reviewers:
Professor Charles B. Higgins, M.D., Ph.D.
Department of Radiology
University of California, San Francisco
USA

Professor Heikki Ruskoaho, M.D., Ph.D.
Molecular and Cellular Biology of
Natriuretic Peptides Biocenter Oulu
Department of Pharmacology and Toxicology
University of Oulu

Opponent:
Professor Albert de Roos, M.D., Ph.D.
Department of Radiology
Leiden University Medical Center
The Netherlands

ISBN 951-27-0389-0
ISBN 951-27-0466-8 (PDF)
ISSN 1235-0303

Kopijyvä
Kuopio 2005
Finland

Sipola, Petri. Magnetic Resonance Imaging in Hypertrophic Cardiomyopathy. Kuopio University Publications D. Medical Sciences 369. 2005. 160 p.
ISBN 951-27-0389-0
ISBN 951-27-0466-8 (PDF)
ISSN 1235-0303

ABSTRACT

Hypertrophic cardiomyopathy (HCM) is a relatively common disease in the general population, with estimated prevalence of 1:500. HCM is caused by mutations in genes encoding sarcomere, a contractile element of cardiomyocyte. Most patients with an HCM-causing mutation have left ventricular hypertrophy (LVH). The severity of LVH is variable, and LVH-modifying factors are largely unknown. HCM is usually benign, but it is associated with increased risk for sudden cardiac death due to malignant arrhythmias in a subgroup of patients. A safe noninvasive method to characterize HCM patients would be valuable.

In the current study cardiac magnetic resonance imaging (MRI) was used to characterize myocardial anatomy, systolic function, perfusion and contrast enhancement in 24 patients with HCM caused by the mutation Asp175Asn in the α-tropomyosin gene. Single photon emission computed tomography imaging with radiolabeled metaiodobenzylguanide, which is an analogue of norepinephrine and acts as a neurotransmitter in the adrenergic system, was used to assess cardiac adrenergic activity.

The maximal wall thickness of the left ventricle (LV) varied from normal to severely hypertrophied. The global ejection fraction in patients with HCM was preserved, but the proportion of hypokinetic segments was increased. The increase in hypokinetic segments was the most important correlate of LVH, supporting the hypothesis that cardiomyocyte systolic dysfunction acts as an initiatior in cascade leading to LVH. In perfusion imaging, an impaired ability to increase myocardial perfusion during adenosine-induced vasodilatation was found. This impairment was also associated with the severity of LVH. The enhancement of the LV myocardium by a gadolinium-diethylenetriaminepentaacetic-acid contrast agent was heterogeneous, indicating that the extracellular space in the LV myocardium is increased in patients with HCM. Enhancement heterogeneity was associated with a biochemical marker of myocardial fibrosis (aminoterminal propeptide of type III collagen), suggesting that the increased extracellular space is caused by myocardial fibrosis. Finally, turnover of a radiolabeled norepinephrine analogue was increased in patients with HCM. The turnover was also associated with the degree of LVH, supporting hypothesis adrenergic innervation contributes to the pathogenesis of LVH in patients with HCM.

The present study shows that cardiac MRI can noninvasively provide multispectral characterization of cardiac anatomy and function without radiation exposure in patients with HCM. Cardiac MRI can be used not only in the characterization of individual patients with HCM but also in the examination of the pathophysiology of HCM, especially when cardiac MRI data is interpreted in conjunction with functional data provided by scintigraphic imaging.

National Library of Medicine Classification: WG 280, WG 141.5.M2, WN 185
Medical subject headings: cardiomyopathy, hypertrophic, familial; genetics; tropomyosin; magnetic resonance imaging; hypertrophy, left ventricular; perfusion; fibrosis; contrast media; procollagen type III-N-terminal peptide; tomography, emission-computed, single-photon; norepinephrine/analog and derivatives; 3-iodobenzylguanidine

ACKNOWLEDGMENTS

I owe my gratitude to professor Seppo Soimakallio, M.D. Ph.D., who was Chairman of the Departments of Clinical Radiology of the Kuopio University Hospital at the time the research project was planned. His favorable attitude towards research project was fundamental to start my project in the Department of Radiology in Kuopio University Hospital.

I wish to express my gratitude to my principal supervisor, docent Hannu J. Aronen, M.D. Ph.D., who encouraged me to become involved in the challenging field of magnetic resonance imaging of the heart. He emphasized the importance of dedicating myself to research to achieve the goal of completing this thesis. He also exhorted me to take part in international scientific congresses, which I found very fruitful for research.

I am greatly indebted to my second supervisor, docent Johanna Kuusisto, M.D. Ph.D., of the Cardiology Unit of the Department of Medicine. She entrusted the very exceptional study subjects she has followed to a novice researcher for this academic dissertation. I appreciate very much Dr. Kuusisto's expertise in scientific writing, and her contribution was crucial in preparation of the manuscripts.

I am greatly indebted to my third supervisor, professor Jyrki T. Kuikka, Ph.D. He is an exemplary scientist, and I was lucky to have this opportunity to work with him. His exhaustive knowledge of the physiology of cardiac function was of great importance throughout the research process. He was aware of the financially, mentally and intellectually challenging steps during this thesis, and he supported me to overcome them.

I owe my gratitude to my fourth supervisor, professor Keijo Peuhkurinen, M.D. Ph.D., of the Cardiology Unit of the Department of Medicine. He had always time to discuss the study with me. I felt he was always truly interested in new data that could be obtained by cardiac MRI, which encouraged me to go on with imaging and image analysis.

I want to thank professor Hannu Manninen, M.D., Ph.D.. His knowledge and practical help in the area of scientific writing and radiological research in general was vitally important during critical steps of my research. Also our common interest in sports provided an important counterbalance to scientific research, the importance of which cannot be emphasized too much.

I am deeply indebted to docent Kirsi Lauerma, M.D., Ph.D.. She actually led me to scientific cardiac MRI. In addition, she planned study protocol, she taught me to image patients, and to write abstracts and articles and she was ready to support me during critical steps in research. Thank you, Kirsi!

I want to thank professor Esko Vanninen, M.D., Ph.D.. His deep knowledge in cardiac imaging and physiology was very helpful to me. He had always time and interest to answer my e-mails.

I want to thank physicist Minna Husso, Ph.Lic.. She was involved in the huge work on image analysis in the perfusion study. We woke up at 5 a.m. to have time to calculate those endless signal intensity versus time curves. Minna, thank you for co-operation!

I want to thank Tomi Laitinen, M.D., Ph.D. Tomi, you tookcare of the patients and controls during the adenosine stress test in the MRI tube, I think they were the first performed in Finland. I appreciate your co-operation very much.

I am indebted to Pertti Jääskeläinen, M.D., Ph.D., and professor Markku Laakso, M.D., Ph.D., who were responsible for genetic analyses of the study subjects and were essential to the planning of the study design and preparation of the manuscripts.

Docent Pekka Niemi, M.D., Ph.D., was a co-author in the perfusion study. We really needed his MRI–knowledge to understand the theoretical basis of the imaging findings.

I am indebted to professor Juha Risteli, M.D., Ph.D., for his co-operation in the collagen analyses and to Sakari Simula, M.D., Ph.D., for his co-operation in the MIBG analyses.

I want to thank all the patients and control subjects who participated in this study. Thank you for your confidence.

I want to express my sincere gratitude to professors Albert de Roos, M.D., Ph.D., and Charles B. Higgins, M.D., Ph.D.. They gave me an idea of becoming a cardiac radiologist. Later on, I had an inconceivable fortune to have them as an opponent and a reviewer of my thesis. It is the greatest honor I can imagine for my research. To have professor Heikki Ruskoaho as another reviewer for my thesis completed my book as a best possible way. I respect his outstanding expertise in the pathophysiology of LVH very much. I am deeply grateful for his helpful advices in the finalization of my thesis.

I am obliged to mention many individuals who were important for my study project. Docents Kaarina Partanen and Ritva Vanninen, the heads of magnetic resonance imaging unit, gave me the possibility to learn and perform our intricate and time-consuming imaging protocols in a busy department. Especially I appreciate your personal support and interest towards my research, which helped me to complete the thesis. We are here now!

I want to thank Paula Syrenius, Jari Räisänen, Jukka Hautakangas, Eila Riekkinen, Isto Lehtonen, Kirsti Ritvanen, Kaija Räisänen, Tuula Ollila, Merja Sihvonen, Jukka Saarela, Erja Väisänen and all other wonderful radiographers in the MRI unit. Without your help and sympathy I could not have done my research. Thank you! I want to thank Aarno Klemola for teaching MR imaging.

I want to thank physicists Pauli Vainio and Mervi Könönen for their help to solve practical problems with scanners, data transfer and image analysis.

I also want to thank my research colleagues Liu Yawu and Jari Karonen. We had many common feelings that nobody else could understand, which gave rise to our own brand of humor and helped us withstand the stresses of research. We also had many, actually very many, congresses with good memories!

I want to thank warmly Marja-Liisa Sutinen for her care of study subjects during their stay in hospital.

Thousands of thanks to Tuula Bruun, Taina Airola and Eija Hassinen for their secretarial help. Especially I want to thank Tuula and Eija for their effort to find subjects for the MRI tube then when I was learning to image the heart by magnetic resonance. There is a street at Petonen, where (almost) all the subjects have been studied by cardiac MRI! Thank you to all of you.

Radiologist Aki Ikonen taught me to perform cardiac MRI in practice. Aki, I won't forget your help.

Also Jukka Lehtovirta, the head of Department of Radiology at Kajaani Central Hospital, taught me the basics of MRI and gave me full support as I found my way to Kuopio and into scientific work.

I'm very thankful to statistician Pirjo Halonen. Her expertise and assiduity to help researchers in statistical analysis by personnel conservations, e-mails and in telephone is irrecoverable. Later on, Vesa Kiviniemi continued this work very nicely. I want to thank Simo Näyhä, Esa Läärä, and Matti Uhari who inspired my interest in biostatistics and epidemiology.

I want to thank docent David Laaksonen of the Department of Medicine for the linguistic revision of my thesis. He had only a few days to go through my thesis, which emphasizes the value of his work.

Cordial thanks to my friends Timo Voivalin, Petteri Röntynen and Lasse Hovi for their total disinterest towards my research. With you I noticed "there may be life out there".

This study was financially supported by many foundations and research grants. Especially I want to thank Kuopio University Hospital for the EVO grants, which gave a real possibility to do full-time research. The role of many foundations has also been essential: the Instrumentarium Science Foundation, Radiological Society of Finland, Aarne Koskelo Foundation, Aarne and Aili Turunen Foundation, Ida Montin Foundation, Research Foundation of Orion Corporation, Research Foundation of Astra, and Finnish Society of Nuclear Medicine have provided grants to my research. I want to thank the reviewers of foundation grant applications. By giving grants you have not only provided the possibility for full-time research, but also strengthened my confidence to carry out research.

Finally, I express my dearest thanks to my family, Marja, Aarne and Auli. My wife Marja gave me the opportunity to concentrate fully on work and to arrange the working hours I needed. At all times I was confident that you would take care of the children and home. I want to thank my children Aarne and Auli for those many lovely drawings that were waiting on the table when I came home. Especially I want to thank you for your encouragement to come home as soon as possible.

On the day of Aleksis Kivi
Siilinjärvi, October 10, 2005
Petri Sipola

ABBREVIATIONS

AU	= arbitrary units
ECG	= electrocardiogram
EF	= ejection fraction
FPR	= first-pass reserve index
FW	= free wall
Gd-DTPA	= gadolinium diethylenetriaminepentaacetic acid
HCM	= hypertrophic cardiomyopathy
H/M	= heart-to-mediastinum
LV	= left ventricle; left ventricular
LVH	= left ventricular hypertrophy
MIBG	= metaiodobenzylguanide
MR	= magnetic resonance
MRI	= magnetic resonance imaging
MWT	= maximal wall thickness
PIIINP	= aminoterminal propeptide of type III collagen
SD	= standard deviation
SPECT	= single photon emission computed tomography
TE	= echo time
TPM1-Asp175Asn	= HCM-causing mutation Asp175Asn in the α-tropomyosin gene
TR	= repetition time

LIST OF ORIGINAL PUBLICATIONS

The thesis is based on the following original articles, which are referred to in the text by their Roman numerals:

I Petri Sipola, Kirsi Lauerma, Pertti Jääskeläinen, Markku Laakso, Keijo Peuhkurinen, Hannu J. Aronen, Johanna Kuusisto. Cine MR imaging of myocardial contractile impairment in patients with hypertrophic cardiomyopathy attributable to Asp175Asn mutation in the α-tropomyosin gene. Radiology 2005;236:815-824. (Study I)

II Petri Sipola, Kirsi Lauerma, Minna Husso-Saastamoinen, Jyrki T. Kuikka, Esko Vanninen, Tomi Laitinen, Hannu Manninen, Pekka Niemi, Keijo Peuhkurinen, Pertti Jääskeläinen, Markku Laakso, Johanna Kuusisto, Hannu J. Aronen. First-pass MR imaging in the assessment of perfusion impairment in patients with hypertrophic cardiomyopathy and the Asp175Asn mutation of the α-tropomyosin gene. Radiology 2003;226:129-137. (Study II)

III Petri Sipola, Keijo Peuhkurinen, Kirsi Lauerma, Minna Husso, Pertti Jääskeläinen, Markku Laakso, Hannu J. Aronen, Juha Risteli, Johanna Kuusisto. Serum amino-terminal propeptide of type III collagen reflects myocardial fibrosis in MRI in patients with hypertrophic cardiomyopathy attributable to the Asp175Asn mutation in the α-tropomyosin gene. Submitted. (Study III)

IV Petri Sipola, Esko Vanninen, Hannu J. Aronen, Kirsi Lauerma, Sakari Simula, Pertti Jääskeläinen, Markku Laakso, Keijo Peuhkurinen, Johanna Kuusisto, Jyrki T. Kuikka. Cardiac adrenergic activity is associated with left ventricular hypertrophy in genetically homogeneous subjects with hypertrophic cardiomyopathy. J Nucl Med 2003;44:487–493. (Study IV)

 Unpublished results are also presented.

CONTENTS

1. INTRODUCTION

Hypertrophic cardiomyopathy (HCM) is a relatively common disease (incidence 1:500) that is characterized by left ventricular (LV) hypertrophy in subjects without other causes such as essential hypertension or aortic stenosis (1-3). During the last decade, HCM has been found to be caused by variable mutations in the contractile element of cardiomyocyte, sarcomere (3-5), and it has been found to be the most common genetically transmitted heart disease.

Transthoracic echocardiography is a clinical standard in the evaluation of a patient with HCM. It usually facilitates the evaluation of LV septal wall thickness, LV outflow tract obstruction and cardiac systolic and diastolic function. Echocardiography, however, is restricted by a variable acoustic window, inadequate LV wall visualization in more distant areas, and inaccuracy of the evaluation of LV mass in patients with asymmetric hypertrophy (6, 7). Cardiac magnetic resonance imaging (MRI), in contrast, provides a comprehensive evaluation of LV function, LV wall thickness and LV mass in patients with HCM (6-9). In addition, MRI with contrast agents provides the potential to study myocardial perfusion abnormalities and myocardial fibrosis, which are pathological features in patients with HCM (1, 3).

Therefore, in the present study, we used multispectral cardiac MRI (anatomy, cine, perfusion, and contrast enhancement) to characterize patients with HCM attributable to a single HCM-causing mutation Asp175Asn in the α-tropomyosin gene. We studied the correlates of LVH, especially the role of adrenergic activity measured by single photon emission computed tomography (SPECT) with the radiolabeled norepinephrine analogue metaiodobenzylguanide (MIBG). We measured myocardial perfusion noninvasively without radiation exposure, and we investigated the

relationship of late-enhancement on gadolinium diethylenetriaminepentaacetic acid (Gd-DTPA) enhanced MRI proposed to represent myocardial fibrosis and aminoterminal propeptide of type III collagen (PIIINP) measured of peripheral blood samples.

2. REVIEW OF LITERATURE

2.1. Definition of HCM

The pathology of HCM was first described by French and German pathologists in the mid 19th and early 20th century (10-12), and modern attention to this disease was brought by Brock and Teare 50 years ago (13, 14). HCM is defined as LV and/or right ventricular hypertrophy without evident causes such as hypertension or LV outflow tract obstruction (Fig 1). Microscopically, hypertrophy is associated with myocardial fiber disarray and fibrosis (1). HCM is a primary and usually familial cardiac disease characterized by a complex pathophysiology and great heterogeneity in its morphological, functional, and clinical features.

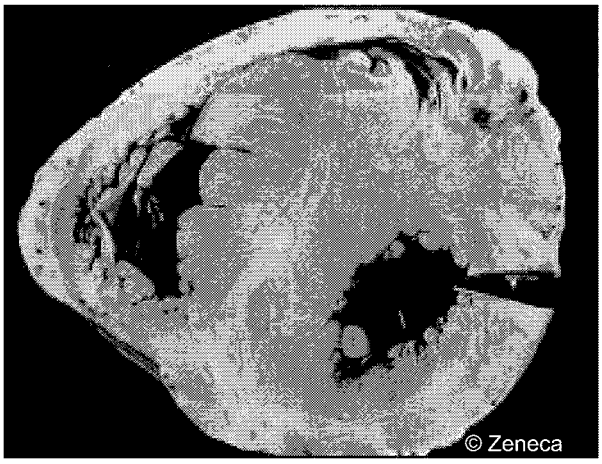

Figure 1. Photograph of the pathology specimen shows the extensive LV septal hypertrophy in a patient with HCM.

2.2. Epidemiology of HCM

In most epidemiological studies, relatively strict morphologic criteria for HCM (i.e., LV wall thickness ≥ 15 mm) could have excluded patients with mild morphologic expressions of the disease (15). According to these criteria, epidemiological

investigations with diverse study designs have shown similar estimates for the prevalence of phenotypically expressed HCM in the adult general population of about 0.2% – 0.3% (1:500 – 1:333) (16-18). In a recent large study among Chinese, a less restrictive cutoff of ≥ 13 mm for LV wall thickness was used, but a similar prevalence was noted: the disease phenotype for HCM was identified in 0.16% of subjects (19). In routine cardiologic practice, HCM is relatively uncommon. Among 714 consecutively studied outpatients with heart disease or suspected heart disease, HCM was found in 0.5% of patients (20).

2.3. Clinical diagnosis of HCM

Conventionally, the clinical diagnosis of HCM is usually established with two-dimensional echocardiography by demonstrating typically asymmetric LVH in the absence of another cardiac or systemic disease (e.g., hypertension or aortic stenosis) capable of producing hypertrophy. The usual clinical diagnostic criterion for HCM is a maximal LV wall thickness greater than or equal to 15 mm. In a recent study, a maximal LV wall thickness greater than or equal to 13 mm was used (19). McKenna et al. have suggested new diagnostic criteria for the first-degree relatives of patients with established HCM (21). Relatives with LV end-diastolic wall thickness of at least 13 mm on two-dimensional echocardiography, or with pathological Q waves, LVH with repolarization changes, or deep T wave inversions on electrocardiogram (ECG), are considered clinically affected.

Laboratory DNA analysis for mutant genes is the most definitive method to establish the diagnosis of HCM. At present, however, there are several difficulties in the translation of genetic research into practical clinical work. HCM may be caused

by multiple different mutations, gene analysis is time-consuming and it requires expensive laboratory techniques. In addition, it is possible that a subject has a disease-causing mutation, but no markers of disease can be found (22).

2.4. Genetics of HCM

HCM is familial in 50% of the cases; the rest of the cases are sporadic. HCM is inherited as a Mendelian autosomal dominant trait, and it is the most common hereditary cardiac disease.

HCM is a genetically heterogeneous disorder, with 12 distinct chromosomal loci mapped to date. Disease-causing genes have been identified in all 12 loci: the first 10 of these genes encoded protein components of the cardiac sarcomere (23). Mutations have been found in four genes that encode components of the thick filament, in five genes that encode thin filament proteins, and in genes that encode the sarcomeric cytoskeletal protein titin (23). Over 150 mutations are recognized (4, 15). Overall, known mutations explain about half of the cases. Currently new disease causing mutations are recognized, and this increases the proportion of the cases with recognized causative mutation.

In the literature, the predominant HCM-causing genes in decreasing frequency are myosin-binding protein C, β-myosin heavy chain, and cardiac troponin-T genes (5, 24-26). In Finland, however, the distribution of HCM causing genes is different. Cardiac myosin-binding protein C gene and α-tropomyosin gene account for most of the cases, i.e. 24% and 11%, respectively (27, 28). β-myosin heavy chain mutations cause 3% of the cases. Figure 2 demonstrates components of the sarcomere.

There are several other diseases that cause thickening of LV, but are not related to sarcomere mutations. These diseases are usually metabolic storage diseases or

are related to disturbances in other cell organs than myocyte sarcomere (for example mutations in the gene encoding the gamma-2-regulatory subunit of the AMP-activated protein kinase, Noonan's syndrome, mitochondrial myopathies, Friedreich's ataxia, metabolic disorders, X-linked deficiency of the lysosomal enzyme α-galactosidase, LV non-compaction, and cardiac amyloidosis). These diseases are usually distinguished from HCM (15, 23).

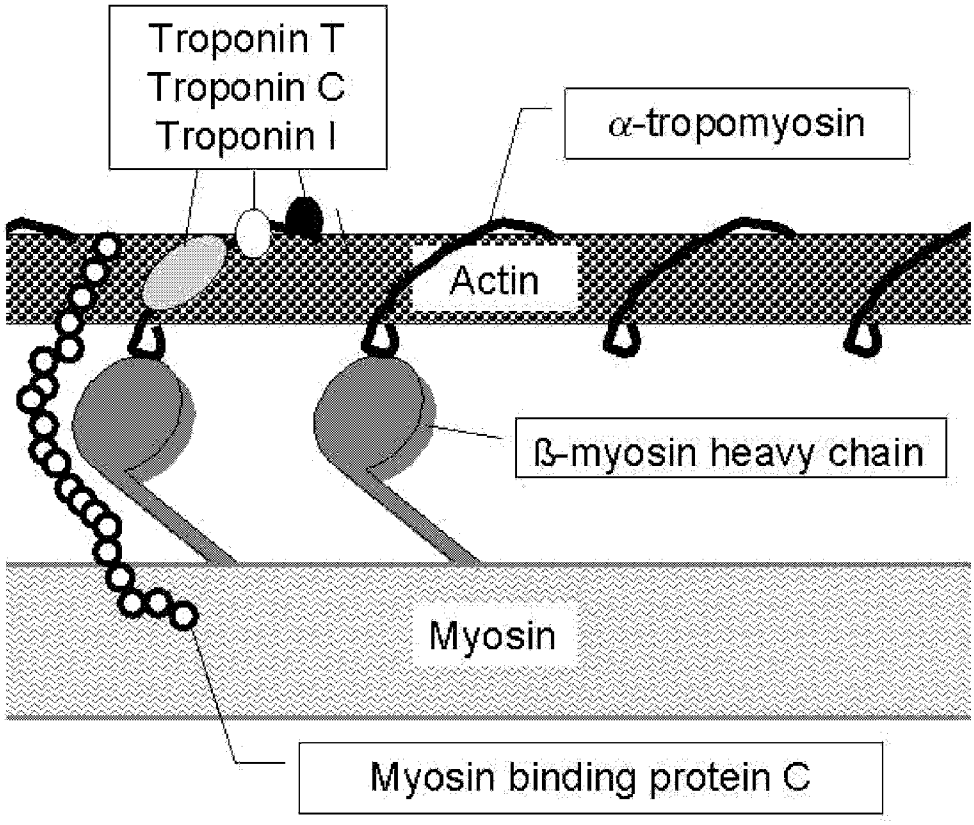

Figure 2. Components of the sarcomere. Cardiac contraction occurs when calcium binds to the troponin complex (subunits C, I, and T) and α-tropomyosin, making possible the myosin–actin interaction. In HCM, mutations may alter protein interactions and contraction properties of the sarcomere (2, 23).

2.5. Histological features in HCM

2.5.1. Myocardial fibrosis

In patients with HCM, both replacement fibrosis (discrete collagen-filled scars visible also to the naked eye) and diffuse interstitial fibrosis (microscopic fibrosis) have been found (29-31). The size of discrete collagen-filled scars has typically been from 5 to 10 mm and scars have been found in half of the HCM patients (31).

In the normal human heart, collagen matrix includes the sheath of connective tissue enveloping bundles of muscle fibers and sarcolemma of individual muscle cells (30). Interstitial fibrosis in HCM patients is characterized as thickened pericellular collagen encasing cardiac muscle cells (30). In addition, fiber components of the matrix have shown a disorganized arrangement compared with normal heart tissue, particularly in areas of cardiac muscle cell disarray (30).

In the histopathological study by Tanaka et al., the percentage area of fibrosis in patients with HCM was 13.1 ± 4.8% (compared to 1.1 ± 0.5% in controls) (32). In a study of adults and young children with HCM who died suddenly, an eightfold amount of matrix collagen was found compared to normal controls (14.1 ± 8.8% vs. 1.8 ± 1%), and a threefold increase compared to patients with hypertension (30).

Tanaka et al. studied myocardial fibrosis between LV septum and free wall (32). The authors found that the percentage area of fibrosis was higher in the LV septum than in the free wall, but that the percentage area of fibrosis was increased also in the LV free wall and right ventricular wall when compared to controls (32).

In normal subjects, interstitial collagen is evenly distributed throughout the middle, inner (adjacent to LV) and outer (adjacent to right ventricle) one-thirds of the septal tissue sections (30). Shirani et al. found more pronounced fibrosis in the middle one-third of the transmural tissue sections (49 ± 9%) than in either the inner (34 ± 13%) or

outer (17 ± 12%) one-third (30) in patients with HCM. Such differences between different LV layers, however, have not been found in all studies (29, 32).

Increased heart weight, LV dilatation and male gender are associated with increased fibrosis in histopathological studies (29, 31, 33). The most fibrosis has been found in patients with a dilated type of HCM (29, 31), and its percentage area has been as much as 37% of total myocardial area and even over 90% in the most affected segments (29). No difference in left atrial fibrosis has been found between HCM patients with and without left atrial dilatation (31). Table 1 summarizes myocardial fibrosis in histopathological studies.

Table 1. Myocardial fibrosis in histopathological studies in patients with HCM and control subjects

Reference	Measured parameter	HCM patients	Controls
(30) Shirani et al.	Total collagen volume	16.7 ± 9.1%	4.0 ± 1.6%
(32) Tanaka et al.	Percentage area of fibrosis	13.1 ± 4.8%	1.1 ± 0.5%
(29) Iida et al.	Percentage area of fibrosis	27.0 ± 7.9%*	NA
(31) Varnava et al.	Percentage area of fibrosis	4.1 ± 4.9%†	NA
(31)Varnava et al.	Percentage area of fibrosis	9.2 ± 7.3%‡	NA
(33) Varnava et al.	Percentage area of fibrosis	2.6 ± 2.8%§	NA
(33) Varnava et al.	Percentage area of fibrosis	0.7 ± 0.4%‖	NA

NA, not available

*Patients with dilated phase of hypertrophic cardiomyopathy in the age range of 50-69 years

† Patients with non-dilated hypertrophic cardiomyopathy

‡ Patients with dilated phase of hypertrophic cardiomyopathy

§Patients with hypertrophic cardiomyopathy with unknown genotype

‖Patients with hypertrophic cardiomyopathy with a Troponin T mutation

Little is known about the differences in the amount of fibrosis between different genotypes. There is some evidence, however, that myocardial fibrosis in patients with defects in troponin T gene is less pronounced as compared to other gene defects (33).

Myocardial fibrosis is suggested to play a crucial role in the pathophysiology of arrhythmias in HCM. The results of the studies on association of sudden cardiac death risk and fibrosis are contradictory, however. In a study by Iida et al. myocardial fibrosis was much greater in HCM patients who suffered sudden cardiac death than in HCM patients with non-cardiac death (29). In contrast, in a large study by Varnava et al. none of the patients aged under 21 years of age had large macroscopic scars, whereas half of the older patients had such scars (34). In a retrospective analysis, however, microscopic fibrosis associated with markers of arrhythmia such as with history of non-sustained ventricular tachycardia or with placement into high-risk zone on paced fractionation testing. In the study by Varnava et al. HCM patients who died of heart failure had more fibrosis than the other HCM patients (34).

Myocardial ischemia (35), production of autocrine fibrotic factors and apoptosis (34) have been suggested as factors behind myocardial fibrosis in HCM.

2.5.2. Myocyte disarray

In histopathological samples, a hallmark of HCM is myocyte disarray and it has been used as a specific marker of the disease (32, 33, 36). In myocyte disarray, cellular disorganization can be seen: longitudinally sectioned cells, or bundles of cells, are aligned perpendicularly or obliquely, or cells are interlaced among transversely oriented cells (30). Some myocyte disarray can be found also in healthy subjects. In normal hearts, however, foci are small and scattered and occupy 2 ± 1%

of septal tissue sections (30). In HCM patients, cellular disarray may be widely distributed, occupying substantial portions of LV, and also RV wall (average, 33% - in some segments over 90%) (29, 34).

Disarray variation within the heart can be substantial (from under 10% in one section to 90% in another). Marked variation in myocyte disarray can be seen even within a single histopathological section, so that that severely disarrayed myocytes have been found to lie adjacent to normally sized and aligned myocytes (29, 37).

Maron et al. and Iida et al. found greatest myocyte disarray in LV septum (mean 40%, range 0 - 95%) in patients with HCM (29, 37). Somewhat less disarray was seen in anterolateral and posterolateral free walls (37). No disarray has been seen in the left atrial free wall (31).

Myocyte disarray has not been found to be different between thin (< 15 mm) and thick (> 30 mm) segments of the LV (38). In correlation analysis within a single heart, no association between LV wall thickness and myocyte disarray has been found either (38). Moreover, in analyses comparing patients, no positive relationships between the LV wall thickness, heart mass and degree of myocyte disarray have been found (31, 38). In contrast, myocyte disarray has been found to be greater in hearts with maximum LV wall thickness of ≤ 20 mm than in those LV wall thickness > 20 mm (31). In HCM patients caused by a troponin-T gene defect, characterized by poor prognosis and mild LVH, the myocyte disarray is extensive, even more pronounced than in other gene defects (33). All these findings suggest differences in pathophysiological pathways in the development of myocyte disarray and LVH in patients with HCM.

No significant difference in the severity of disarray has been observed between male and female patients (31). Disarray has been found to be more prominent in typical HCM than in the dilated type of HCM (31).

The amount of disarray associates with correlates of sudden cardiac death such as the number of family members suffering sudden cardiac death before the age of 40 years, symptom onset before the age of 21 years, or an abnormal response to exercise (34). Myocyte disarray has not been found to increase with age (34). In contrast, the most pronounced disarray has been found in young patients who die of their disease (for example up to 80% of the myocardium in a six-year-old patient) (31). As the amount of disarray is associated with chest pain, it is considered as a potential causative factor behind myocardial ischemia, promoting inefficient contraction leading to increasing energy demand (34).

2.5.3. Coronary artery abnormalities

Coronary artery abnormalities have been frequently described in histopathological studies of HCM patients. The most common abnormalities are decreased arterial lumina, but dilated lumina have also been found (35, 39, 40). Arterial walls are usually thickened, and the external diameter of the vessel has been found to be increased (35, 39). Increased wall thickness, which may be asymmetric, is caused by proliferation of medial or intimal components, particularly smooth muscle cells and collagen (30, 35). Increased number of elastic fibers and mucoid deposits have also been found (35). In addition, collagen matrix in perivascular adventitia have been found to be increased (30). Another reported abnormality is somewhat decreased capillary density (40).

Abnormal intramural coronary arteries have been found in the majority of HCM patients and also in infants suffering from HCM (35). Most often abnormal vessels have been found in LV septum (35), and at that segment abnormalities have been found to be the most marked (39). No abnormal vessels have been found in atria (31).

Both Varnava et al. and Tanaka et al. found that a small percentual vessel lumen area associates with increased heart weight (31, 39). In addition, Varnava et al. found that small vessel disease associates with segmental thickness within individual heart (35). In contrast, Maron et al. found no association between LV wall thickness and the frequency of abnormal arteries (31). No correlation between small vessel disease and disarray has been found (35, 39). The results of the association between small vessel disease and fibrosis are contradictory (35, 39). Severely dysplastic small vessels have been found in areas without marked fibrosis, while sections with widespread fibrosis often contained normal small vessels (35, 39). On the other hand, the correlation between small luminal area and the amount of myocardial fibrosis has also been found (35, 39). Krams et al. found that small arteriolar lumen size is associated with impaired coronary flow reserve, decreased capillary density and increased LV hypertrophy (40).

To conclude, abnormal intramural coronary arteries, characterized by thickened walls with increased intimal and medial collagen and a narrowed lumen, are characteristic in patients with HCM. These architectural alterations of the microvasculature are supposed to be one of the causative factors to explain the low coronary vasodilator reserve in patients with HCM.

2.6. Clinical course in HCM

2.6.1. Development of LVH

LV wall thickening often does not appear until adolescence, and phenotypic expression may not be complete until full growth and maturation is achieved; therefore, many children with HCM will not show LV wall thickening identifiable by 2-dimensional echocardiography before adolescence (41-43). Although it appears that the remodeling process is usually overtly complete by about the age of 18 years, one serial echocardiographic study in patients with mutations in myosin-binding protein C gene has demonstrated a delayed appearance of LVH in mid-life and even later (44). Elderly HCM patients (≥ 75 years) have been reported to compose as much as 25% of an HCM cohort (45).

2.6.2. Symptoms and risk of sudden cardiac death

The clinical course in patients with HCM is highly variable, with some patients remain asymptomatic throughout life and others develop severe symptoms of heart failure; some die prematurely, either suddenly (often in the absence of prior symptoms) or due to progressive heart failure (1-3, 15). HCM appears to be a more benign condition in unselected patient populations, which are more representative of the overall disease spectrum, than in those patients who are part of preferentially selected and high-risk cohorts from a few tertiary referral centers (3).

Clinical symptoms in patients with HCM are variable. Many patients are asymptomatic. Exertional dyspnea and disability, often associated with chest pain, dizziness, presyncope and syncope, usually occur. Chest pain may be typical of angina pectoris or atypical (occurs without exertion or is prolonged > 30 minutes) in character (2, 46). Patients may have impaired exercise performance with reduced

oxygen consumption at peak exercise (15). Women with HCM generally experience little difficulty during pregnancy and delivery, with the exception of some of those with advanced disease (47). In patients with obstructive HCM symptoms such as dyspnea, angina, presyncope and/or syncope on exertion, may be more severe. Congestive heart failure is rarely seen in HCM in normal sinus rhythm, but it may be seen in patients with severe obstruction to outflow or in patients with severe systolic and/or diastolic dysfunction, and in the presence of atrial fibrillation (3).

Patients with HCM have an increased risk for sudden cardiac death. The risk of sudden cardiac death has perhaps been overestimated because frequently cited studies are based on tertiary-center experience (annual mortality rates of 3% to 6%). Recent reports throughout the last 7 years from less selected regional or community-based HCM patient cohorts cite much lower annual mortality rates of about 1%, not dissimilar to that for the general adult US population (1-3, 15). Studies of HCM in children report annual mortality rates of 2% (community-based populations) to 6% (tertiary referral cohorts) (3).

Although annual mortality rate within the broad spectrum of patients with HCM is similar to that of normal population, there exist small subset of patients at a much higher risk (perhaps at least 5% annually) (3). Sudden death occurs most commonly in children and young adults, and the risk extends across a wide age range through midlife and beyond (48). Sudden death can be the initial manifestation of HCM, and such patients usually have no or only mild prior symptoms (3). The majority of HCM patients (55%) do not demonstrate any of the acknowledged risk factors, and it is exceedingly uncommon for such patients to die suddenly (49). The highest risk for sudden death in HCM has been associated with any of the following noninvasive clinical markers: prior cardiac arrest or spontaneous sustained ventricular

tachycardia, family history of premature HCM-related death, syncope, bursts of nonsustained ventricular tachycardia on serial ambulatory (Holter) ECG recordings hypotensive blood pressure response to exercise, and extreme LVH with maximum wall thickness ≥ 30 mm, particularly in adolescents and young adults. Exceptions to LVH being a determinant of prognosis in HCM are a few HCM families carrying troponin T mutations. In these families multiple sudden deaths despite only mild LVH have been recognized (33, 50, 51). In children with HCM, QT dispersion on ECG, presence of ventricular tachycardia on ambulatory monitoring, and the presence of myocardial bridging on coronary angiography have been found to be associated with reduced survival (52).

2.6.3. Atrial fibrillation

Atrial fibrillation is a common complication of HCM. It has been found in over one third of patients at ≤ 50 years of age (3). Usually, atrial fibrillation has been found in patients with increased size of left atrium. Annual HCM-related mortality is higher in HCM patients with atrial fibrillation and it is explained by an excess stroke- and heart failure–related mortality. In a study by Olivotto et al. ischemic stroke was found in 21% of the patients with atrial fibrillation. Ischemic strokes were 8 times more frequent among HCM patients with atrial fibrillation than among those in sinus rhythm (53).

2.6.4. LV outflow tract obstruction

Septal hypertrophy may cause obstruction to LV ejection (hypertrophic obstructive cardiomyopathy), which may be an important cause of limiting symptoms in a minority of patients. By convention, LV outflow tract obstruction is defined by a

pressure gradient greater than or equal to 30 mmHg. Above 50 mmHg, the percentage of ventricular ejection that occurs before mitral-septal contact rapidly declines (25). In a tertiary center study, LV outflow tract obstruction in children was found in 59% of patients, with a mean peak instantaneous gradient of 44 ± 33 mmHg (52). The conceptions of clinical importance of LV outflow obstruction are controversial. LV outflow tract obstruction is commonly found in HCM patients with advanced age as well suggesting that subaortic gradients may be well tolerated for long periods without adverse consequences (15). On the other hand, LV outflow tract obstruction has been linked to increased risk for sudden cardiac death (15).

2.6.5. Treatment of HCM

At present, an implantable cardioverter-defibrillator appears to be the most effective treatment modality for the high-risk HCM patient (3). In a large multicenter study, implantable cardioverter-defibrillators aborted potentially lethal ventricular tachyarrhythmias and restored sinus rhythm in almost 25% of patients throughout a 3-year follow-up. Appropriate device interventions occurred at 11% annually for secondary prevention (implant following cardiac arrest) and 5% annually for primary prevention (implant based on risk factors), usually in patients with no or only mild prior symptoms (54). Historically, drug-based treatment strategies to reduce risk for sudden death have been used. However, there are only few studies showing that prophylactic pharmacological strategies and rhythm-modulating drugs can reduce risk for sudden death (3, 55).

In patients with exertional symptoms of heart failure, it is conventional to initiate pharmacological therapy with negative inotropic drugs such as β-blockers or verapamil. Some investigators favor disopyramide (often with β-blockers) for severely

symptomatic patients with obstruction. Patients who develop severe symptoms of heart failure associated with systolic dysfunction and deteriorate into the end stage require alternative drug treatment with diuretics, vasodilators, and digitalis (3, 25). Amiodarone is effective in preventing atrial fibrillation and thromboembolism in HCM (3, 25).

In patients with hypertrophic obstructive cardiomyopathy whose symptoms persist despite treatment, septal myotomy-myectomy can be performed (56). In this surgical treatment, muscle is removed from the interventricular septum via an aortic approach. An alternative to surgery is alcohol ablation of the interventricular septum by using percutaneous transcoronary septal myocardial ablation or transcoronary alcohol septal ablation (57). Ultimately, cardiac transplantation might be necessary in patients with refractory heart failure symptoms (25). Figure 3 summarizes the principal clinical presentations of HCM.

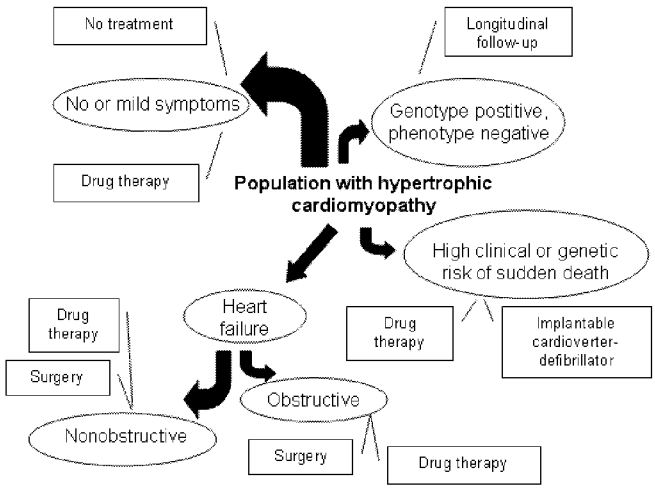

Figure 3. The principal clinical presentations of HCM and corresponding treatment strategies. The size of the arrows indicates the approximate proportion of patients with HCM in each subgroup (modified from reference (2)).

2.7. Morphology and cardiac function in HCM

2.7.1 LVH

2.7.1.1. LVH location

Heterogeneity in LVH is considerable in HCM. There is no single pattern of LVH regarded as typical (3). Ventricular septal hypertrophy is the most common type of asymmetrical hypertrophy in Anglo-Americans (3, 31), whereas apical hypertrophy has been prevalent in Asian populations (58, 59). Although many patients show diffusely distributed LVH, almost one third have mild wall thickening localized to a single segment (31).

In a large histopathological study, right ventricular wall thickness equal or over 4 mm was found in over half of the patients, including 28% of the patients with thickness $\geq$ 8 mm (31). Left or right atrial wall hypertrophy, or both, was found in about 10% of the patients (31).

2.7.1.2. LVH magnitude

In a histopathological study of normal subjects, the interventricular septal and LV free wall thicknesses varied from 10 to 15 mm (30). In histopathological studies in patients with HCM, LV wall thicknesses has varied widely from mild (13-15 mm) to massive ($\geq$ 30 mm) hypertrophy and even up to 60 mm, the most substantial in any cardiac disease (3, 30, 33). In children, the mean ratio of interventricular septum to LV freewall thickness has been 2.3 ± 1.1 (upper limit in normals 1.5) in diagnostic echocardiograms and 16% of the childhood HCM has had both right ventricular hypertrophy and LVH (52).

In a histopathological study by Shirani et al., heart weights were 320 to 970 g (mean 518 ± 156 g) in asymptomatic HCM subjects who died at the age < 35 years

(normal limits < 350 g in women; < 400 g in men) (30). In s study by Varnava et al. including 72 patients with HCM of all ages and also patients with dilated type of disease, heart weights were from 170 to 1770 g (mean 530 ± 222 g) (33).

2.7.1.3. LVH correlates

Little is known about the correlates of LVH in HCM. In a large histopathological study by Varnava et al. patients aged ≤ 30 years (but over 12 years) had a greater wall thickness than those > 30 years (31). However, no linear correlation between the maximum wall thickness and age was observed. Maximum LV wall thickness has been found to be greater in males than in females (31). No association between age and heart weight has been observed either (33). However, three patients with massive heart weights (> 900 g) were under 30 years of age. No significant difference in heart weights between patients with HCM or dilated HCM was found (33).

Some gene defects, particularly those in the β-myosin heavy-chain gene, are associated with marked LVH, whereas many gene defects (e. g. those of troponin T gene) generally induce mild LVH (50, 60, 61). However, in genotype-phenotype correlation studies significant variability in the phenotype expression of HCM among affected individuals with identical causative mutations has been observed. Thus, causal mutations account only a fraction of the variability of phenotypes. The possible individual modifier genes for HCM remain largely unknown. The insertion/deletion polymorphism of the angiotensin-I converting enzyme gene is most consistently reported to be related to LVH in HCM patients with identical causative mutations, accounting for 10 - 15% of the variability in LVH (62-64).

2.7.2. Systolic function in HCM

Systolic function in HCM is a contradictory topic. Some authors have suggested that systolic function in HCM is normal or even augmented (65), but others have found that HCM patients have hypocontractile systolic kinetics (66). In addition, LV systolic asynchrony has been reported (67, 68).

Echocardiographic studies

Cohen et al. was one of the first who investigated cardiac regional function in patients with HCM (nominated as subjects with idiopathic subaortic stenosis) (66). The authors used M-mode echocardiography and found that fractional thickening in LV septum was decreased in HCM patients and that the septum thickened up to the one-third of that of the posterior wall. In addition, the septum in HCM patients contracted more slowly than the normal septum or posterior wall in patients with HCM. However, the posterior wall velocity in HCM patients was more rapid than that measured in normal ventricles – possibly to compensate for the impaired movement in LV septum. Kaul et al. used echocardiographic two-dimensional apical four-chamber view still-images with fixed and floating reference system and investigated regional systolic function in HCM patients (65). The authors found that in a fixed reference system, septal movement was reduced and in a floating reference system, septal movement was normal or increased. The authors preferred a floating reference system and argued that interventricular septum in HCM exhibits normal or increased excursion during systole (65). Hattori et al. investigated direction-dependent contraction in HCM patients in an echocardiographic study (69). The authors suggested that meridional shortening (long-axis function) was depressed, but

circumferential shortening (short-axis function) was maintained in HCM. This finding was based on increased circumferential to meridional shortening ratio.

LV cineangiography studies

Gibson et al. used LV cineangiography (iodinated contrast agent injection into the LV cavity during x-ray imaging at a rate of approximately 50 frames per second) and found that ejection fraction in patients with HCM was supranormal (84 ± 4%). The maximum rate of reduction of LV volume was identical to that observed in control subjects (690 ± 280 ml/s) (70). In control subjects, the LV anterior wall initiated LV movement. In contrast, in the majority of HCM patients, the apical region was the first to move. In addition, eventhough abnormal delay in the onset of inward movement was found, the peak rate of inward movement was found to be increased. Pouler et al. used cineangiography and found increased ejection fraction and increased mean velocity of fiber shortening in HCM patients (68). Betocchi et al. found hyperkinesia in the LV free wall, whereas the septum exhibited normal wall motion (67). The authors concluded that LV movement was asynchronic and asynergic in patients with HCM.

2.7.3. Diastolic function in HCM

Diastolic dysfunction is a common finding in patients with HCM and it is supposed to result from loss of myocardial compliance owing to fibrosis and hypertrophy (56). On the other hand, diastolic dysfunction can occur independently of LVH and it can also precede subsequent development of LVH (42, 71, 72). Measurement of diastolic dysfunction noninvasively is difficult because conventionally used echocardiographic parameters are affected by loading conditions (73). Tissue Doppler imaging is a

promising method to diagnose and evaluate diastolic function in children and adult HCM (71-73).

2.7.4. Adrenergic activity in HCM

Mammalian heart is innervated by thousands of adrenergic nerve fibers (74). Adrenergic nerves acts as an important regulatory mechanism of cardiac function (75). A hypothesis has been presented that the primary abnormality in the pathogenesis of HCM is decreased contractility of cardiac myocytes that causes cell stress and increased cardiac adrenergic activation, which in turn induces expression of stress-responsive trophic factors and LVH (61). Thus it is rationale to investigate whether adrenergic activity is augmented in patients with HCM.

Lefroy et al. found impaired β-adrenoceptor density in patients with HCM by using positron emission tomography with ^{11}C-labeled S-enantiomer of the nonselective β-blocker CGB 12177 (76). Impairment was homogeneous through the LV without association to LV wall thickness measured by echocardiography. The authors suggest that this reflects receptor downregulation secondary to increased myocardial concentrations of norepinephrine. Li et al. used ^{18}F-labeled 6-fluorodopamine, a norepinephrine analogue, that is taken up by presynaptic adrenergic nerve endings, and found an impaired transmitter-perfusion ratio in echocardiographically hypertrophied regions of LV compared to non-hypertrophied regions (77). In non-hypertrophied myocardium, neuronal uptake was similar to controls. The authors suggest that impaired presynaptic neurotransmitter uptake would augment delivery of local catecholamines to adrenoceptors of cardiomyocytes. Schäfers et al. used both a norepinephrine analogue measuring presynaptic uptake and a β-adrenoceptor analogue measuring β-adrenoceptor density in a positron emission tomography study

and found that both presynaptic uptake and β-adrenoceptor density are impaired, suggesting increased local catecholamine levels in the synapse cleft (78). Tracer distribution between different regions was not different from that in controls indicating homogeneous impairment throughout the LV.

Radioiodinated metaiodobentzylguanide (^{123}I-MIBG) provides an opportunity to noninvasively explore cardiac adrenergic neuronal function *in vivo*. ^{123}I-MIBG shares the same neuronal transport and storage mechanisms with norepinephrine (79). Several clinical conditions associated with increased cardiac adrenergic tone have been shown to be characterized by accelerated ^{123}I-MIBG washout (80, 81). Terai et al. investigated ^{123}I-MIBG kinetics in patients with HCM (82). The authors found that those patients who had increased LV end-diastolic diameter, impaired fractional shortening and thinner septal thickness (end-stage HCM) had impaired early uptake, impaired delayed uptake and increased ^{123}I-MIBG washout. Thus, it is possible that chronic adrenergic overactivity contributes to the development of LVH and also LV dilatation in later stages of the disease.

2.7.5. Myocardial ischemia

Myocardial ischemia is considered, together with myocardial fibrosis, causative of fatal arrhythmias in patients with HCM (34, 83). Ischemia is supposed to promote enhanced automatism of the myocardium, leading eventually to the development of secondary, fatal arrhythmias.

2.7.5.1. Gamma camera studies

Abnormal myocardial rest and stress perfusion have been frequently found in scintigraphic studies in patients with HCM. Weiss et al. used radioactive ^{133}Xenon injected as a bolus into the left coronary artery and multiple crystal scintillation camera and found impaired myocardial blood flow per unit mass of tissue in HCM patients at rest (84). Other investigators have used peripheral tracer injections. Rubin et al. studied 10 patients with obstructive HCM who suffered from anginal symptoms. In ^{201}Tl imaging, 9 of 10 patients had no significant perfusion defects and one patient had reversible perfusion defect (85). Based on these findings, the authors considered perfusion imaging a useful technique in ruling out the presence of significant coronary artery stenoses in HCM patients. In a later studies, however, reversible perfusion abnormalities have been found to be common in HCM, and it has been suggested that scintigraphy cannot be used as a method to exclude or diagnose coronary artery disease in patients with HCM (86).

In a large studies by Yoshida et al. (105 patients) and O'Gara et al. (72 patients) fixed perfusion defects, reversible perfusion defects, and LV cavity dilatation were found in 30%, 60% and 16% and 42%, 58%, and 36% of the HCM patients, respectively (87, 88). Cannon et al. found reversible defects in 37 of 50 HCM (89). In a study by Udelson et al. 15 of 29 relatively young HCM patients (mean age 28 years) had perfusion defects during exercise in ^{201}Tl imaging. The majority of patients had complete normalization of perfusion abnormalities after one week treatment with verapamil Ca^{2+}-channel blocker (90).

In stress studies using pharmacological vasodilatation of coronary arteries, perfusion defects have been frequently found as well. Takata et al. studied 82 HCM patients with ^{201}Tl at rest and during dipyridamole-induced vasodilatation. Thirty-nine

percent of the patients showed reversible defects of which 18% were large (91). von Dohlen et al. found dipyridamole-induced defects in 11 of 39 patients (92).

The location of perfusion defect has been variable but somewhat more often they have been found in interventricular septum (86, 89, 93). In a large study by Cannon et al. one third of the defects were in the anterior septum, one fourth in the anterior free wall and one fourth in the posteroinferior free wall (89). In a study by O'Gara et al. 35%, 24% and 20% of the completely reversible defects located in the anterior septum, posterior free wall and apex, respectively. Most fixed defects were observed in patients with ejection fraction < 50%, whereas reversible defects were usually in patients with normal ejection fraction. Fixed defects have been found to be located evenly in different locations of LV (88). Thus, in scintigraphy studies perfusion defects may locate in any segment of LV without any clear predilection site.

In a study by O'Gara et al. less than 10% of fixed defects appeared in regions of LV wall thickness $\geq$ 20 mm. In contrast, 41% of completely reversible defects occurred in areas of LV wall thickness $\geq$ 20 mm, and 50% of these patients had subaortic obstruction, which was more than in patients with fixed defects or with no defects (88). In a study by Cannon et al. reversible defects disappeared completely in 11 of 15 patients 6 months after surgical relief of LV outflow tract obstruction (94). Accordingly, reversible defects perfusion defects suggesting myocardial ischemia seem to be more frequently found in hypertrophied segments of LV and LV outflow tract obstruction seems to one cause of perfusion defects.

Patient symptoms between patients with fixed and reversible perfusion defects seem to differ. In patients with fixed defects, dyspnea and fatigue have been frequently found (88). In one study, reversible exercise-induced perfusion defects were found in all young HCM patients who had suffered from cardiac arrest or

syncope (93). Subsequent verapamil-treatment improved thallium uptake in most patients. In a study by Yoshida et al. LV cavity dilatation was associated with the failure of systolic blood pressure to increase by ≥ 25 mmHg above the resting value, suggesting an association between pathological blood pressure response and ischemia.

Comparison of perfusion imaging and great cardiac vein lactate measurements during atrial pacing has been used to study whether perfusion defects reflect true metabolic ischemia at the cardiomyocyte level. Hanrath et al. found no association between perfusion defects and pathological myocardial lactate extraction (= impaired lactate extraction or lactate production) during rapid atrial pacing. Neither did LV outflow tract obstruction correlate with pathological myocardial lactate extraction (86). In contrast, in a large study of 50 HCM patients Cannon et al. found that in 82% of HCM patients with reversible defects had lactate production indicative of myocardial ischemia (89). This percentage was higher than that found in patients without reversible defects (31%). Postpacing LV end-diastolic pressure was found to be higher in HCM patients with reversible defects than in others, supporting the concept that reversible perfusion defects have a pathophysiological importance. Impaired lactate extraction has been found more frequently in patients with stress-induced LV cavity dilatation, suggesting that LV cavity dilatation in scintigraphic study is also a correlate of myocardial ischemia in patients with HCM (89). However, no correlation between the presence of reversible or fixed defects and chest pain on exertion has been observed (85, 88, 91, 92). The results of myocardial perfusion findings in SPECT studies are summarized in Table 2.

Table 2. Myocardial perfusion imaging findings in SPECT studies

Reference	Tracer	Stressor	No of patients	Findings
(88) O'Gara	^{201}Tl	Treadmill exercise	72	Fixed defects 24% Reversible defects 33%
(91) Yoshida	^{201}Tl	Bicycle ergometer	105	Fixed defects 30% Reversible defects 60%
(95) Cannon	^{201}Tl	Treadmill exercise	50	Fixed defects 30% Reversible defects 52%
(91) Takata	^{201}Tl	Dipyridamole	82	Fixed defects 33% Reversible defects 39%
(92) von Dohlen	^{201}Tl	Treadmill exercise	28	Abnormal rest or stress scan 39%

2.7.5.2. Positron emission tomography studies

Rest studies

The results of myocardial blood flow measurements at rest between hypertrophied and nonhypertrophied LV wall in positron emission tomography studies have been controversial. Camici et al. found that myocardial blood flow was increased in the hypertrophied septum compared with that in the nonhypertrophied myocardium (96). In contrast, Nienami et al., Grover-McKay et al. and Nienebar et al. found rest flow to be significantly lowered in hypertrophied myocardium compared with normal myocardium (97, 98), and finally, Perrone-Filardi et al., Tadamura et al., and Li et al. found no differences between flows in hypertrophied and nonhypertrophied myocardium (77, 95, 98-100). However, in aforementioned studies echocardiographically measured LV wall thicknesses were used to correct for the partial volume effect, which does not necessarily enable correction of the true partial volume effect due to marked regional differences in LV wall thickness throughout LV.

Partial volume effect correction had significant impact on results and conclusions as found in a study by Grover-McKay et al. (98).

Perrone-Filardi et al. (99) and Grover-Mckay et al. found impaired septal glucose uptake arguing against ischemia. In a study by Grover-Mckay et al., the tissue clearance kinetics of ^{11}C was identical between septum and lateral wall and between HCM patients and controls. This normality does not support hypothesis of global or septal ischemia in HCM either (98). Perrone-Filardi et al. found that lowered glucose uptake associated with impaired systolic thickening compared with the lateral wall (99) and the authors suggest that heterogeneity in regional glucose uptake is parallel to systolic function and does not necessarily represent a metabolic abnormality at the cellular level.

The results of myocardial perfusion at rest in HCM patients, compared with controls, have also been controversial. In the positron emission tomography study by Posma et al., absolute rest perfusion (ml/min/tissue gram) was found to be increased in HCM patients (101). Camici et al. and Lefroy et al., however, did not find differences between HCM patients and controls (76, 96).

Rest-stress studies

The results of quantitative myocardial perfusion rest-stress measurements are summarized in Table 3.

Table 3. Myocardial flow reserve or perfusion reserve in patients with HCM and control subjects

Reference	Method/	Measured parameter	Stressor	HCM patients	Controls
(96) Camici	^{13}N-ammonia-PET	Myocardial blood flow	iv dipyridamole	IVS 1.6 ± 0.6	3.0 ± 1.0
				FW 1.5 ± 0.6	2.4 ± 0.8
(95) Tadamura	^{13}N-ammonia-PET	Myocardial blood flow	iv dipyridamole	IVS 1.4 ± 0.3	2.9 ± 0.3
				FW 1.8 ± 0.4	2.9 ± 0.7
(102) Cecchi	^{13}N-ammonia-PET	Myocardial blood flow	iv dipyridamole	1.8 ± 0.7	2.7 ± 0.9
(103) Memmola	Transesophageal	Stress/rest flow velocity	iv dipyridamole	1.8 ± 0.3*	3.1 ± 0.5*
	Doppler	ratio in coronary artery		1.2 ± 0.1†	2.3 ± 0.7 †
(40) Krams	Doppler wire in LAD	Stress/rest flow velocity	Intracoronary	1.8 ± 0.9	2.6 ± 0.8
		ratio in coronary artery	adenosine		
(95) ‡Tadamura	^{13}N-ammonia-PET	Myocardial blood flow	iv dipyridamole	IVS 0.8 ± 0.3	2.9 ± 0.3
				FW 2.7 ± 0.9	2.9 ± 0.7
(104) Kawada	Flow in coronary sinus	Stress/rest flow ratio	iv dipyridamole	1.7 ± 0.5	3.0 ± 0.8

* Systole

† Diastole

‡ Pediatric HCM

IVS = interventricular septum, FW = free wall, PET = positron emission tomography, LAD = left anterior descending artery

Stress flow, stress perfusion, stress-rest flow ratio, and stress-rest perfusion ratio have been found to be consistently impaired in HCM patients (40, 96, 97, 101, 105). Perfusion reserve in pediatric HCM patients is probably more severely impaired than in adult HCM patients (95).

Camici et al. found that in HCM patients during dipyridamole infusion, myocardial perfusion increased 1.5 times higher as compared to rest values, whereas in control subjects the corresponding increment was 3.0–fold (96). In a study by Cecchi et al. the values were very near to those obtained by Camici et al. (102). These studies, however, may include the same patients. In the study by Cecchi et al., impaired rest perfusion values and an impaired stress-rest perfusion ratio were associated with a poor prognosis during follow-up (102).

In a study by Posma et al. myocardial blood flow ml/min per tissue gram was comparable to controls during dipyridamole-induced vasodilatation (101). However, also in this study, perfusion reserve was lower due to increased rest perfusion in HCM patients. In a study by Nienaber et al. normal glucose utilization, but reduced myocardial flow during a supine bicycle exercise test was found, suggesting the presence of myocardial ischemia in patients with HCM (97).

Camici et al. and Tadamura et al. found that dipyridamole induced vasodilatation impairment somewhat more in the septum than in the free wall, but the differences were not statistically significant (96, 100). In pediatric HCM patients, however, myocardial blood flow reserve was clearly impaired in hypertrophied septum, but not in the LV free wall, compared with healthy controls (95).

2.7.5.3. Doppler studies

Memmola et al. found that diastolic velocity in coronary artery measured by transesophageal Doppler echo was increased, whereas systolic velocity was decreased in HCM patients (103). During dipyridamole stress, the increment in flow velocities was depressed in both systolic and diastolic components, resulting in impaired velocity reserve in HCM patients (Table 3). In a study by Dimitrow et al. systolic blood flow velocity was observed to be reversed in HCM patients (contrary to controls), whereas peak diastolic velocity and diastolic time-velocity integrals were increased in transthoracic Doppler-echo, measured distal of left anterior descending coronary artery (106).

2.7.5.4. Biochemical measurements

In a study by Cannon et al. and Pasternack et al. lactate metabolism was found to be different between HCM patients and controls during atrial pacing (105, 107). In controls, pacing increased lactate consumption, whereas in patients with HCM decreased lactate consumption or even lactate production was found. In a study by Cannon et al. great cardiac vein - arterial O_2 difference decreased during cardiac pacing in HCM patients, but not in controls (105). These findings indicate difficulties in oxygen extraction and true myocardial ischemia in HCM during atrial pacing in HCM.

2.7.5.5. Coronary angiography

In a study by Yetman et al. myocardial bridging with compression of an epicardial artery was found in 28% of pediatric HCM patients (108). In all 10 patients, the site of systolic compression was in the middle third of the left anterior descending coronary

artery, just distal to the origin of the first diagonal branch. The degree of systolic narrowing was greater than 90 percent. In general, the coronary arteries remained compressed over half of the length of diastole. When compared with patients without bridging, patients with bridging more frequently had chest pain, cardiac arrest with subsequent resuscitation and ventricular tachycardia. The patients with bridging had a reduction in systolic blood pressure with exercise when compared with an elevation of 43 ± 31 mmHg in those without bridging. The patients with bridging also had greater ST-segment depression with exercise, shorter duration of exercise and greater degree of dispersion of the QT interval. The proportion of patients who had died or had cardiac arrest with subsequent resuscitation was higher among patients with bridging (108).

2.7.5.6. Etiology of ischemia in HCM

Several potential mechanisms have been presented to account for perfusion abnormalities. The various possible factors include insufficient widening of the epicardial coronary arteries related to increased heart weight (109), small-vessel disease with decreased vasodilator capacity (3, 35, 105, 107, 110), septal perforator artery compression (111, 112), myocardial bridging (108, 112), inadequate capillary density ratio (105), decreased coronary perfusion pressure due to increased LV end-diastolic pressure (105), decreased oxygen extraction (105) and obstruction of the LV outflow tract (112). Evidence of causative factors behind ischemia, however, is limited, and existing results are contradictory.

2.8. Findings in HCM caused by TPM1-Asp175Asn

TPM1-Asp175Asn is a missense mutation that results in the substitution of asparagine for aspartic acid at amino acid position 175 in the α-tropomysin gene. TPM1-Asp175Asn occurs in a troponin T binding region of α-tropomyosin. α-tropomyosin belongs to thin filaments in cardiac sarcomere (Figure 2). Cardiac contraction occurs when calcium binds the troponin complex and α -tropomyosin, making possible the myosin–actin interaction (2).

A transgenic mouse that expresses mutant TPM1-Asp175Asn in the adult heart has been developed (113). In a study by Muthuchamy et al., severe impairment of both contractility and relaxation in the hearts of the TPM1- Asp175Asn mice were found in vivo (113). Rates of contraction (+dP/dt) and relaxation (-dP/dt) were found to be significantly reduced in mutant hearts, and time to peak pressure and time to half relaxation were found to be prolonged. Myofilaments that contained mutated protein demonstrated increased sensitivity to Ca^{2+} when compared with non-mutated myofilaments during force development. Even though functional differences between mutated and control mice were found, septal and posterior wall thickness in echocardiography or LV mass in echocardiography were similar in both groups. Thus based on these findings systolic dysfunction develops before LVH. Interestingly, functional changes were developed, if the proportion of the mutant protein was 60%. The mice that expressed < 40% of the TPM1-Asp175Asn protein did not show any differences in physiological measurements. However, in a recent study, Wernicke et al. found decreased Ca^{2+} sensitivity and accelerated contraction and relaxation, all findings contrary to that found by mouse- model by Muthuchamy et al. in transgenic rats with TPM1-Asp175Asn (107).

In human studies, the penetrance of TPM1-Asp175Asn mutation, i.e. the proportion of patients with mutation and HCM phenotype, in adult patients has been estimated to be 100% (114-116). In a study by Coviello et al., most patients with TPM1-Asp175Asn were asymptomatic, or they had only mild symptoms. LV maximal wall thickness on echocardiography varied from 13 to 28 mm (116). The distribution of LV hypertrophy was generally uniform in the family members and predominantly involved the anterior septum.

2.9. MRI findings in HCM patients

2.9.1. MRI techniques to study patients with HCM

The first MR image of the human heart was published in 1982 (117). Image acquisition time was 8 minutes and it was obtained without cardiac gating. The first ECG-gated images from the beating heart were published in 1984 from anesthetized dogs (118). As early as 1985 Been et al. and Higgins et al. used cardiac MRI to investigate LV anatomy in patients with HCM (8, 119). In the study by Been et al., no cardiac gating was used, and imaging was performed using a very low-field scanner (0.08 T). Higgins et al. used a 0.35 T scanner and ECG-gated image acquisition. Park et al. were the first who utilized a high-field MR scanner to image patients with HCM (9).

In the first studies, a body coil was used as a receiver, and image acquisition was performed using black-blood spin-echo sequences. In spin-echo imaging, some investigators have used saturation pulses to improve myocardium-blood delineation (120). Pixel dimensions in the phase-encoding orientation have varied from 1.25 to 3.4 mm. In the frequency-encoding orientation pixel dimension has been equal or smaller. Slice thicknesses have varied between 7 and 10 mm. In the first studies,

only transverse, sagittal or coronal orientations were used. Since 1992, double-oblique LV long- and short-axis views have been used to image patients with HCM (121).

Sardanelli et al. were the first to perform cine MRI to investigate patients with HCM (122). The authors reported the results of cardiac anatomy, LV wall systolic thickening and flow void in the LV outflow tract. In later studies, spin-echo imaging was largely replaced by cine imaging in anatomical and functional imaging. At the beginning, cine images were obtained with free breathing (122, 123). Later 1990s, studies were usually performed by cine imaging with breath holding, which facilitated an accurate assessment of cardiac function in less than 5 minutes (124). In general, the duration of the whole imaging protocol in cardiac MRI has ranged between 20 and 90 minutes. Currently, the fast low-angle shot cine sequence has been replaced by a steady-state precession that is associated with higher contrast-to-noise ratio and better detection of endocardial border than the fast low-angle shot cine sequence (125). The temporal resolution in cine imaging has been varied from 16 to 32 phases/cardiac cycle.

In 1992, the first tagging results from subjects with HCM were published (126). Tagging imaging facilitates the noninvasive analysis of the complicated contraction pattern of the human cardiac left ventricle (126-129). Image analysis is performed by specific softwares not commercially available (126-129). During image postprocessing, myocardial tagging stripes have been claimed to use subpixel resolution (127).

Gd-DTPA-enhanced segmented inversion recovery imaging (130) have been used in fibrosis imaging and in imaging to detect tissue changes after septal ablation (131-136). Contrast-agent doses for contrast-enhanced imaging have varied between

0.1 mmol/kg to 0.2 mmol/kg, inversion time has typically been 250 msec and delay between injection and imaging has varied from 5 to 10 minutes (131-136).

T2-weighted imaging has had limited value in HCM characterization. In a recent study, however, Amano et al. used T2-weighted fast spin-echo imaging with breath holding a double inversion recovery pulse pair and with or without fat-suppression to detect tissue edema after percutaneous transluminal septal myocardial ablation in patients with obstructive HCM (136).

2.9.2 The accuracy and reproducibility of LV mass measurement

Excellent reproducibility and accuracy in LV mass measurements by using MRI have been found (137). Katz et al. used a spin-echo sequence to measure LV mass in ex vivo hearts in 40 subjects (138). The standard error of the measurements in ex vivo study was 6.8 g ($r = 0.99$), and the standard error of intraobserver and interobserver measurements was 11.1 g ($r = 0.96$) and 17.8 g ($r = 0.91$), respectively. Allison et al. imaged LV mass in ex vivo hearts and in patients with HCM by using spin-echo sequence (6). MRI evaluations of LV mass in ex-vivo hearts were within 8% of the mass determined by weighing the hearts ($r = 0.99$). MRI is considered a golden standard in LV mass measurements (137).

2.9.3. Regions of LVH and LV maximal wall thickness

In studies of HCM patients with European descent, asymmetrical septal hypertrophy has been the most common finding. The mean LV maximal wall thickness (MWT) has typically been between 20 and 25 mm (Table 4). The highest LV wall thickness found by MRI has been 37 mm (139).

Sardanelli et al. investigated 23 HCM patients with an echocardiographic diagnosis of HCM (122). Half of the patients had asymmetric and half symmetric LVH. Apical hypertrophy or papillary muscle hypertrophy were rare findings in the aforementioned study. In a study by Arrivé et al., most HCM patients had asymmetric septal hypertrophy. In addition, hypertrophy of the entire septum and of the LV posterolateral wall were found. The mean posterolateral wall thickness did not differ from that in control subjects (140).

Park et al. found apical hypertrophy in one third of patients with HCM (9). The rest of the patients had asymmetric septal hypertrophy. The mean LV wall thickness in apical hypertrophy was 25 mm compared with 24 mm in patients with asymmetric septal hypertrophy. Thus, apical hypertrophy is usually advanced upon diagnosis. Suzuki et al. described a form of HCM, in which LVH was confined to a small region of the septum of the anterior or lateral wall at the apical level (141). Soler et al. found that apical hypertrophy was confined to true apex only in 5 of 21 HCM patients with apical LVH (142).

2.9.4. LV mass

Been et al. measured only the LV septal area, a precursor of LV mass, rather than LV mass itself in one of the first MRI studies published on HCM patients (119). The LV septal area was increased compared with controls. In a study by Allison et al. the mean LV mass/body weight -ratio was 3.77 g/kg in HCM patients, which was significantly higher than that in control subjects (1.80 g/kg) (6). The following studies have confirmed these findings that LV mass is increased in patients with HCM, but not as markedly as supposed based on LV mass measurements in

echocardiographic studies (143). The results of quantitative LV anatomical and functional characteristics in MRI studies in HCM patients are summarized in Table 4.

Table 4. Left ventricular anatomical and functional characteristics in patients with HCM in MRI studies

Left ventricular	Result	Author	Patients
Mass (g)	242 ± 81	(104) Kawada et al.	29
Mass (g)	159 ± 56	(134) Bogaert et al.	29
Mass (range) (g)	238 ± 88 (95 – 427)	(131) Choudhury et al.	21
Mass index (range) (g/kg)	3.8 ± 0.9 (3.3 – 5.6)	(6) Allison et al.	12
Mass index (g/m^2)	106 ± 20	(139) Schwammenthal et al.	7
Maximal wall thickness (mm)	Highest 34	(144) Arrivé et al.	10
Maximal wall thickness (mm)	25 ± 8 (11 – 37)	(139) Choudhury et al.	21
Maximal wall thickness (mm)	23 ± 8 (11* – 32)	(134) Bogaert et al.	21
Mass/end-diastolic volume (g/ml)	2.4 ± 0.52	(139) Schwammenthal et al.	7
End-diastolic volume (ml)	100 ± 42	(134) Bogaert et al.	11
End-diastolic volume index (ml/m^2)	146 ± 24	(139) Schwammenthal et al.	7
End-systolic volume index (ml)	45 ± 9	(139) Schwammenthal et al.	7
Stroke volume (ml)	69 ± 36	(134) Bogaert et al.	11

Ejection fraction (%)	66 ± 7	(144) Dong et al.	11
Ejection fraction (%)	71 ± 7	(134) Bogaert et al.	11
Ejection fraction (%)	70 ± 11	(139) Choudhury et al.	21
Ejection fraction (%)	80 ± 7	(139) Schwammenthal et al.	7
Sinus coronaries flow reserve	1.72 ± 0.49	(104) Kawada et al.	29

* the lowest value was obtained in a 10-year-old girl

2.9.5. LV function

No difference has been found in LV global ejection fraction between HCM patients and control subjects in studies using three-dimensional cine MRI (104, 144) (Table 4). LV regional systolic function has been investigated in many MRI studies. Arrivé et al. found that the average thickening of the basal septum was markedly reduced compared with that in control subjects (140). In a study by Perrone-Filardi et al., lateral wall thickening was found to be increased compared with the septum. In addition, in positron emission tomography imaging, ^{18}fluorodeoxyglucose activity in lateral wall, describing metabolic activity, was higher in the lateral wall parallel to increased systolic function (99). In a study by Choudhury et al., the average LV systolic thickening was 77 ± 63% in patients with HCM (131). In the aforementioned study, LV systolic thickening impairment was associated more closely with increased LV end-diastolic thickness (r^2 = 0.30) than with myocardial contrast-enhancement (r^2 = 0.04). This suggests that regional hypokinesia is more closely associated with LVH than with myocardial fibrosis.

In a study by Kramer et al. using cine tagging imaging, percentage shortening at short axis orientation and at long axis orientation was impaired in HCM in the septal, inferior, and anterior regions of LV, but not in the lateral region of the LV (145). These findings are in concordance with findings by Maier et al., Perrone-Filardi et al. and Dong et al. who found that LV lateral wall movement was increased compared with the LV septum (99, 144, 146). However, the radial displacement of septum has been found to be lowest also in normal subjects (144). The authors found also that total LV shortening occurred earlier in systole in HCM patients than in control subjects (145) (In contrast Gibson et al. found an abnormal delay in the onset of movement in a cineangiography study (70)).

In a tagging study by Young et al., radial motion (measured in short axis images) was less reduced than longitudinal displacement (measured in long axis images) (127). This finding is in concordance with echocardiographic findings by Hattori et al. (69). In terms of three-dimensional movements, the most significant systolic impairment was found in the basal septum and LV anterior wall. In contrast, LV torsion was found to be increased in HCM patients compared to controls (20 vs. 15 degrees). In control subjects, early counterclockwise rotation reversed to clockwise in later systole. In HCM patients, normal clockwise rotation was abolished, resulting a net increase in counterclockwise torsion (127). Increased counterclockwise torsion has previously found to be related to increased inotropic stimulation (147). Thus, increased counterclockwise rotation could be related to augmented adrenergic activity, which has been suggested to be increased in HCM patients. In a study by Maier et al. however, the average rotation was similar between HCM patients and controls (126).

Dong et al. investigated radial displacement differences between LV layers. The authors found that radial displacement especially in the midwall and epicardial layers was less in patients with HCM (144). In a study by Maier et al. radial displacement of all myocardial layers was impaired in septal and inferior LV segments (126). In the posterior and anterior segments, in contrast, decreased radial displacement was observed only in the epicardial and midwall layers.

Bergey and Axel have shown patient examples in which myocardial tagging imaging helped to detect myocardial contraction in highly localized LVH, which indicated a diagnosis of HCM instead of neoplasm (129).

2.9.6. LV outflow tract obstruction, mitral regurgitation and systolic anterior motion of mitral valve leaflet

MRI has had only a limited role in the assessment of LV outflow tract obstruction, mitral regurgitation and systolic anterior motion of the mitral valve leaflet in characterization of HCM patients. Sardanelli et al. found a correlation between signal void duration in cine MRI and signal turbulence duration in Doppler echocardiography in the LV outflow tract and left atrium suggestive of LV subaortic stenosis and mitral insufficiency, respectively (122). In all patients with signal void in MRI, a pressure gradient in echocardiography was present. The same association between signal void in LV outflow tract and LV outflow tract obstruction was found by Arrivé et al. (140) and Scheffknecht et al. (120). Schulz-Menger et al. used cine MRI to document therapeutic response after septal embolization (121). Twelve months after embolization, the non-turbulent area in LV outflow tract was increased, and the improvement was associated with the amelioration of symptoms.

2.9.7. Contrast-enhanced MRI

At present, myocardial tissue characterization using contrast-enhanced MRI is one of the main interests in imaging of HCM patients. Aso et al. was one of the first to investigate the accumulation of contrast agent in the cardiomyopathic heart. The authors studied cardiomyopathic hamsters by contrast-enhanced (0.1 mmol/kg Gd-DTPA) spin-echo imaging (148). The Gd-DTPA they used was labeled by ^{14}C, which enabled the accurate detection Gd-DTPA in histopathological sections. In cardiomyopathic hamsters, autoradiograms showed a nonuniform distribution with patchy or linear areas with increased uptake of Gd-DTPA compared with controls. Areas of patchy accumulation of Gd-DTPA corresponded to “replacement fibrosis”,

and areas of linear accumulation to interstitial fibrosis separating myocardial fibers. Histologically, "replacement fibrosis" was shown to have more capillaries and cellularity than interstitial fibrosis. Accodingly, the mean Gd-DTPA concentration was highest in myocardial fibrosis with high cellularity, proliferation of new vessels, and loose collagen and it was lowest in myocardial fibrosis with dense collagen, few vessels, and low cellularity (148).

In patients with coronary artery disease the association between myocardial fibrosis and hyperenhancement is well established (149-152). In HCM, according to findings by Aso et al., the most hyperenhancement was shown in relatively young animals that histologically demonstrated markers of inflammation, neovascularization and earlier phases of interstitial fibrosis than dense scars filled only with collagen (148). Contrast-enhancement was associated with inflammation, fibrosis and vessel proliferation in a hamster study by Nanjo et al. as well (153). The concepts of inflammatory changes and neovascularization are novel mechanisms implicated in the pathophysiology of HCM.

Sequences with a preparatory inversion pulse have been shown to best delineate abnormal contrast enhancement in humans (130). The segmented breath-hold sequences can provide images with higher resolution and with a better contrast-to-noise ratio than images obtained with single-shot sequences (130). Choudhury et al. used a contrast-enhanced (gadoteridol, 0.1 mmol/kg) segmented inversion-recovery sequence in 21 patients with HCM. Eight of the 21 patients were examined based on clinical symptoms and the rest were examined as part of family screening or due to the findings of an asymptomatic murmur (131). Altogether 81% of the patients had hyperenhanced myocardium. Contrast enhancement occurred in a patchy distribution with multiple discrete foci within hypertrophied regions of the interventricular septum

and in the anterior and posterior walls but not in the lateral free wall. The mass of scar tissue ranged from 0 to 143 g (mean, 22 ±- 31 g), and it constituted 8 ± 9% of the LV mass. On a regional basis, weak relationship between hyperenhancement and end-diastolic wall thickness was observed. None of the LV segments under 10 mm thick had any hyperenhancement. The extent of hyperenhancement associated weakly with impaired fractional or absolute segmental thickening. The extent of hyperenhancement, as a percentage of the LV mass, correlated weakly with the maximum LV end-diastolic wall thickness and the LV mass, and modestly with the LV ejection fraction (131).

Boggiest et al. used contrast-enhanced (Gd-DTPA 0.2 mmol/kg) inversion-recovery T1-weighted imaging and found abnormal enhancement in 7 of 8 patients with echocardiograph diagnosis of HCM (134). Both patchy and homogeneous enhancement was observed. Hyperenhancement was associated with regional LVH and hypocontractility.

Teraoka et al. investigated 59 patients with HCM with an inversion-recovery FLASH sequence 15 minutes after 0.1 mmol/kg Gd-DTPA injection and found contrast enhancement in 76% of the patients (135). Hyperenhancement was found most frequently in the region where the right ventricle was attached to the LV. LV mass in patients with and without hyperenhancement was not different. The number of hyperenhanced segments was associated with an impaired ejection fraction. Hyperenhancement was associated with ventricular tachycardia in 24-h Holter monitoring (135).

Amano et al. investigated the association between myocardial fibrosis evaluated by contrast-enhanced MRI and fatty acid metabolism evaluated using uptake of an ^{123}I labeled fatty acid analogue in SPECT. The authors found that in both methods,

the most marked abnormalities were found in interventricular septum. but that the agreement between the methods in detecting myocardial abnormalities was fair (154).

In a study by Moon et al., myocardial enhancement was found in 42 of 53 HCM patients affecting 0 - 48% of myocardial mass (mean 11%) (133). In patients with a decrease in LV wall thickness and an increase in LV end-systolic dimensions during follow up on serial echocardiograms had more hyperenhancement than other patients. In addition, patients with two or more risk factors for sudden death had more hyperenhancement than other HCM patients. Hyperenhancement was correlated weakly with LV mass index, LV end-diastolic volume, LV end-systolic volume, and inversely with ejection fraction.

Recently, the first study of hyperenhancement in HCM patients with identified disease causing mutations was published (155). In aforementioned study Moon et al. investigated 30 patients with the TNNI3 mutation in the troponin I gene (155). The authors found hyperenhancement in 12 patients (80%) with LVH in echocardiography and in 2 patients (13%) without LVH. The extent of hyperenhancement was positively associated with clinical markers of sudden death risk and LV mass and was inversely associated with LV ejection fraction.

In a study investigating one HCM patient who underwent late gadolinium enhancement MRI and 49 days later heart transplantation, regions of myocardial late enhancement were found to represent regions of myocardial collagen in histological sections (132).

The role of T1-weighted spin-echo imaging has been limited in tissue characterization in HCM patients. Nishimura et al. used contrast-enhanced (0.1 mmol/kg Gd-DTPA) spin-echo imaging 5-10 minutes after injection in patient with

HCM and found increased signal intensity at subendocardial layers in 10 of 16 HCM patients. In this study, however, no control subjects were studied (156). Schulz-Menger et al. used T1-weighted spin-echo sequences, after 0.1 mmol/kg Gd-DTPA to visualize myocardial infarction after septal embolization (121). The infarcted zone was visible on contrast-enhanced images.

Two studies have described myocardial signal intensity differences without contrast agent in HCM patients (157, 158). The role of such measurements seems to be minor.

2.9.8. Coronary sinus flow measurements

Blood flow in coronary sinus represents approximately 96% of the total myocardial blood flow. Kawada et al. investigated coronary sinus flow by using velocity encoded cine MRI during breath-hold (104). The authors used 12.7 cm circular surface coil, 5 mm section thickness, and 2.9 mm spatial resolution. Temporal resolution in imaging was 60 msec, and it allowed 9 to 13 flow phases within a single breath hold. Imaging was performed at rest and during dipyridamole-induced vasodilatation. At baseline state, coronary blood flow per gram of myocardial mass was 0.74 ml/min/g ± 0.23 in patients with HCM, not significantly different from that in healthy subjects. After administration of dipyridamole, coronary blood flow per gram of myocardial mass was lower in patients with HCM than in controls (1.03 ± 0.40 ml/min/g vs. 2.14 ± 0.51 ml/min/g), reflecting a lower coronary flow reserve in HCM patients (Table 3). A significant negative correlation was found between the coronary flow reserve and LV mass index when both control subjects and HCM patients were included in the same analysis (104).

2.9.9. MR spectroscopy

De Roos et al. and Jung et al. found that patients with HCM had increased inorganic phosphate-to-phosphocreatine ratio and decreased phosphocreatine-to-adenosine triphosphate ratio (159, 160). The phosphocreatine-to-adenosine triphosphate ratio correlated negatively and inorganic phosphate-to-phosphocreatine ratio positively with the extent of LVH (160). These abnormalities are similar to those found in ischemic myocardium. Interestingly, a decreased phosphocreatine-to-adenosine triphosphate ratio has also been found in Himalayan natives, Sherpas, and it is supposed to reflect adaptation to hypoxic circumstances (161). In a study by Jung et al., an increase in the phosphomonoester-to-phosphocreatine ratio was also observed, indicating altered glucose metabolism (160). De Roos et al. found lowered myocardial pH values measured with MR spectroscopy in symptomatic patients, indicating myocardial ischemia (159). In a study by Jung et al. no differences in pH values between HCM patients and controls was observed (160). However, patients in the study by de Roos et al. were symptomatic. In contrast, Jung et al. studied young asymptomatic patients, which may explain the difference in pH values. The aforementioned metabolic abnormalities can theoretically be caused by (1) increased workload of the heart under resting conditions, (2) limitation in oxygen supply severe enough to invoke a significant increase in anaerobic metabolites and disturbances in oxidative phosphorylation and in the ATP production contribution to ATP turnover rates, and (3) altered energy sources fueling the cardiac "engine" (161).

2.9.10. Comparison of MRI and echocardiography in the assessment of LVH in patients with HCM

Many studies have compared MRI and echocardiography in the assessment of LVH in patients with HCM (122, 143, 162, 163). Devlin et al. compared LV wall thickness measurements obtained by transthoracic echocardiography and MRI between LV segments (143). The best agreement between M-mode echocardiography and MRI was observed in LV anterior septum and anterior free wall. Posma et al. compared MR imaging and echocardiography in the Spirito-Maron and Wigle hypertrophy score calculations. MRI yielded complete assessment of anatomic features and allowed calculation of hypertrophy scores in 49 patients (94%), which was significantly more than echocardiography (33 patients; 63%) (7). The LV anterior free wall, posterior septum, posterior free wall and apex are the regions that are difficult to evaluate by echocardiography (7, 141, 143).

In LV mass measurements in patients with HCM, a poor correlation between LV mass obtained by MRI using Simpson's LV mass measurement formula three-dimensional method) and echocardiography by using Devereux LV mass measurement formula has been found (6, 143). The main reason appears to be asymmetric LVH in patients with HCM, a feature not considered in most echocardiographic LV mass measurement formulas.

In conclusion, in the assessment of regional wall thicknesses MRI is a more comprehensive method than echocardiography. In LV mass measurements in patients with asymmetrically thickened LV, three-dimensional methods such as MRI are methods of reference.

2.9.11. Differential diagnosis between HCM and other diseases causing LVH

In one study, the differential diagnosis between HCM and other diseases causing LVH, such as amyloidosis, has been attempted. Fattori et al. compared imaging findings between patients with symmetric HCM and biopsy-proven amyloidosis. In patients with amyloidosis, the interatrial septum, right atrial free wall, and right ventricular anterior wall were claimed to be thicker in patients with amyloidosis than in patients with HCM (158). All these structures, however, are relatively thin, masked by other structures, such as trabeculations of RV, or complex in shape. Due to these difficulties, they may be difficult to measure accurately with the current level of image quality.

3. AIMS

The general aim of this study was to evaluate the role of cardiac MRI in the characterization of LV anatomy, systolic function, perfusion and contrast enhancement in patients with HCM caused by the mutation Asp175Asn in the α-tropomyosin gene. More specifically, the objectives were:

1. To investigate the relationship between myocardial contractile impairment and LVH in HCM (Study I).
2. To assess first-pass MRI a) in the evaluation of perfusion impairment in patients with HCM and b) to evaluate the association between first-pass perfusion and LVH in HCM (Study II).
3. To investigate the relationship of myocardial enhancement with gadolinium-DTPA in MRI with serum concentrations of a collagen synthesis marker (the aminoterminal propeptide of type III collagen) (Study III).
4. To determine the relationship between hypertrophy and cardiac adrenergic activity measured by ^{123}I-MIBG in HCM (Study IV).

4. PATIENTS AND METHODS

The study protocol was approved by the Kuopio University Hospital Ethics committee, and all subjects gave written informed consent.

4.1. Selection of patients with HCM

The Kuopio University Hospital region in Eastern Finland covers a population of approximately 250,000 inhabitants. All patients with suspected or confirmed HCM in this area are referred to Cardiology Unit, Department of Medicine of Kuopio University Hospital for diagnosis and treatment. All available unrelated patients from this region with suspected or confirmed HCM according to hospital records have been previously evaluated by the same cardiologist at our hospital. Altogether 36 unrelated patients aged over 16 years and fulfilling the criteria for definite HCM were identified (164).

4.1.1. Clinical diagnosis of HCM

In index patients, the clinical diagnosis of HCM was based on the demonstration of maximum LV wall thickness of at least 15 mm on two-dimensional echocardiography in the absence of other causes for LVH, such as hypertension or aortic stenosis. Because the above mentioned clinical criteria are too insensitive to diagnose HCM in first-degree relatives of HCM patients, clinical diagnosis of HCM in adult relatives of the index patients was based on the diagnostic criteria suggested by McKenna et al. (21). Relatives with LV wall thickness of at least 13 mm on two-dimensional echocardiography, or with pathological Q waves, LVH with repolarization changes, or deep T wave inversions on ECG, were considered clinically affected.

4.1.2. Genetic analysis

The genetic screening of variants in TPM1 was performed with the polymerase chain reaction – single strand conformation polymorphism analysis and direct sequencing, as previously described (28). Haplotype analysis in patients with TPM1-Asp175Asn was performed as previously described (28, 164).

4.1.3. Control subjects

Seventeen healthy volunteers without history of previous cardiac disease or medications, and with gender and age distribution similar to the HCM patients, were recruited.

4.1.4. Clinical and echocardiographic evaluation

All patients with HCM and control subjects underwent an interview, physical examination, 12-lead ECG recording and echocardiography. Transmitral flow recordings were obtained from the apical four-chamber view, with the pulsed Doppler sample volume placed at the level of the mitral leaflet tips. Peak early (E) and late (A) transmitral flow velocities, E wave deceleration time and E/A ratio were determined. Isovolumic relaxation time was measured by positioning the continuous wave Doppler cursor between the mitral valve and LV outflow tract, and the time between aortic closure and the onset of transmitral flow was measured. Measurements were performed in two beats and averaged.

4.1.5. Cardiac catheterization and coronary angiography

Right and left heart catheterization and coronary angiography were performed on 21 of the 24 HCM patients by the percutaneous femoral approach using standard

angiographic techniques by the same cardiologist as previously described (165). Three HCM patients who did not undergo angiography were 33 to 38-year-old females from the same family, in which there was no history of HCM-related sudden cardiac deaths. These three patients had definite HCM, but no cardiovascular risk factors.

Control subjects aged over 45 years (two men and three women) had undergone diagnostic coronary angiography within the previous year, showing normal coronary arteries. Other control subjects did not undergo cardiac catheterization or coronary angiography.

4.1.6. Subjects with the TPM1-Asp175Asn

Of the 36 aforementioned unrelated patients with HCM, four were heterozygous carriers of the TPM1-Asp175Asn mutation. All available relatives of the index patients were examined, and 23 relatives were found to have the TPM1-Asp175Asn mutation. In addition, one family with four affected family members from western Finland with the identical TPM1 mutation was included in the study. Thus, altogether 31 patients with the TPM1-Asp175Asn mutation were identified. No consanguinity was found between the five families in genealogical studies tracing ancestors of the families up to 3-5 generations. However, a conserved haplotype between an intragenic microsatellite marker $HTM_{\alpha CA}$ and two extragenic microsatellite markers (D15S1036 and D15S108), spanning a region of about 3 centimorgans and co-segregating with the mutation was observed in five families, suggesting a founder effect (164).

One subject with the TPM1-Asp175Asn mutation and definite HCM was not included in the study because she had had a coronary by-pass operation, and six HCM subjects with the TPM1-Asp175Asn mutation were not willing to participate.

The final population of the present study consisted of 24 adult subjects from four families with the TPM1-Asp175Asn.

In a study investigating LVH and systolic function, LVH was evaluated in all study subjects (100%) (Study I). LV end-systolic dimensions were determined in all but one patient, who had atrial fibrillation (23 of 24, 96%) (Study I). For the perfusion study (Study II), two patients could not be imaged with the phased-array coil because of obesity. Two patients with bronchial asthma were excluded because adenosine stress was contraindicated in these patients in an MR imaging environment. ECG triggering failed during the first-pass of contrast medium in two patients. Contrast medium injection was mistimed in one patient. Thus the population of the rest-stress perfusion study ultimately consisted of 17 of 24 subjects (71%). In the fibrosis study, two subjects could not be imaged with the phased-array coil due to obesity, and one subject became exhausted before the time for post-contrast imaging. Thus the population of the fibrosis study (Study III) ultimately consisted of 21 of 24 subjects (88%). In the study investigating adrenergic activity, three patients could not be studied because ^{123}I-MIBG-tracer could not be supplied by the manufacturer during the study day. Thus the population of study IV included 21 of 24 subjects (88%).

4.1.7. Clinical characteristics

None of the HCM subjects had intracardiac defibrillator or a history of heart failure. There were sudden cardiac deaths at a young age related HCM in three of the four families with the TPM1-Asp175Asn mutation (164). About one third of the patients used cardiac medication, most often β-blocking agents. None of the patients used angiotensin II receptor blockers or statins. Clinical characteristics of the patients with HCM are summarized in Table 5. The mean age was 37 years (range 17-53).

Patients had similar blood pressure values as controls. On two-dimensional echocardiography, the maximal end-diastolic thickness of the septum was 19 ± 6 mm (range 8 - 29 mm). LV end-diastolic and end-systolic dimensions were within the normal range in all patients with HCM. None of the subjects with HCM had significant LV outflow tract obstruction (> 30 mmHg). Patients with HCM had a higher isovolumic relaxation time, deceleration time and E/A ratio than control subjects.

Table 5. Clinical characteristics of the patients with HCM attributable to the Asp175Asn mutation in the TPM1 gene and control subjects

Characteristic	HCM patients n = 24	Control subjects n = 17
Men/Women	11/13	8/9
Age (y)	42 ± 13	38 ± 12
Systolic blood pressure (mmHg)	133 ± 16	128 ± 15
Diastolic blood pressure (mmHg)	84 ± 11	78 ± 10
Echocardiographic findings		
Maximal septal thickness on 2D-mode (mm)	18.6 ± 6.1*	9.1 ± 1.7
Left ventricular end-diastolic diameter (mm)	42 ± 5*	50 ± 4
Left ventricular end-systolic diameter (mm)	26 ± 4*	31 ± 3
V_{max} in left ventricular outflow tract (m/sec)	1.4 ± 0.5	1.3 ± 0.2
Isovolumic relaxation time (msec)	268 ± 280†	82 ± 22
Deceleration time (msec)	237 ± 66*	190 ± 56
E/A ratio	1.57 ± 0.32*	1.18 ± 0.43
Ejection fraction (%)	68 ± 10	67 ± 7
V_{max} at LVOT (m/s)	1.4 ± 0.5	1.3 ± 0.2

Data are means ± SDs

2D, two-dimensional; E/A –ratio, the ratio of early-to-late ventricular filling; V_{max} at LVOT, maximal velocity at left ventricular outflow tract

*P < 0.05

†P < 0.001

‡P < 0.01

On coronary angiography, one patient with HCM had < 50% stenoses in the left anterior descending coronary artery, and another patient had < 50% stenosis in the left anterior descending, intermediate and right coronary arteries. All other HCM

patients and all control subjects in whom coronary angiography was performed had normal coronary arteries. In patients with HCM, LV end-diastolic pressure was 9 ± 5 mmHg (range 0 – 20 mmHg) and pulmonary capillary wedge pressure 8 ± 4 mmHg (range 3 - 16 mmHg). All control subjects had normal blood pressure and normal findings on echocardiography (Table 5) and ECG.

4.2. MRI protocol

MRI was performed with a 1.5-T clinical MRI unit (Magnetom Vision; Siemens Medical Systems, Erlangen, Germany). A phased-array body coil was used as a receiver. ECG readings, blood pressure, pulse waves and peripheral oxygen saturation were monitored during the study with an MR-compatible control monitor (Datex-Ohmeda AS/3 MRI patient monitor; Instrumentarium, Datex-Ohmeda Division, Helsinki, Finland). In addition, precordial electrodes were applied for ECG gating of the image acquisition. All study subjects were imaged by the same radiologist. Two patients were imaged by body coil due to obesity, whereas the others were imaged by phased-array coil.

4.2.1. Rest perfusion imaging

After scout views were obtained, the first-pass of the contrast medium was assessed with acquisition of images at three LV short-axis planes: at the levels of mitral valve chordae, papillary muscle and apex. The first-pass in the myocardium was observed with an inversion-recovery snapshot fast low-angle shot sequence (166). The parameters for first-pass MRI were as follows: repetition time msec/echo time msec/inversion time msec, 4.5/2.2/300; 8° flip angle; 128 x 128 data matrix; 10-mm section thickness; and a 250 – 280 mm field of view with a 256 x 256 interpolated

matrix. Before imaging with contrast medium was performed, the baseline signal intensity (SI) level was assessed. Myocardial first-pass was assessed after injection of a 0.05 mmol bolus of Gd-DTPA (Magnevist; Schering, Berlin, Germany) per kilogram of body weight into the right antecubital vein through an 18-gauge cannula. The volume of the bolus was 5–13 ml (0.1 ml/kg). The injection was performed at a speed of 5 ml/sec with an MR-compatible power injector (Spectris, Medrad, Pittsburgh, Pa, USA). The bolus of contrast medium was followed by a 10 ml bolus of saline. Immediately after injection of the contrast agent, the patient was asked to hold his or her breath. An image at each anatomic position listed above was acquired every 3–4 seconds, for a total of 15 images at each level.

4.2.2. Cine imaging

After rest perfusion images were obtained, cine imaging was started. Cine images were acquired in 10-mm sections with no gap in the short axis orientation, extending from base of the heart to apex using Turbo-Flash cine sequence (124, 125). The parameters for cine imaging were as follows: repetition time msec/echo time msec, 60/4.8 with fivefold k-space segmentation; 20° flip angle; 110 x 256 data matrix; and a 280–320-mm field of view with a 256 x 256 interpolated matrix. Imaging was performed during multiple breath holds (one slice for each breath hold). An average length of time for one breath hold was 20 seconds. The mean number of slices needed to image the whole LV at shot axis orientation was 9.6 ± 1.3 (range 8 - 14). In addition, two-chamber and four-chamber long-axis views were obtained to evaluate the thickness of cardiac apex. Time resolution in cine imaging was 30 msec. Due to variable R-R-intervals, 24 ± 5 cardiac phases were obtained (range 13 – 35).

4.2.3. Fibrosis imaging

After rest perfusion and cine images were obtained, fibrosis imaging was performed at the level of tips of the mitral valve leaflets and at the level of papillary muscles using the same T1-weighed single-shot inversion-recovery FLASH sequence that was used during perfusion imaging. Typically, images were obtained about 15 minutes after Gd-DTPA (Magnevist, Schering AG, Berlin, Germany) injection into antecubital vein (0.05 mmol per kilogram of body weight). Fibrosis imaging was performed by phased-array coil only.

4.2.4. Stress perfusion imaging

About half an hour after previous rest injection of Gd-DTPA, maximal vasodilatation was induced with a continuous infusion of 140 μg/kg/min of adenosine (Adenoscan; Sanofi Winthrop Pharmaceuticals, Morrisville, Pa, USA). Each patient had refrained from ingesting caffeine for 24 hours before the examination. The first-pass MRI sequence was performed 3 minutes after the initiation of adenosine with continuous adenosine infusion. Gd-DTPA was injected through a separate line to prevent an adverse bolus effect of adenosine. Stress perfusion imaging was performed by phased-array coil only.

Seventeen HCM patients underwent MR imaging at rest and during adenosine infusion (rest-stress injections). Five control subjects (the rest-stress injection control group) underwent MR imaging at rest and during adenosine infusion and 7 control subjects (the two-injections-at-rest control group) underwent MR imaging without stress. The second injection of gadopentetate dimeglumine was administered half an hour after the first in both control groups. To observe the effect of adenosine on first-pass reserve index (FPR) parameters, results in the rest-stress injection control

group were compared with results in the two-injections-at-rest control group. To observe the differences in FPR between patients with HCM and control subjects, FPR parameters in patients with HCM were compared with those in subjects in the rest-stress injection control group.

4.2.5. Image analysis

4.2.5.1. Anatomical measurements

All anatomic measurements on MR images were performed with Numaris software provided with the MR system (Siemens, Erlangen, Germany) by the same radiologist. LV end-diastolic wall thickness, end-systolic wall thickness and systolic thickening were evaluated in short-axis orientation at the basal (tips of the mitral valve leaflets), mid-cavity (papillary muscles) and apical (beyond papillary muscles but before cavity ends) levels (Fig 4). The end-diastolic image was the first image acquired after the R-wave of the ECG signal, and the end-systolic image was the image with the smallest LV area at the mid-ventricular level. Short axis slices were divided into 16 segments according to a recent statement from the Cardiac Imaging Committee of the Council on Clinical Cardiology of the American Heart Association (167), including 6 segments for the basal and mid-cavity level and 4 segments for the apical level in short axis plane (Fig 4). In addition, the end-diastolic wall thickness for true apex was measured from long-axis images. However, due to insufficient endocardial delineation on Turbo-Flash cine images (125), end-systolic thickness at the apex was not measured. The maximal end-diastolic wall thickness in the LV at any location (LV MWT) was recorded.

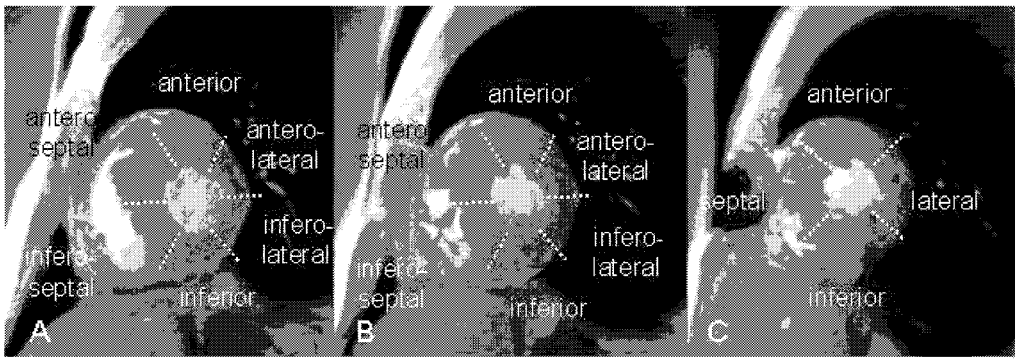

Figure 4. Basal (A), mid-cavity (B) and apical (C) end-diastolic cine images in a patient with HCM showing the location of segments at short-axis orientation according to American Heart Association statement of standardized myocardial segmentation for tomographic imaging (167). The basal image is at the level of tips of the mitral valve leaflets, mid-cavity image at the level of papillary muscles and apical image beyond papillary muscles.

To evaluate LV mass, the endocardium and epicardium, excluding papillary muscles and trabeculations, were manually traced using end-diastolic images. The total myocardial volume of the LV was calculated with Simpson's method by multiplying each traced myocardial area by the section thickness (10 mm) and by summing the volumes of separate slices together. LV end-diastolic and end-systolic volumes were computed in a similar fashion using short-axis end-diastolic or end-systolic areas, respectively. Stroke volume was calculated by subtracting LV end-systolic volume from LV end-diastolic volume. Myocardial mass was calculated by multiplying myocardial volume by myocardial density (1.05 g/ml). In one patient with atrial fibrillation, end-systolic dimensions were not measured.

The LV mass index, LV volume indices, and LV maximal wall thickness index were calculated by dividing the mass of the LV by the body surface area, which was calculated by following equation ((weight (kg) x height (cm))/3600)$^{0.5}$ (168).

4.2.5.2. Measurement of LV contractility by MRI

The global ejection fraction was calculated as the stroke volume divided by the end-diastolic volume. The percentage of fractional thickening in each of the 16 LV short-axis segments was calculated as follows: ((end-systolic wall thickness minus end-diastolic wall thickness) divided by end-diastolic wall thickness) multiplied by 100%. A segment with fractional thickening < 30% was considered hypokinetic (169). The proportion of hypokinetic segments was calculated by dividing the number of hypokinetic segments by the total number of all measured LV segments. Fractional thickening was not measured in one patient with atrial fibrillation. In addition, in 27 of 270 segments (10%), fractional thickening could not be measured due to insufficient image quality, masking of LV wall thickness by papillary muscles, or closeness of outflow tract of LV.

4.2.5.3. Analysis of first-pass MR images

For MR first-pass imaging, regions of interest for tissue segments were drawn by the same radiologist on the first-pass MR images. All of the SI versus time curves were fitted by the same physicist, who was blinded to all the clinical data of the subjects. Data points were fitted with the extended Freundlich model of the right-skewed curve with Origin 5.0 software (Microcal Software, Northampton, MA, USA) according to the following equation:

$$y = ax^{bx^{-c}}$$

where *x* is time, *y* is signal intensity, and *a*, *b*, and *c* are the fitting parameters.

Only first-pass data points (7.2 points ± 1.2 (mean ± standard deviation (SD)) were included in the fitting procedure to avoid the effect of recirculation. Maximal SI increase was determined from the fitted curves. The SI change rate was calculated as SI increase versus time. The FPR was calculated as the ratio of the SI change rate at stress to that at rest according to the following equation:

$$FPR = \frac{SI\ change\ rate_{stress}}{SI\ change\ rate_{rest}}$$

Each patient's global FPR was calculated as the mean of the segmental FPR values; the global FPR was assumed to represent an estimation of the global myocardial perfusion reserve index. If a SI curve was continuously ascending, or if it ended in plateau, the curve was excluded from the analysis.

4.2.5.4. Assessment of reproducibility of perfusion measurements

For the evaluation of intraobserver variation in the assessment of perfusion parameters, one radiologist drew new regions of interest for 30 myocardial segments 1 month after the original analysis. A physicist fitted SI versus time curves to these new data. For the evaluation of interobserver variation, 30 myocardial segments were drawn by a physicist and fitted by the radiologist.

4.2.5.5. Assessment of myocardial fibrosis by MRI

To evaluate myocardial fibrosis, LV short-axis images at the levels of tips of the mitral valve leaflets and papillary muscles were divided to anterior and posterior

septum and LV free wall. In each segment, the visually brightest and darkest regions of myocardium were selected and manually outlined. SI values in arbitrary units (AU) at these two regions and epicardial fat were measured with Cheshire v1.18 -software (Hayden Image Processing Group, Boston, MA, USA). Segmental enhancement heterogeneity was determined by subtracting the lowest SI value from the highest SI value in each segment and normalizing the difference to epicardial fat as follows:

$$\left(\frac{SI_{Highest} - SI_{Lowest}}{SI_{Epicardial\ fat}}\right) \times 100$$

Myocardial fibrosis index in MRI was calculated as the mean of the six segmental enhancement heterogeneity values. Maximal myocardial fibrosis index was the highest enhancement heterogeneity among six segments.

4.3. Assessment of cardiac adrenergic activity with ^{123}I-MIBG

In HCM patients, ^{123}I-MIBG imaging was performed during the same day as MRI. All imaging was performed with a MultiSPECT3 gamma camera (Siemens Medical Systems, Inc., Hoffman Estates, IL, USA) equipped with high-resolution collimators. A dose of 200MBq of ^{123}I-MIBG (specific activity, 26,000 MBq/mmol) (MAP Medical Technologies Oy, Helsinki, Finland) was injected into the antecubital vein during rest. The energy window of ^{123}I was set at 162 keV (150–174 keV). The first acquisition was started 15 min after injection, and the second acquisition was started 4 h later using the same image settings. An anterior planar study was acquired using a 5-min acquisition time and a 128 x 128 matrix size. During SPECT acquisition, 3 detectors (3 x 120°) acquired 30 views in 4° steps of 40 s per view with a 64 x 64 matrix size. In the healthy volunteers, imaging was done in a similar way.

To assess the ^{123}I-MIBG uptake differences between HCM patients and healthy volunteers, data of initial and delayed planar imaging were used. Similarly sized rectangular regions of interest were used, which facilitated the normalization of mean planar cardiac ^{123}I-MIBG counts by the mean upper mediastinal counts of the respective image, expressed as the heart-to-mediastinum (H/M) ratio (170). ^{123}I-MIBG washout between 15 min and 4 h was calculated as follows: ((A-B)/A)) x 100%, where A is ^{123}I-MIBG uptake in the initial image and B is ^{123}I-MIBG uptake in the delayed image. No physical decay correction of ^{123}I was applied.

To assess the association between LVH and global and segmental ^{123}I-MIBG washout, data from SPECT imaging were used. The SPECT technique overcomes the limitations related to planar imaging, such as superposition of noncardiac structures, and enables the assessment of regional radioligand uptake. The raw data of ^{123}I-MIBG SPECT were reconstructed using a Butterworth-filtered (order, 6; cutoff frequency, 0.5/cm) back projection technique. Global myocardial washout was calculated as a mean value of 4 different segmental washouts (anterior, septal, lateral and inferior myocardial regions). The utmost apical and basal slices of each region were excluded to ensure the myocardial origin of detected activities.

4.4. Laboratory tests

Venous blood samples were obtained between 07.00 and 08.00 am after a 12-hour fast. The following laboratory tests were obtained to investigate their association to LVH: hematocrit, norepinephrine, epinephrine, somatomedin, renin, aldosterone, fasting glucose and fasting insulin (171). PIIINP was collected in EDTA tubes on ice and immediately spun, and sera were analyzed with commercially available

radioimmunoassay (Orion Diagnostica, Espoo, Finland) as previously described in detail (172-175).

4.5. Statistical analysis

Parameter transformations: Because LV mass, MRI fibrosis index, isovolumic relaxation time, deceleration time, collagen turnover byproducts, plasma renin, serum aldosterone and fasting plasma insulin were not normally distributed, they were log-transformed in all statistical analyses.

Analysing data from multiple segments per patient: Because segmental wall thickness and segmental fractional thickening were measured in multiple segments per patient, the differences in segments between groups were analyzed using appropriate least square mean differences (and their corresponding p-values) estimated from the mixed model accounting for the possible dependencies of the measurements within subjects (176).

Investigating the linear association between two variables: Univariate linear regression analysis was used to investigate the association of the proportion of hypokinetic segments, ^{123}I-MIBG washout and other correlates of LVH with LV mass and LV MWT as well as the association of LV segmental end-diastolic wall thickness with fractional thickening. Univariate linear regression analysis was used also to investigate the association of PIIINP collagen markers with clinical and MRI parameters.

Investigating the linear association between multiple variables: Correlates that reached statistical significance ($P < 0.05$) in univariate analysis were included in multiple regression analysis. Multicollinearity of variables in multivariate analysis was investigated by using collinearity statistics tolerance. The tolerance limit of > 0.7 was

used for non-multicollinearity. Variables were entered or removed stepwise from the model if the probability of the F value was less than 0.05 or greater than 0.10, respectively, and R square change was used to assess the contribution of each variable to LV mass.

Analysing data with normal or near normal distribution: The independent samples t test was used to study the differences in continuous variables with normal or near normal distribution between the study groups. One-way analysis of variance followed by the Scheffé test was used to compare the values of PIIINP between MRI fibrosis tertiles and controls.

Analysing data without normal or near normal distribution: In perfusion measurements, the Mann-Whitney test was used to evaluate the differences in hemodynamic response, and FPR parameters between the groups. The Spearman correlation was used to assess the correlations within each group between LV mass index and global FPR, LV maximal end-diastolic wall thickness and global FPR, and segmental wall thickness and segmental FPR.

Investigating the equality of variation and test for linearity association: Levene's test for equality of variances was used to study the difference of LV MWT variability between HCM patients and control subjects. To assess the association between PIIINP and myocardial fibrosis tertiles, the test for linear association was used.

Mixed model analysis was performed with SAS for Windows version 8.02 (SAS Institute, Cary, NC, USA) and all other statistical analyses with SPSS for Windows version 11.5.1 (SPSS, Chicago, IL, USA). Data are presented as means ± SDs.

5. RESULTS

5.1. LVH and systolic function in MRI (Study I)

5.1.1 LV mass and volumes in MRI

The main anatomical and functional parameters in MRI study are summarized in Table 6. No statistically significant difference was seen in LV mass or LV mass index between patients with HCM and control subjects, although there was a trend towards increased LV mass in HCM patients (151 ± 57 g vs. 123 ± 32 g, P = 0.064; and 77 ± 24 g/m^2 vs. 66 ± 12 g/m^2, P = 0.099, respectively) (Fig 5A). Patients with HCM had smaller LV end-diastolic volume (Table 6). Accordingly, volume adjusted LV mass was higher in HCM patients compared to control subjects (1.27 ± 0.33 g/ml vs. 0.86 ± 0.22 g/ml, P < 0.001). LV end-systolic volume was similar in both groups, but stroke volume was smaller in patients with HCM (70 ± 24 ml vs. 90 ± 18 ml, P = 0.008).

Table 6. Left ventricular characteristics in patients with HCM and control subjects in cine MRI study

	HCM patients (n=24) Mean ± SD (Range)	Control subjects (n=17) Mean ± SD (Range)	P*
LV MWT (mm)	19.5 ± 4.9 (10 – 31)	9.7 ± 1.7 (7 – 12)	< 0.0001
LV mass (g)	151 ± 57 (80 – 313)	123 ± 32 (74 – 197)	0.064
LV EDV (ml)	122 ± 45 (71 – 287)	146 ± 25 (100 – 195)	0.038
LV ESV (ml)	52 ± 29 (33 – 176)	56 ± 15 (37 – 95)	0.565
Stroke volume (ml)	70 ± 24 (23 – 136)	90 ± 18 (47 – 118)	0.008

LV MWT, left ventricular maximal wall thickness; LV EDV, left ventricular end-diastolic volume; LV ESV, left ventricular end-systolic volume

*independent samples t-test

5.1.2. LV MWT in MRI

In patients with HCM, LV MWT was increased (19.4 ± 4.9 mm) compared to control subjects (9.7 ± 1.7 mm; P < 0.0001) (Fig 5B). In Levene's test, LV MWT was more variable in patients with HCM than in control subjects (P = 0.014) (Fig 6AB). Three of the 24 patients with the TPM1-Asp175Asn mutation had LV MWT less than 13 mm in MRI (two patients had 11 mm and one patient 10 mm). The highest LV MWT in patients with HCM was 31 mm.

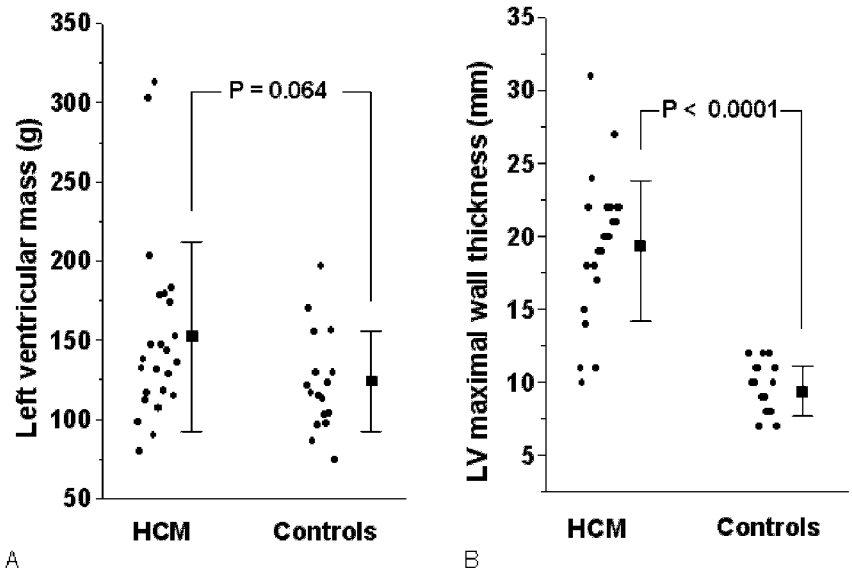

Figure 5. LV mass (A) and LV maximal wall thickness (B) by MRI in 24 patients with HCM caused by TPM1-Asp175Asn and in 17 healthy controls. A significant difference in LV maximal wall thickness between patients with HCM caused by TPM1-Asp175Asn and control subjects is demonstrated.

5.1.3. Segmental wall thickness in MRI

End-diastolic wall thickness values in 17 LV segments in patients with HCM and control subjects are summarized in Table 7. The anterior segment at basal level was the thickest segment in patients with HCM (16.8 ± 6.4 mm). Segments in the anterior septum at the basal level and inferoseptal wall at the mid-cavity level were most often hypertrophied (≥ 13 mm in 75% of patients with HCM). The anterolateral segment at the mid-cavity level was not hypertrophied in any of the HCM patients, and the apex was hypertrophied (≥ 13 mm) only in one patient.

Figure 6. End-diastolic cine MR images (TR msec/TE msec, 60/4.8; FA 20°) demonstrate a great variability in LVH between two cousins with TPM1-Asp175Asn. (A) Images in a 19-year-old man show extensive LV hypertrophy (arrows). (B) Images in a 17 year-old woman show no hypertrophy (LV maximal wall thickness 10 mm).

Table 7. LV segmental end-diastolic wall thicknesses and fractional thickening values in patients with HCM and control subjects

	HCM patients		Healthy controls	
17-segment system	End-diastolic wall thickness (mm) Mean ± SD (range)	Fractional thickening (%) Mean ± SD	End-diastolic wall thickness (mm) Mean ± SD (range)	Fractional thickening (%) Mean ± SD
Basal				
anterior	16.8 ± 6.3 (6 - 31)	30 ± 29	7.9 ± 1.6* (5 – 10)	55 ± 22†
anterolateral	8.0 ± 2.3 (5 - 15)	73 ± 34	7.2 ± 1.7 (5 – 10)	65 ± 29
inferolateral	9.6 ± 2.8 (5 - 15)	52 ± 36	7.6 ± 1.2† (5 – 10)	60 ± 24
inferior	13.6 ± 3.7 (8 - 20)	26 ± 21	9.5 ± 1.5‡ (6 – 12)	42 ± 18§
inferoseptal	11.9 ± 3.7 (6 - 19)	14 ± 14	7.9 ± 1.6‡ (6 – 10)	42 ± 23*
anteroseptal	14 ± 3.5 (9 - 22)	17 ± 13	8.4 ± 1.8* (5 – 11)	48 ± 22*
Mid-Cavity				
anterior	12.8 ± 6.2 (6 - 27)	39 ± 30	6.8 ± 1.9‡ (4 – 10)	80 ± 42‡
anterolateral	8.3 ± 1.9 (5 - 11)	69 ± 21	7.1 ± 2.1 (4 – 11)	70 ± 35
inferolateral	11 ± 4.8 (6 - 28)	52 ± 24	7.1 ± 1.8† (5 – 11)	75 ± 38§
inferior	13.7 ± 5.1 (6 - 28)	41 ± 28	9.1 ± 2.2† (6 – 12)	69 ± 24†

inferoseptal	14.8 ± 5.0 (7 - 30)	31 ± 21	8.8 ± 1.7* (6 – 11)	54 ± 21[†]
anteroseptal	13.5 ± 4.4 (6 - 21)	32 ± 21	7.2 ± 1.8* (5 – 12)	66 ± 28[‡]
Apical				
anterior	10 ± 4.1 (6 - 21)	64 ± 43	7.9 ± 2.2[§] (4 – 12)	81 ± 45[§]
lateral	10.2 ± 3.6 (6 - 22)	54 ± 30	8.1 ± 2.2[§] (5 – 12)	77 ± 32[§]
inferior	9.4 ± 2.7 (6 - 19)	61 ± 30	8.6 ± 2.0 (5 – 12)	52 ± 28
septal	11.3 ± 3.6 (6 - 20)	51 ± 25	8.1 ± 1.8 [†] (5 – 12)	62 ± 28
apex	8.5 ± 2.5 (5 - 16)		7.2 ± 1.6 (3 – 10)	
Total	11.6 ± 4.7 (5 - 31)	44 ± 32	7.9 ± 1.9[*] (3 - 12)	62 ± 31[‡]

*P < 0.0001

[†]P < 0.01

[‡]P < 0.001

[§]P < 0.05

Note.— The p-values are calculated for the least square means differences estimated from the model accounting for the dependencies of the measurements within subjects (176).

5.1.4. LV contractility by MRI

Global LV ejection fraction by MRI was similar in patients with HCM and control subjects (58 ± 7 vs. 61 ± 7%; P = 0.227). However, segmental fractional thickening values were lower in patients with HCM than in control subjects (44 ± 32% vs. 62 ± 31%; P < 0.001, respectively). Also in three patients with the TPM1-Asp175Asn mutation, but normal LV wall thickness on MRI, mean fractional thickening was decreased compared with control subjects (52 ± 26% vs. 63 ± 31%; P = 0.045). The proportion of hypokinetic segments was higher in patients with HCM compared to control subjects (37 ± 20% (range 6 – 81%) vs. 12 ± 12%, (range 0 – 31%); P < 0.0001).

In patients with HCM, most (11/16) segments had less fractional thickening than in controls. Some segments, particularly in the anterolateral and apical area, had similar fractional thickening values compared with those of control subjects (Table 7).

5.1.5. Association of LV contractility with LV mass and MWT in patients with HCM

At segmental level, LV end-diastolic wall thickness correlated negatively with fractional thickening of the segment (r = -0.741; P < 0.0001). Mean fractional thickening did not significantly correlate with LV mass (r = -0.406; P = 0.055) or LV MWT (r = 0.236; P = 0.278). However, the proportion of hypokinetic LV segments was strongly associated with LV mass (r = 0.647; P = 0.0008; Fig 7A) and LV MWT (r = 0.691; P = 0.0003; Fig 7B). If three patients with the TPM1-Asp175Asn mutation, but no LVH, and one patient with previous myectomy were excluded from the analyses, the associations between the proportion of hypokinetic segments and LV mass and LV MWT remained statistically significant (r = 0.638; P = 0.003, and r = 0.613; P = 0.005, respectively). If the proportion of hypokinetic segments was

calculated using mid-cavity segments only, the association between proportion of hypokinetic segments and LV mass and LV MWT was also significant (r = 0.605; P = 0.002 in both analyses). MR cine images in Figure 8A-D demonstrate two patients with the TPM1-Asp175Asn mutation and with the different proportion of hypokinetic segments. Patient 1 (Fig 8AB) has no LVH and only one hypokinetic segment, whereas patient 2 (Fig 8CD) has marked LV hypertrophy and numerous hypokinetic segments.

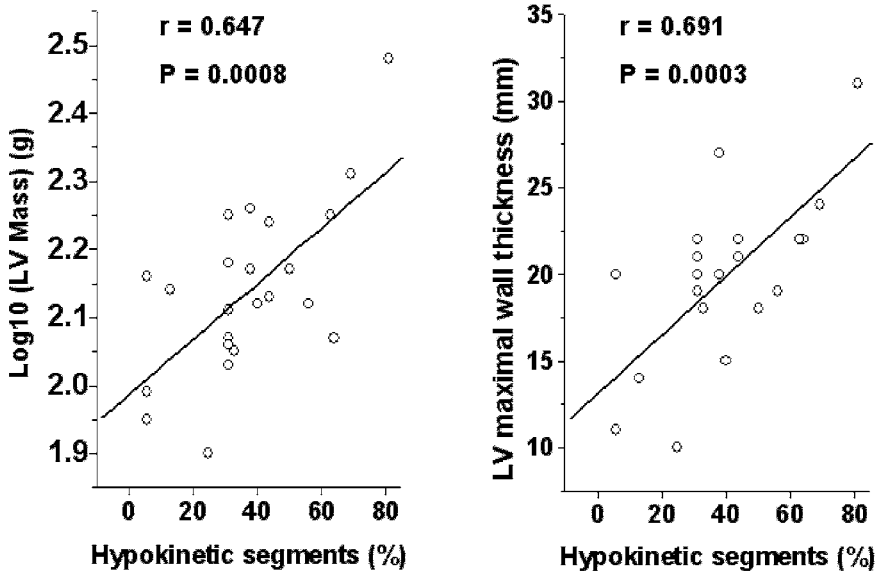

Figure 7. Association of LV mass (A) and LV maximal wall thickness (B) with the proportion of hypokinetic LV segments in patients with TPM1-Asp175Asn. The proportion of hypokinetic segments is significantly associated with LV mass and LV maximal wall thickness.

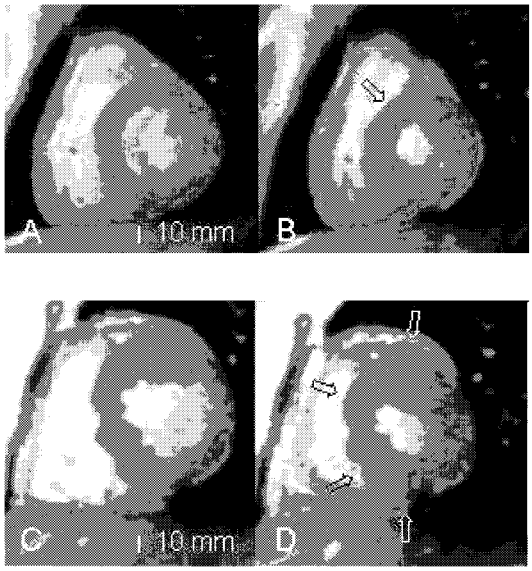

Figure 8. The short axis end-diastolic (A) and end-systolic (B) LV cine MR images (TR msec/TE msec, 60/4.8; FA 20°) in a 23-year-old man with the TPM1-Asp175Asn. The patient had mild LVH and only one hypokinetic segment (anteroseptal segment at basal level; arrow). Corresponding images (C, D) in a 22-year-old man with the TPM1-Asp175Asn and marked LVH and several hypokinetic segments (arrows). All cine images are shown as movies on web site: http://radiology.rsnajnls.org/cgi/content/full/2363041165/DC1

5.1.6. Correlates of LV mass and MWT in linear regression analysis in patients with HCM

The correlates of LV mass and LV MWT in linear regression analyses in patients with HCM are shown in Tables 8 and 9. In univariate analyses (Table 8), gender, body surface area, systolic blood pressure, LV end-diastolic and end-systolic volumes, stroke volume, the proportion of hypokinetic segments, and fasting plasma glucose were associated with LV mass. Only the proportion of hypokinetic segments was associated with LV MWT, explaining 48% of LV MWT variability ($P < 0.001$).

Table 8. Correlation coefficients of LV mass and maximal wall thickness in patients with HCM in univariate linear regression analysis

	LV mass*	LV MWT
Age	0.103	-0.148
Gender (0=female, 1=male)	0.480†	0.086
Body surface area	0.558‡	0.214
Systolic blood pressure	0.439†	0.137
Diastolic blood pressure	-0.040	-0.368
LV end-diastolic volume	0.710§	0.152
LV end-systolic volume	0.621‡	0.009
LV stroke volume	0.606‡	0.278
LV ejection fraction	-0.236	0.126
Proportion of hypokinetic LV segments	0.647§	0.691§
ACE gene polymorphism‖	0.322	0.321
Hematocrit	0.025	-0.171
Plasma norepinephrine	-0.145	-0.020
Plasma epinephrine*	-0.111	-0.220
Serum somatomedin	-0.284	-0.287
Plasma renin*	-0.101	-0.307
Serum aldosterone*	-0.097	-0.355
Plasma glucose	0.491†	-0.360
Plasma insulin*	0.214	-0.254
Glucose/Insulin ratio*	-0.008	0.214

LV, left ventricular; MWT, maximal wall thickness

*Log 10 transformed

† $P < 0.05$

‡ $P < 0.01$

§ $P < 0.001$

‖ Number of D-alleles = 0,1, or 2

To investigate which variables were independently associated with LV mass, stepwise linear regression analysis was performed. No statistically significant multicollinearity between the proportion of hypokinetic segments and other variables included in the multiple linear regression analyses was found. The best stepwise multivariate model, explaining 75% of LV mass variability, included the proportion of hypokinetic segments, LV end-diastolic volume, and male gender (Table 9). The proportion of hypokinetic segments contributed 42% ($P < 0.0001$), LV end-diastolic volume 24% ($P = 0.003$) and male gender 10% ($P = 0.014$) to LV mass variability.

Table 9. Stepwise multiple linear regression analysis of correlates of left ventricular mass in patients with HCM

	β	P
Proportion of hypokinetic segments	0.574	< 0.0001
Left ventricular end-diastolic volume	0.412	0.003
Gender (0 = female, 1 = male)	0.320	0.014

5.2. First-pass imaging (Study II)

5.2.1. Hemodynamics at rest and during adenosine stress

There was no statistically significant difference in hemodynamic response between the patients with HCM and the subjects in the rest-stress injection control group (data not shown). In all individuals who underwent adenosine stress MRI (17 patients with HCM and five control subjects), the mean heart rate increased during adenosine infusion from 67 ± 9 beats per minute to 87 ± 10 beats per minute ($P < 0.001$). The mean systolic blood pressure was 153 ± 18 mmHg at rest; it remained at the same level (156 ± 25 mmHg) during adenosine infusion ($P = 0.087$). The

corresponding values for diastolic blood pressure were 79 ± 18 mmHg and 74 ± 11 mmHg (P = 0.360). Thus, because heart rate changed, the mean rate-pressure product increased from 10,279 ± 2,057 to 13,586 ± 2,927 (P < 0.001).

5.2.2. Effect of adenosine on first-pass parameters

Figure 9 demonstrates typical SI versus times curves at rest and during adenosine stress. The effect of adenosine on first-pass parameters was studied by comparing results in the rest-stress injection control group with those in the two-injections-at-rest control group. The results are summarized in Table 10. At rest, no significant difference was observed in time-to-peak values, SI increase, or SI change rate between the rest-stress injection control group and the two-injections-at-rest control group. For the second injection, the time to peak was shorter and the SI change rate was higher in the rest-stress injection control group than in the two-injections-at-rest control group. As a result, the mean SI change rate ratio was, on average, 2.6 times higher in the rest-stress injection control group than in the two-injections-at-rest control group (1.80 ± 0.58 vs. 0.71 ± 0.16, P = 0.003).

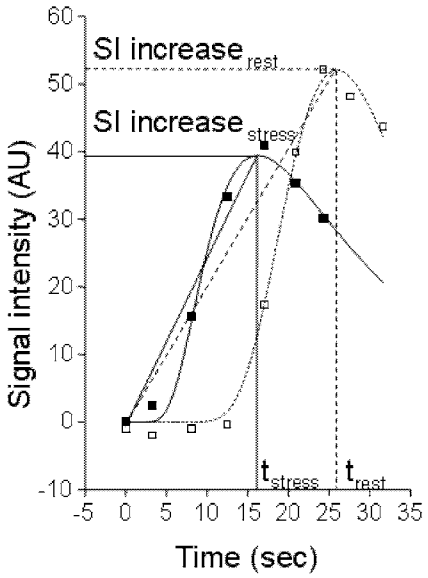

Figure 9. Graph depicts data obtained in a 48-year-old man with the TPM1-Asp175Asn, but no hypertrophy at MRI. Time is displayed along the x axis, and myocardial SI is displayed along the y axis. The curved lines show the fitted power curves. The dashed line indicates SI change rate during imaging at rest. The continuous line indicates SI change rate during adenosine stress MRI. At rest, the SI change rate (calculated as SI $increase_{rest}$ divided by t_{rest}) was 1.9 arbitrary units (AU)/sec, and during stress, the SI change rate (calculated as SI $increase_{stress}$ divided by t_{stress}) was 2.3 AU/sec, resulting in an FPR value (calculated as SI change $rate_{stress}$ divided by SI change $rate_{rest}$) of 1.2.

Table 10. Effect of adenosine on first-pass parameters in control subjects

	Two-injections-at-rest control group (n=7)	Rest-stress injection control group (n=5)	P-value*
First injection			
Time-to-peak (sec)†	13.1 ± 5.8	10.8 ± 1.3	0.639
SI increase (AU)	58 ± 15	65 ± 17	1
SI change rate (AU/sec)	5.5 ± 2.8	6.2 ± 1.6	0.755
Second injection			
Time-to-peak (sec)†	14.5 ± 4.4	6.6 ± 1.6	0.005
SI increase (AU)	46 ± 13	58 ± 12	0.202
SI change rate (AU/sec)	3.7 ± 2.0	10.1 ± 2.2	0.003
SI change rate ratio	0.71 ± 0.16	1.80 ± 0.58	0.003

AU = arbitrary units; SI = signal intensity

*Mann-Whitney test

† Time difference between the myocardial signal intensity maximum and arrival of contrast agent in the left ventricle

5.2.3. Comparison of first-pass parameters between patients with HCM and subjects in the rest-stress injection control group

Mean time-to-peak was longer in the patients with HCM than in the subjects in the rest-stress injection control group, both at rest (16.6 ± 4.0 seconds vs. 10.8 ± 1.3 seconds, P = 0.001) and during stress (11.6 ± 4.2 seconds vs. 6.6 ± 1.6 seconds, P = 0.002). At rest, the patients with HCM and the subjects in the rest-stress injection control group showed nearly equal levels of SI increase (62 ± 16 AU vs. 65 ± 17 AU, P = 0.762). During adenosine stress, however, the SI increase in the patients with HCM was lower than it was in the subjects in the rest-stress injection control group

(43 ± 13 AU vs. 58 ± 12 AU, P = 0.025). This difference did not result from a difference in baseline values between the patients with HCM and the subjects in the rest-stress injection control group, because baseline levels before the at-rest injection (15 ± 6 AU vs. 15 ± 5 AU, P = 0.866) and before the stress injection were nearly equal (35 ± 16 AU vs. 37 ± 10 AU, P = 0.933) in both groups. Due to the longer time to peak and the smaller SI increase, global FPR was smaller in the patients with HCM than in the subjects in the rest-stress injection control group (1.12 ± 0.35 vs. 1.80 ± 0.58, P = 0.015).

There was no significant difference between patients with HCM and subjects in the rest-stress injection control group in the number of segments per person that were included in the analysis (9.7 ± 2.4 vs. 9.0 ± 3.0, P = 0.704).

5.2.4. Correlation of first-pass parameters with LV hypertrophy

In patients with HCM, maximal LV wall thickness and LV mass index correlated negatively with global FPR (r = -0.723, P =0 .001 and r = -0.598, P = 0.011, Fig 10, respectively). Figure 11 demonstrates largely impaired first-pass enhancement during adenosine stress in a 22-year-old man with the TPM1-Asp175Asn and extensive LVH. In the rest-stress injection control group, no correlation between global FPR and LVH was observed (data not shown).

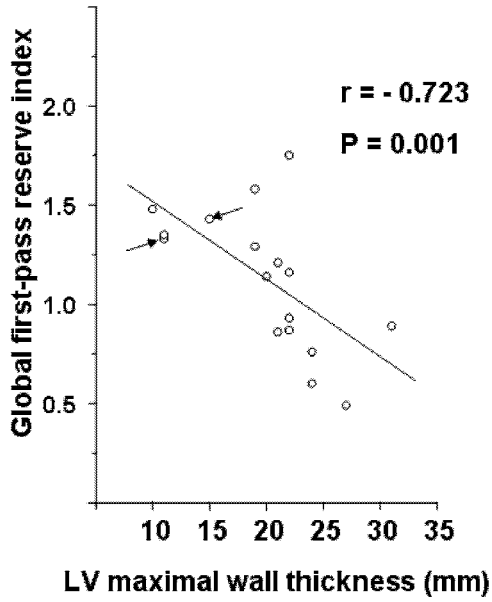

Figure 10. Scatterplot depicts the negative correlation between global FPR and maximal LV wall thickness in 17 patients with the TPM1-Asp175Asn. Arrows indicate two patients with HCM who had moderate coronary artery disease.

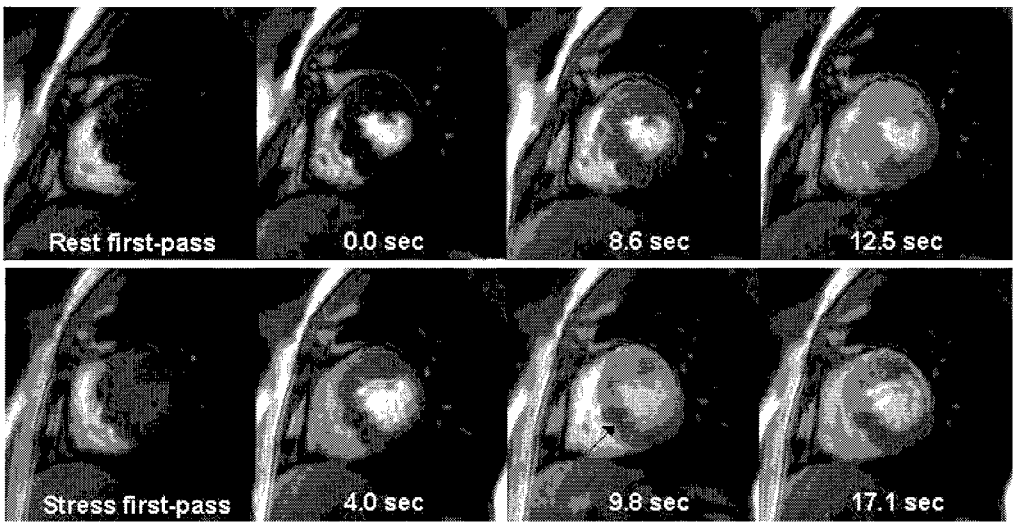

(Figure legend on the next page)

Figure 11. Images in a 22-year-old man with the TPM1-Asp175Asn and extensive LV hypertrophy. Upper row: In a series of short-axis MR images of the LV at the papillary muscle level obtained during a breath hold with the patient at rest and during the first-pass of 0.05 mmol/kg of Gd-DTPA with a turbo fast low-angle shot sequence (4.5/2.2/300, 8° flip angle, 10-mm section thickness, 250 x 250-mm field of view, and 128 x 128 matrix), the delay time for the arrival of the contrast agent in the LV blood is displayed in each image. There were no signs of impaired first-pass enhancement in this patient at rest. Lower row: A series of short-axis first-pass MR images of the same section obtained during adenosine stress shows that first-pass enhancement is markedly impaired. The poorest enhancement was observed in the hypertrophied (25-mm) posterior septum (arrow), in which the FPR was 0.2.

5.2.5. Intra- and interobserver reproducibility of MRI first-pass perfusion measurements

The results of reproducibility measurements are summarized in Table 11. The individual components of first-pass perfusion indices were highly reproducible. Reproducibility was best in the assessment of the SI increase of the first-pass curves. Because of the nature of the FPR measure (which is a combination of four indices), the reproducibility of assessments of FPR was somewhat weaker than the reproducibility of time-to-peak or SI increase values, but was still reasonably good (intraobserver $r = 0.791$, $P < 0.001$, mean difference = 0.0 ± 0.4; interobserver $r = 0.710$, $P < 0.001$, mean difference = 0.1 ± 0.4).

Table 11. Reproducibility of first-pass parameters

		Intraobserver difference			Interobserver difference		
		Mean difference*	P-value†	r‡	Mean difference*	P-value†	r‡
Rest	Time-to-peak (sec)	0.2 ± 2.1	0.556	0.844	0.1 ± 2.2	0.843	0.836
	SI increase (AU)	-1.1 ± 4.3	0.171	0.986	-0.8 ± 9.5	0.634	0.926
	SI change rate (AU/sec)	-0.5 ± 0.8	0.003	0.968	0.2 ± 1.1	0.253	0.928
Stress	Time-to-peak (sec)	-0.3 ± 1.3	0.157	0.867	-0.3 ± 1.3	0.180	0.854
	SI increase (AU)	-2.2 ± 6.5	0.071	0.964	-0.8 ± 5.6	0.456	0.975
	SI change rate (AU/sec)	0.2 ± 1.5	0.520	0.965	0.2 ± 1.7	0.532	0.950
FPR		0.0 ± 0.4	0.209	0.791	0.1 ± 0.4	0.569	0.710

AU = arbitrary units; FPR, First-pass reserve index; SI = signal intensity

*Values are the mean plus or minus SD

†Paired samples T-test

‡Pearson correlation coefficient

5.3. Myocardial fibrosis (Study III)

5.3.1. Myocardial fibrosis by MRI

If LV segments both at the levels of tips of the mitral valve leaflets and papillary muscles were selected for image analysis, no statistically significant difference was seen in the mean MRI fibrosis index between HCM patients and control subjects (5 ± 5% vs. 5 ± 4%; P = ns). However, if LV segments only at the papillary muscle level were included in the image analysis, HCM patients had a higher MRI fibrosis index than control subjects (12 ± 7 (range 3 – 31) vs. 7 ± 3% (range 0 – 13), P< 0.01 (Fig 12)). Figure 13 shows contrast-enhanced T1-weighted inversion recovery images in a 52-year-old control subject and in a 45-year-old male HCM patient with intramyocardial focal high-signal areas indicative of fibrosis.

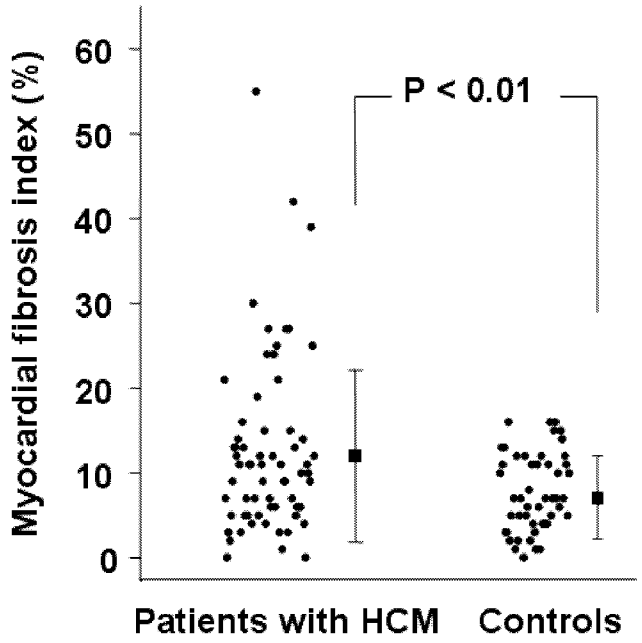

Figure 12. Graph depicts MRI fibrosis values at the papillary muscle level in patients with HCM caused by TPM1-Asp175Asn and in 17 healthy controls.

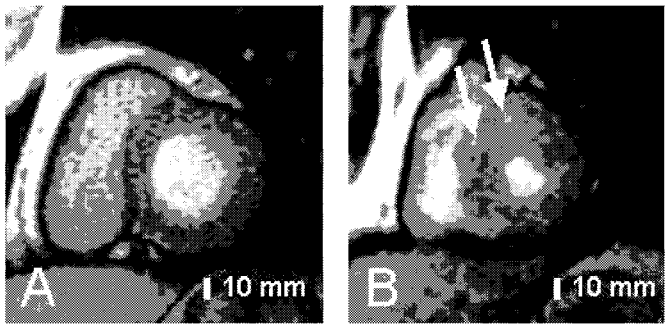

Figure 13. Contrast-enhanced T1-weighted inversion recovery images in a 52-year-old control subject (A), and in a 45-year-old male with HCM (B). Focal intramyocardial areas with a high signal indicative of fibrosis were found at the mid-ventricular level at the junction of the interventricular septum and the right ventricular free wall (arrows).

5.3.2. The PIIINP-marker of collagen metabolism and its association with MRI fibrosis index (Study III)

PIIINP levels were higher in patients with HCM than in control subjects (3.6 ± 1.3 µg/l vs. 2.8 ± 0.8 µg/l; $P < 0.05$). In patients with HCM, PIIINP levels were significantly associated with myocardial fibrosis in MRI. In HCM patients from the lowest to the highest tertile of myocardial fibrosis in MRI, the respective PIIINP values were 2.84 ± 0.94 µg/l, 3.54 ± 0.72 µg/l and 4.46 ± 1.93 µg/l ($P < 0.01$) (Fig 14). In pairwise multiple comparisons, statistically significant differences in PIIINP values were seen only between HCM patients in the highest tertile of myocardial fibrosis in MRI and controls ($P < 0.05$).

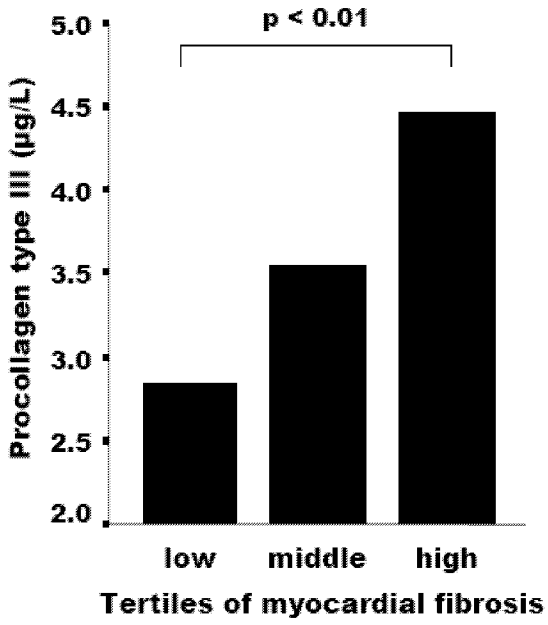

Figure 14. Graph depicts PIIINP levels in HCM patients according to tertiles of myocardial fibrosis in MRI

5.3.3. Association of clinical, invasive and MRI parameters with PIIINP in linear regression analyses

Correlates of PIIINP in univariate linear regression analyses in patients with HCM and control subjects are shown in Table 12. Age ($r = -0.565$, $P < 0.01$), diastolic blood pressure ($r = -0.443$, $P < 0.05$), LV mass index ($r = 0.439$, $P < 0.05$) and myocardial fibrosis in MRI ($r = 0.485$, $P < 0.05$; Fig 15) were significantly associated with PIIINP levels in patients with HCM. Age ($r = -0.508$, $P < 0.05$) and LV ejection fraction ($r = -0.578$, $P < 0.05$) were significantly associated with PIIINP levels in univariate regression analyses in control subjects (Table 12).

Table 12. Correlates of procollagen type III propeptide in patients with hypertrophic cardiomyopathy and control subjects in univariate linear regression analysis

	HCM Patients	Controls
Age	-0.565*	-0.508†
Systolic blood pressure	-0.146	-0.345
Diastolic blood pressure	-0.443†	-0.273
LVEDV index	0.308	-0.130
LVESV index	0.409	0.396
LV ejection fraction	-0.213	-0.578†
LV mass index ‡	0.439†	0.404
LV maximal wall thickness in MRI	0.182	0.364
Myocardial fibrosis in MRI	0.485†	-0.102
LV end-diastolic pressure	-0.392	
PCWP	0.090	
Isovolumic relaxation time‡	0.350	-0.232
Deceleration time‡	0.233	-0.406
E/A –ratio	0.143	0.164

E/A-ratio = the ratio of early-to-late ventricular filling; LV = left ventricular; LVEDV = left-ventricular end-diastolic volume; LVESV = left ventricular end-systolic volume; MRI = magnetic resonance imaging; PCWP = pulmonary-capillary wedge pressure

*P < 0.01

†P < 0.05

‡Log 10 transformed values

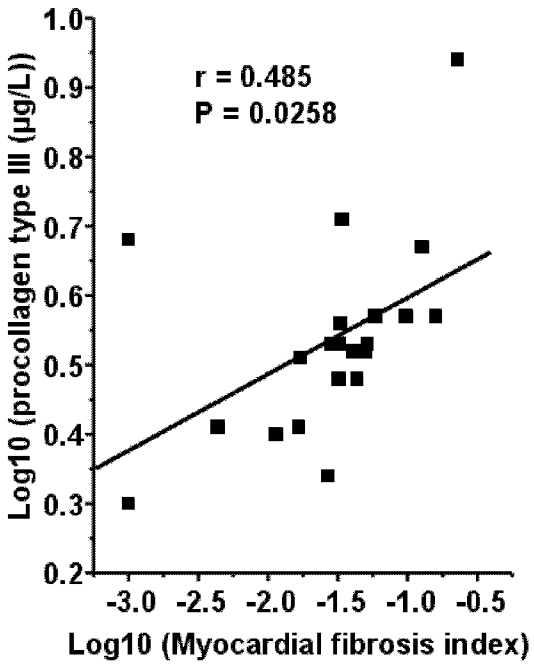

Figure 15. Logarithmic plot of MRI fibrosis index and procollagen type III amino-terminal propeptide level in patients with HCM caused by the Asp175Asn mutation of the α-tropomyosin gene.

No multicollinearity between age, diastolic blood pressure, LV mass index and myocardial fibrosis in MRI was found in patients with HCM. Thus, all above mentioned variables were entered into a stepwise multiple linear regression analysis. Only age ($\beta = -0.487$, $P < 0.05$) and myocardial fibrosis in MRI ($\beta = 0.381$, $P < 0.05$) contributed independently to PIIINP variability in patients with HCM. The model explained 46% of PIIINP variability, age contributing 32% and myocardial fibrosis in MRI 14% to the total variability. In controls, no multiple regression analysis was performed because of multicollinearity of age and ejection fraction (collinearity statistics tolerance 0.32).

5.4. Cardiac adrenergic activity in HCM patients and control subjects and its association with LVH (Study IV)

At 15 minutes, the H/M uptake ratio was similar between patients with HCM and control subjects (1.70 ± 0.15 vs. 1.67 ± 0.09, P = 0.689). At 4h, the H/M ratio was lower in HCM patients than in control subjects (1.57 ± 0.16 vs. 1.77 ± 0.20, P = 0.008). Thus, due to higher turnover of ^{123}I-MIBG, global washout was faster in HCM patients than in control subjects (50 ± 9% vs. 37 ± 8%, P = 0.001) (Fig 16).

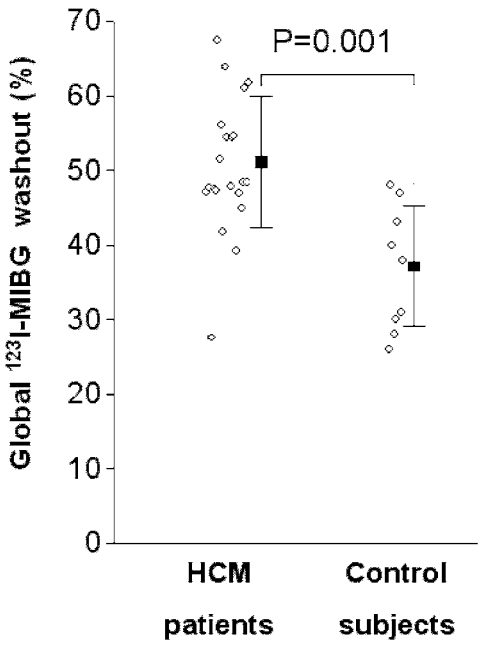

Figure 16. Global ^{123}I-MIBG washout in patients with HCM caused by Asp175Asn mutation of α-tropomyosin gene and in healthy volunteers.

In linear regression analysis, global ^{123}I-MIBG washout was associated with the LV mass index and LV maximal wall thickness index in HCM patients (r = 0.512, P = 0.018; Fig 17 and r = 0.478, P = 0.028, respectively).

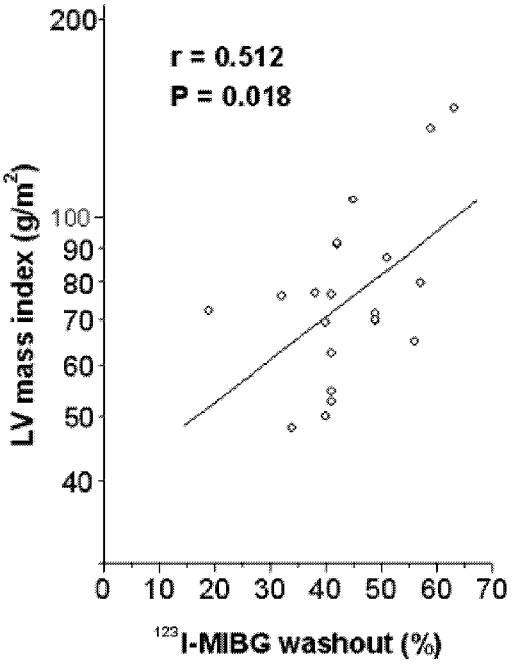

Figure 17. Linear-logarithmic plot of global ^{123}I-MIBG washout and LV mass index in patients with HCM caused by Asp175Asn mutation of α-tropomyosin gene.

6. DISCUSSION

6.1. LVH and LV systolic function on cine images

6.1.1. Assessing cardiac anatomy and systolic function by cardiac MRI

Cardiac MRI is considered the standard of reference for measurement of LV end-diastolic and end-systolic volume, mass, and ejection fraction (6, 7, 137, 177, 178). Cine MRI with a segmented k-space turbo-gradient echo technique facilitates accurate and reproducible wall thickness and thickening assessment (179, 180). Systolic wall thickening has been shown to reflect myocardial function in a single region during normal and abnormal cardiac states, and it has been shown to be more precise than wall motion analysis (181, 182). In patients with myocardial infarction, wall thickening analysis has been shown to have high specificity and moderate sensitivity for detecting dysfunctional myocardium (169).

In the present study cine MRI was shown to be a feasible method to investigate not only LVH, but also the extent of contractile impairment in HCM. Hypokinetic LV segment was defined as segment with fractional thickening < 30%. In patients with previous myocardial infarction, the mean fractional thickening in infarct-related myocardium has been shown to be 31% (169). Consequently, LV segments with fractional thickening less than 30% probably represent physiologically significant hypokinesia.

6.1.2. Myocardial contractility and its relationship with LVH in HCM

In the present study on HCM patients with the TPM1-Asp175Asn mutation, the global ejection fraction was normal, but the stroke volume was decreased. In HCM, global systolic contractility measured by ejection fraction is usually well preserved, and could be even hyperkinetic. However, global systolic function measured by using

endocardial shortening provides an overestimate of myocardial function in concentric LVH caused by arterial hypertension (183, 184). Also in patients with HCM, two MRI studies have shown that in spite of preserved global ejection fraction, regional systolic function can be impaired (127, 144). Accordingly, in the present study, regional LV contractile function measured by mean fractional thickening or the proportion of hypokinetic segments was impaired. Some LV segments, however, had normal systolic contractility in HCM patients. Variable regional systolic function is in accordance with previous studies and appears to be a characteristic feature in patients with HCM (67, 126, 127).

In the present study fractional thickening was related to the end-diastolic thickness of the segment in each LV segment, which is in accordance with the findings by Dong et al. (144). Moreover, the extent of impaired contractility measured as the proportion of hypokinetic LV segments by MRI was an independent and strongest correlate of both LV mass and LV maximal thickness. In spite of the fact that all HCM subjects of the present study shared the same causative mutation, there were marked differences in contractility and LVH in these patients. In a transgenic animal model, cardiac-specific expression of the mutant TPM1-protein has been shown to be dose-dependently associated with the extent of cardiac dysfunction (113, 185). Also in human HCM the variability of expression of mutant protein may influence myocardial contractility. The extent of cardiac systolic impairment, in turn, may activate expression of stress-responsive trophic factors, such as adrenergic mediators triggering LVH.

What is the evidence that impaired contractility precedes LVH in HCM? Both in transgenic animal models of HCM, and also in human studies, reduced myocardial contraction has been detected in disease-causing mutation carriers without LVH (42,

71, 72) and to predict later development of LVH (72). Accordingly, in the current study, LV fractional thickening by MRI was decreased in patients with the TPM1-Asp175Asn mutation, but with normal wall thickness and LV mass, supporting the notion that impaired contractility precedes LVH. However, as systolic impairment was more severe in HCM patients with marked LVH, it cannot be ruled out that severe or moderate LVH further impairs contractile function by mechanical interference between myocardial cells or increased connective tissue. Only three patients with the TPM1-Asp175Asn had normal LV wall thickness. Accordingly, larger study is needed to confirm whether systolic impairment really precedes, and initiates, development of LVH.

6.1.3. Heart morphology in HCM patients with the TPM1-Asp175Asn

TPM1-Asp175Asn is a well-established HCM-causing mutation (28, 115, 116). To our best knowledge, our study is the first to utilize cardiac MRI in the assessment of genotype-phenotype in patients with TPM1-Asp175Asn mutation. HCM caused by the TPM1-Asp175Asn mutation is characterized by highly variable LVH, as shown by present and previous studies (50, 114-116). The penetrance of this mutation in adult patients has been estimated to be 100% (50, 114-116), but in our study there were three patients of at least 17 years of age with LV maximal wall thickness less than 13 mm. Only one of the HCM patients had a maximal LV thickness over 3 cm. The septum and LV anterior free wall were the areas most often hypertrophied. Anterolateral segment at mid-cavity level was not hypertrophied in any of the HCM patients. Of global parameters, LV end-diastolic volume was smaller in HCM patients compared to controls. Further MRI studies from the other HCM patients caused by other genes are needed to show whether this phenotype is characteristic to TPM1-

Asp175Asn gene or whether it is common with other HCM causing mutations. It is important to use the same LV segmentation to obtain comparable results (17-segment model according to American Heart Assosiation recommendation for tomographic imaging modalities (167).

6.2. Measurement of myocardial perfusion by MRI

In this study, a relatively low-dose (0.05 mmol/kg) bolus of Gd-DTPA was injected into a peripheral vein, and the first-pass of the bolus was observed with an inversion-recovery gradient-echo sequence. SI versus time curves were fitted, and the SI increase, time to peak, and maximal SI increase were calculated. The segmental FPR was derived as a ratio of SI change rate values observed in the adenosine stress MRI to those observed in the MRI at rest.

Findings of impaired perfusion in patients with HCM are in concordance with positron emission tomography (95, 96, 104), Doppler echocardiography (40, 103) and velocity-encoded cine MRI (104) studies. In the current study perfusion impairment was found to be associated with the extent of LVH. This relationship has also been found in most, but not all, previous studies in patients with HCM. The present study has some improvements in design compared with previous studies. The most important advantage is that in all patients with HCM, the disease was caused by a single mutation. Accordingly, perfusion differences between phenotypes are not caused by different causative mutations, but instead are really associated with the extent of LVH. Second, the perfusion impairment was found to be associated not only with LV MWT but also with LV mass, which characterizes LVH at a more global level than LV MWT. Third, study patients of the present study included subjects with the TPM1-Asp175Asn, but no LVH (clinically healthy mutation carriers)

and also patients with marked LV hypertrophy (LV maximal wall thickness 31 mm). A large range in measured variable values improves the possibility to detect or exclude an association between variables. MRI can be recommended in perfusion studies of clinically unaffected subjects because MRI is a safe noninvasive method that facilitates measurement of perfusion without radiation exposure or use of nephrotoxic contrast agents. Quantitative perfusion estimates have been shown to have a high clinical value in HCM patients, because they are associated with prognosis, also when obtained at rest (102).

6.3. Myocardial fibrosis

6.3.1. MR imaging of fibrosis

In the present study, Gd-DTPA as a contrast agent and a T1-weighted inversion recovery sequence 15 minutes after injection of the contrast agent were used to detect myocardial fibrosis. In previous study, this method has been used to detect nonviable myocardium in patients with coronary artery disease (186). Myocardial enhancement heterogeneity, based on numerical SI values, was quantitatively measured, enabling to make comparisons between controls and HCM patients and also to investigate correlations between enhancement heterogeneity, suggestive of myocardial fibrosis, and features of cardiac phenotype in HCM patients.

Gd-DTPA contrast agent is a biologically inert tracer that distributes in the extracellular space, but is unable to cross the intact cell membrane (187-189). Normal myocardium is uniformly tightly packed with cardiomyocytes, and there is low gadolinium concentration and low signal in MRI fifteen minutes after Gd-DTPA injection. In areas of myocardial fibrosis, the extracellular compartment is expanded (190, 191), allowing contrast agent a larger space to spread out (192). In addition,

gadolinium wash out from the expanded interstitial space back to peripheral circulation is decreased (193). These conditions lead to a higher gadolinium concentration on the late enhancement scan in areas of myocardial fibrosis, which is seen as a bright signal. Gadolinium-enhanced MRI has been considered to be a unique tool to detect myocardial fibrosis, with high sensitivity, good spatial resolution, low cost and without radiation exposure, both in patients with coronary artery disease and in patients with cardiomyopathies (149-152), including HCM (151, 152).

6.3.2. Association of PIIINP values with MRI-derived LV characteristics in HCM patients with the TPM1-Asp175Asn mutation

There is only one previous study on procollagens in HCM, and there are no previous studies on myocardial fibrosis or PIIINP values in HCM patients with identified disease-causing mutations. In the study by Lombardi and coworkers, patients with HCM had increased levels of PIIINP (194). In the present study, we found also increased levels of PIIINP in patients with HCM. In contrast to the study by Lombardi and coworkers, in which PIIINP was inversely related to LV size measured as LV end-diastolic diameter, we found no relationship between PIIINP and LV volumes measured by MRI. In the present study, PIIINP levels correlated significantly with young age in both HCM patients and controls. Accordingly, normal children have been shown to have higher PIIINP values than adults, reflecting high turnover of soft tissue during childhood growth (195-197).

In HCM patients PIIINP levels were associated with myocardial fibrosis evaluated by MRI so that HCM patients without myocardial fibrosis in MRI had relatively low PIIINP values, and PIIINP levels increased linearly with increasing myocardial fibrosis. Many of the patients with the TPM1-Asp175Asn had normal myocardial

enhancement, which suggests that myocardial fibrosis is not a primary phenotype determined by the genotype. Accordingly, in a transgenic rabbit model recapitulating the phenotype of human HCM, fibrosis was not a primary phenotype (198).

6.4. Increased adrenergic activity in HCM

Many clinical features of HCM and previous studies (76-78, 199) suggest accentuated cardiac adrenergic activity in this disease. In the present study, ^{123}I-MIBG washout was faster in HCM patients with the TPM1-Asp175Asn than in healthy volunteers, which is in concordance with enhanced cardiac adrenergic activity in HCM. Moreover, in patients with HCM, global ^{123}I-MIBG washout correlated with LV mass and LV maximal wall thickness, suggesting that enhanced cardiac adrenergic activity is one factor explaining the variability of LVH in HCM patients with the TPM1-Asp175Asn. The current study has methodological advantages compared with previous studies. In this study, HCM patients represented a wide spectrum of hypertrophy, since the study group included patients with no hypertrophy, patients with mild LVH, and patients with marked LVH. In addition, LVH was measured with MRI, which allows a more accurate and more reproducible LVH evaluation than echocardiography (6, 7). Finally, all previous studies on cardiac adrenergic activity in HCM have been performed in patients who have not been genetically characterized (76-78, 199, 200). Although some of these studies have shown that adrenergic activity is associated with the extent of LVH, these findings could be explained by different genetic defects causing HCM. Namely different defects in sarcomeric genes induce LVH to a variable extent, and variable myocardial sympathetic activity might also be related to different causal mutations. In the present study, however, all patients had the same gene defect of the TPM-1 gene. Consequently, the

association between accentuated adrenergic activity and LVH shown by the present study cannot be attributed to variable causal mutations.

6.5. Insertion/deletion polymorphism of the angiotensin-I converting enzyme

We observed a positive trend between the number of D alleles of the angiotensin-I converting enzyme gene and both LV mass and LV MWT in patients with the Asp175Asn mutation in *TPM1,* but the association was not statistically significant. Although the possibility of a statistical type II error cannot be excluded, our results are in accordance with previous studies that indicate a relatively minor influence of the ACE gene polymorphism on LV hypertrophy in patients with HCM (62, 201).

The insertion/deletion polymorphism of the angiotensin-I converting enzyme is supposed to influence plasma ACE activity so that plasma ACE activity is significantly higher in individuals with the deletion allele than in individuals with the I allele. This, in turn, could activate the systemic renin-angiotensin system, which regulates sodium balance and intravascular volume and interacts with other blood pressure control mechanisms, including the sympathetic nervous system and baroreflexes (202). In other words, patients with deletion polymorphism could have increased activity of systemic renin-angiotensin system which, in turn, could induce LVH. On the other hand, the II genotype of the ACE gene has been suggested to be a risk factor for atrial fibrillation in patients with HCM (202) which could be triggered by hypotension and paradoxal peripheral vasodilatation during central volume unloading (203, 204). More studies on the relationship between ACE activity, LV mass, left atrial size and function, and peripheral vasoreactivity are needed. MRI should be employed in such studies, because it facilitates accurate measurements of LVH (137, 178), left atrium size (205) and also peripheral vasoreactivity (204).

6.6. Study limitations

6.6.1. Study subjects

The present study included a relatively limited number of HCM patients with a single causative mutation. Although most sarcomeric mutations are considered hypo-contractile (23) the findings of the present study cannot necessarily be extrapolated to all HCM-causing mutations. On the other hand, as demonstrated by the present study, an adequate number of HCM patients with an identical disease causing mutation are needed to investigate the relationship between contractility and LVH, since different causal mutations induce both contractile deficits and LVH to a variable degree.

6.6.2. Methodological limitations in cine MRI

First, when measuring LV wall thickness at end systole by cine MRI, the endocardial surface can be obliterated by papillary muscles and trabeculations. However, by observing the moving structures in cine series image by image, it is usually possible to detect the endocardium in end systole. Only a few segments had to be excluded from image analysis in the present study due to endocardial surface obliteration. Second, plane motion of the heart can lead to myocardium moving out of plane at end systole with respect to end diastole, which might disturb assessment of the relationship between contractility and LVH. To exclude this error, we investigated the relationship between LV contractility and LVH by using segments at the mid-ventricular level only, where longitudinal movement of LV is relatively minor (4 mm) (127, 144). This approach did not influence the results.

With the MRI myocardial tissue tagging method, it is possible to determine regional myocardial shortening three-dimensionally (126-128, 206, 207). Tissue

tagging images are easy to obtain, but image analysis is complicated and no commercial software packages are available. Fractional thickening analysis, in contrast, is easy to define and analysis can be performed with any software that can measure distance. Measurement of regional systolic function accurately is a great challenge in cardiac imaging. Better imaging sequences and image analysis programs and methods are still needed.

6.6.3. Limitations of MR first-pass perfusion imaging

In the current study, first-pass parameters were used to obtain a semiquantitative estimate of myocardial perfusion. With optimal conditions, as when contrast medium is injected into the left atrium, this approach has been proved to yield measurements that have a close correlation with myocardial blood flow measurements made using radiolabeled microspheres (208). This method has also been shown to be sensitive in the detection of perfusion abnormalities in patients with coronary artery disease (209, 210). However, to the best of our knowledge, the present study was the first in which the first-pass MR technique was used to depict perfusion abnormalities in patients with HCM.

The changes in parameters derived of signal-intensity versus time curves at rest and during adenosine-induced vasodilatation do not necessarily reflect alterations in perfusion only. Rather, they also reflect alterations in the systemic circulation and dispersion in the bolus of contrast agent. More importantly, during the first-pass of agent through the capillary network, about half of the agent leaks out of the vessel into the interstitial space (211, 212). Thus, the alteration in the SI increase may be due not only to altered flow, but also to changes in the interstitial space or extraction efficiency.

If one were to perform a perfusion study with both an intravascular contrast agent and a small molecular compound such as Gd-DTPA, one could possibly differentiate the specific components of perfusion malfunction, i.e. intravascular flow and extraction through the capillary network. This approach may be especially informative in patients with HCM, since the basic cause of perfusion abnormalities is unknown.

The calculated SI change rate ratio in the two-injections-at-rest control group was only 0.71 instead of the anticipated 1.00. This result implies that these methods tend to underestimate the true perfusion reserve. This is in concordance of our numerical estimates of perfusion reserve: In patients with HCM and healthy controls, the mean perfusion reserve in our study was 1.1 and 1.8, respectively, compared to 1.6 and 2.8 in previous studies (Table 3). One reason for this underestimation is probably related to the influence of residual myocardial gadolinium in the second first-pass curve. Residual gadolinium, however, can not explain the impaired slope at stress in patients with HCM, because baseline signal intensity values before rest and stress injection did not differ between HCM patients and controls. Accordingly, to reduce methodological errors in the assessment of perfusion in patients with HCM, only a single high-dose injection should be performed in a single imaging session.

6.6.4. Study limitations in the estimation of fibrosis

In linear regression analyses, the correlation coefficient between PIIINP and myocardial fibrosis was relatively low. This is not surprising because there are multiple possibilities that may weaken this correlation. First, not all PIIINP is derived from the heart (213). Second, the half-life of PIIINP is relatively short, and PIIINP levels may reflect short time alteration in collagen metabolism. Contrast-enhancement, however, represents anatomical changes and are probably more

stable (214). Third, myocardial fibrosis in HCM may comprise also other collagens, such as collagen I (215). It is also important to note, that image analysis method used does not recognize diffusely distributed myocardial fibrosis, because enhancement heterogeneity only was measured. Further studies are needed to clarify whether contrast-enhanced MRI can detect diffusely distributed fibrosis or a diffusely enlarged interstitial space, which is a common finding in cardiomyopathies according to histopathological studies (29-32). In the current study, only six LV segments and two one centimeter thick short-axis LV slices were used for image analysis. Thus measurement sample covered less than 50% of the total myocardial volume. Whole LV imaging with pixel by pixel image analysis would be preferable.

The late-enhancement imaging sequence used in the current study (single-shot Turbo-Flash with a stable 300 msec inversion time) does not represent state-of-the art sequence to detect delayed hyperenhancement (130, 151). Basically, imaging findings in the Turbo-Flash sequence are the same as in segmented inversion recovery images, but tissue contrast is clearly inferior to modern sequences (130).

6.6.5. Study limitations in the estimation of adrenergic activity and its association with LVH

In the current study, we measured cardiac adrenergic activation by using washout kinetics of ^{123}I-MIBG, which is a norepinephrine analogue. Experimental and human studies link ^{123}I-MIBG tracer activity closely to the adrenergic nervous system (216). However, further studies of the ^{123}I-MIBG kinetics at the cellular level are needed to understand the exact background of increased ^{123}I-MIBG washout in HCM.

In the current study, an association between adrenergic activity and LVH could be found. In a cross-sectional study-setting, however, the degree of confidence in the

direction and nature of causality is weaker than in a longitudinal study. However, other results support the conception that adrenergic activity could cause LVH. For example, without endogenous norepinephrine and epinephrine (neurotransmitters of adrenergic system) no activation in the pathways signaling LVH occur (217). In addition, transgenic mice lacking both $G\alpha_q$ and $G\alpha_{11}$ in cardiomyocytes, receptors coupled to endothelin-1, norepinephrine or angiotensin II, a complete lack of LVH in response to pressure overload has been found (218). In contrast, to our best knowledge, no studies have indicated that LVH induces enhanced adrenergic activity.

6.7. Clinical implications

6.7.1. Association of contractile impairment and adrenergic activity with LVH

The extent of myocardial contractile impairment by cine MRI was a strong correlate of LV hypertrophy, supporting the concept that LVH in HCM is secondary. The notion that cardiac adrenergic activity is associated with LVH in genetically identical patients is a novel finding that raises new questions. For example, could LVH be prevented by modifying sympathetic activity in HCM?

6.7.2. Myocardial ischemia in HCM

The role of myocardial perfusion in the evaluation risk for sudden cardiac death has been investigated in one study (102). In that study, impaired capability to increase myocardial perfusion during drug-induced vasodilation was found to be a risk factor for sudden cardiac death in patients with HCM (102). First-pass MR perfusion imaging is a widely available noninvasive method to measure myocardial perfusion without ionizing radiation. This facilitates the use of perfusion measurement

in the risk stratification of HCM patients. This could be useful especially in patients with an intermediate risk (patients with one intermediate or weak risk factor) after assessment of conventional clinical risk factors. However, prospective studies of the importance of the MRI-derived perfusion abnormalities are needed before MRI perfusion imaging can be used routinely in the clinic.

In previous studies, the extent of LV hypertrophy seems to be related to the risk of sudden cardiac death (49, 219, 220). In the current study, a strong association between LVH and impaired stress perfusion was found. Accordingly, the present study suggests that one factor explaining the increased risk of sudden death in patients with HCM and severe LV hypertrophy might be myocardial ischemia.

6.7.3. Myocardial fibrosis in HCM

Prevention of fibrosis formation might be a target for the treatment of patients with HCM. Two animal studies have suggested that myocardial fibrosis in HCM might be reversible. Angiotensin II blockade by losartan reversed interstitial fibrosis in hearts of transgenic cTnT-Q^{92} mice (221). Simvastatin, which inhibits angiotensin II–mediated myocyte hypertrophy (222, 223), induced regression of hypertrophy and fibrosis in transgenic β-myosin heavy chain-Q^{403} rabbits (224). Human studies have been lacking so far, but are needed to investigate whether myocardial fibrosis in HCM, as evaluated quantitatively by MRI, could be prevented or diminished by drugs.

7. SUMMARY AND CONCLUSIONS

The main findings of the present study were as follows:

1) Despite the fact HCM was caused by the same causal mutation in all study subjects, LVH varied from normal to severe. The proportion of hypokinetic segments was increased in HCM patients with TPM1-Asp175Asn. Moreover, the proportion of hypokinetic segments was the only correlate of LV MWT, and the most important correlate of LV mass, explaining 48% and 42% of LV MWT and LV mass variability, respectively.

2) Detection of perfusion abnormalities in patients with HCM with the first-pass MRI technique is feasible. The global FPR was decreased in patients with HCM, indicating that the ability to increase myocardial perfusion during adenosine-induced maximal vasodilatation is impaired in these patients. In addition, global FPR impairment was associated with the extent of LVH in patients with HCM. Because HCM was caused by an identical gene defect in all study patients, the perfusion impairment in HCM in this study was related not to the genotype, but to the phenotype — in other words, to the extent of LVH.

3) The myocardium was enhanced heterogeneously by Gd-DTPA in patients with HCM caused by TPM1-Asp175Asn. The heterogeneity was associated with increased levels of PIIINP, indicating that enhancement heterogeneity is associated with a fibrotic process in the heart.

4) ^{123}I-MIBG washout was augmented in HCM patients with the TPM1-Asp175Asn indicating enhanced cardiac adrenergic activity in HCM. Moreover, in patients with HCM, global ^{123}I-MIBG washout correlated with the LV mass

and LV maximal wall thickness, supporting the hypothesis that cardiac adrenergic activity is a hypertrophy-modifying factor in HCM.

To conclude, cine MRI is a feasible method to detect not only LV hypertrophy but also the extent of contractile impairment in HCM. In patients with HCM caused by the Asp175Asn mutation in the α-tropomyosin gene, LV hypertrophy and segmental contractility are highly variable, and the extent of the myocardial contractile impairment is a strong correlate of LV hypertrophy. First-pass MR perfusion imaging is a promising method that may have the role in the risk stratification of HCM patients. Enhancement heterogeneity in HCM is related to altered collagen metabolism, indicating that enhancement heterogeneity on MRI reflects a myocardial fibrotic process in patients with HCM. Finally, increased cardiac adrenergic drive, possibly induced by systolic hypokinesia, is associated with LVH, indicating that adrenergic activity modifies LVH in HCM. Figure 18 summarizes the hypothesis for the pathogenesis of HCM supported by findings of the present study.

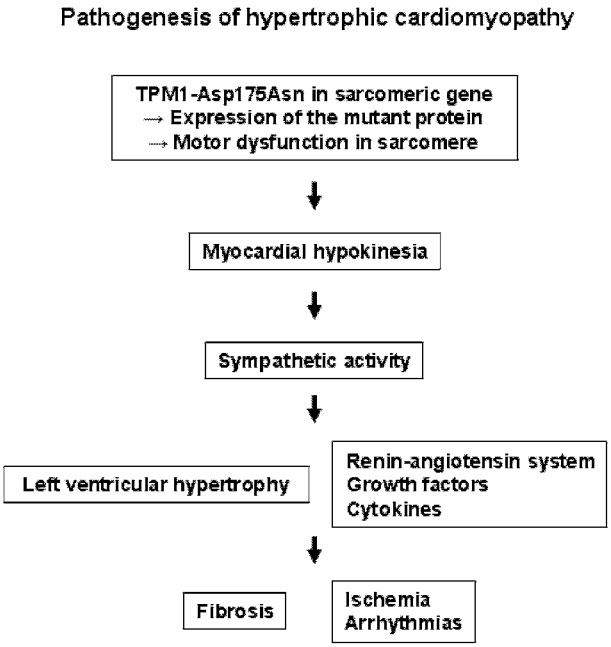

Figure 18. Hypothesis for the pathogenesis of hypertrophic cardiomyopathy phenotypes.

The present study shows that MRI can without radiation exposure provide a noninvasive and multispectral characterization of cardiac anatomy and function in patients with HCM. Cardiac MRI can be used not only in the characterization of individual patients with HCM, but also in the examination of pathophysiology of HCM, especially when cardiac MRI data is interpreted in conjunction with functional data provided by scintigraphic imaging.

8. REFERENCES

1. Wigle ED, Rakowski H, Kimball BP, Williams WG. Hypertrophic cardiomyopathy. Clinical spectrum and treatment. Circulation 1995;92(7):1680-92.
2. Spirito P, Seidman CE, McKenna WJ, Maron BJ. The management of hypertrophic cardiomyopathy. N Engl J Med 1997;336(11):775-85.
3. Maron BJ. Hypertrophic cardiomyopathy: a systematic review. JAMA 2002;287(10):1308-20.
4. Marian AJ, Roberts R. The molecular genetic basis for hypertrophic cardiomyopathy. J Mol Cell Cardiol 2001;33(4):655-70.
5. Niimura H, Patton KK, McKenna WJ, Soults J, Maron BJ, Seidman JG, et al. Sarcomere protein gene mutations in hypertrophic cardiomyopathy of the elderly. Circulation 2002;105(4):446-51.
6. Allison JD, Flickinger FW, Wright JC, Falls DGd, Prisant LM, VonDohlen TW, et al. Measurement of left ventricular mass in hypertrophic cardiomyopathy using MRI: comparison with echocardiography. Magn Reson Imaging 1993;11(3):329-34.
7. Posma JL, Blanksma PK, van der Wall EE, Hamer HP, Mooyaart EL, Lie KI. Assessment of quantitative hypertrophy scores in hypertrophic cardiomyopathy: magnetic resonance imaging versus echocardiography. Am Heart J 1996;132(5):1020-27.
8. Higgins CB, Byrd BF III, Stark D, McNamara M, Lanzer P, Lipton MJ, et al. Magnetic resonance imaging in hypertrophic cardiomyopathy. Am J Cardiol 1985;55(9):1121-26.

9. Park JH, Kim YM, Chung JW, Park YB, Han JK, Han MC. MR imaging of hypertrophic cardiomyopathy. Radiology 1992;185(2):441-46.

10. Hallopeau L. Rétrécissement ventriculo-aortique. Gaz Med Paris 1869;24:683-84.

11. Liouville H. Rétrécissement cardiaque sous aortique. Gaz Med Paris 1869;24:161-63.

12. Schmincke A. Ueber linksseitige muskulose Conusstenosen. Dtsch Med Wochenschr 1907;33:2082.

13. Brock R. Functional obstruction of the left ventricle; acquired aortic subvalvar stenosis. Guys Hosp Rep 1957;106(4):221-38.

14. Teare D. Asymmetrical hypertrophy of the heart in young adults. Br Heart J 1958;20(1):1-8.

15. Maron BJ, McKenna WJ, Danielson GK, Kappenberger LJ, Kuhn HJ, Seidman CE, et al. American College of Cardiology/European Society of Cardiology clinical expert consensus document on hypertrophic cardiomyopathy: A report of the American College of Cardiology Foundation Task Force on clinical expert consensus documents and the European Society of Cardiology committee for practice guidelines. J Am Coll Cardiol 2003;42(9):1687-1713.

16. Maron BJ, Gardin JM, Flack JM, Gidding SS, Kurosaki TT, Bild DE. Prevalence of hypertrophic cardiomyopathy in a general population of young adults. Echocardiographic analysis of 4111 subjects in the CARDIA Study. Coronary Artery Risk Development in (Young) Adults. Circulation 1995;92(4):785-89.

17. Maron BJ, Mathenge R, Casey SA, Poliac LC, Longe TF. Clinical profile of hypertrophic cardiomyopathy identified de novo in rural communities. Journal of the American College of Cardiology 1999;33(6):1590-95.

18. Maron BJ, Spirito P, Roman MJ, Paranicas M, Okin PM, Best LG, et al. Prevalence of hypertrophic cardiomyopathy in a population-based sample of American indians aged 51 to 77 years (the Strong Heart Study),. The American Journal of Cardiology 2004;93(12):1510-14.

19. Zou Y, Song L, Wang Z, Ma A, Liu T, Gu H, et al. Prevalence of idiopathic hypertrophic cardiomyopathy in China: a population-based echocardiographic analysis of 8080 adults. The American Journal of Medicine 2004;116(1):14-18.

20. Maron BJ, Peterson EE, Maron MS, Peterson JE. Prevalence of hypertrophic cardiomyopathy in an outpatient population referred for echocardiographic study. Am J Cardiol 1994;73(8):577-80.

21. McKenna WJ, Spirito P, Desnos M, Dubourg O, Komajda M. Experience from clinical genetics in hypertrophic cardiomyopathy: proposal for new diagnostic criteria in adult members of affected families. Heart 1997;77(2):130-32.

22. Maron BJ, Moller JH, Seidman CE, Vincent GM, Dietz HC, Moss AJ, et al. Impact of laboratory molecular diagnosis on contemporary diagnostic criteria for genetically transmitted cardiovascular diseases: hypertrophic Cardiomyopathy, long-QT Syndrome, and Marfan syndrome : a statement for healthcare professionals from the Councils on Clinical Cardiology, Cardiovascular Disease in the Young, and Basic Science, American Heart Association. Circulation 1998;98(14):1460-71.

23. Fatkin D, Graham RM. Molecular mechanisms of inherited cardiomyopathies. Physiol. Rev. 2002;82(4):945-80.

24. Morner S, Richard P, Kazzam E, Hellman U, Hainque B, Schwartz K, et al. Identification of the genotypes causing hypertrophic cardiomyopathy in northern Sweden. J Mol Cell Cardiol 2003;35(7):841-49.

25. Elliott P, McKenna WJ. Hypertrophic cardiomyopathy. The Lancet 2004;363(9424):1881-91.

26. Perrot A, Schmidt-Traub H, Hoffmann B, Prager M, Bit-Avragim N, Rudenko RI, et al. Prevalence of cardiac β-myosin heavy chain gene mutations in patients with hypertrophic cardiomyopathy. J Mol Med 2005;83(6):468-77.

27. Jääskeläinen P, Kuusisto J, Miettinen R, Kärkkäinen P, Kärkkäinen S, Heikkinen S, et al. Mutations in the cardiac myosin-binding protein C gene are the predominant cause of familial hypertrophic cardiomyopathy in eastern Finland. J Mol Med 2002;80(7):412-22.

28. Jääskeläinen P, Soranta M, Miettinen R, Saarinen L, Pihlajamäki J, Silvennoinen K, et al. The cardiac β-myosin heavy chain gene is not the predominant gene for hypertrophic cardiomyopathy in the Finnish population. J Am Coll Cardiol 1998;32(6):1709-16.

29. Iida K, Yutani C, Imakita M, Ishibashi-Ueda H. Comparison of percentage area of myocardial fibrosis and disarray in patients with classical form and dilated phase of hypertrophic cardiomyopathy. J Cardiol 1998;32(3):173-80.

30. Shirani J, Pick R, Roberts WC, Maron BJ. Morphology and significance of the left ventricular collagen network in young patients with hypertrophic cardiomyopathy and sudden cardiac death. J Am Coll Cardiol 2000;35(1):36-44.

31. Varnava AM, Elliott PM, Sharma S, McKenna WJ, Davies MJ. Hypertrophic cardiomyopathy: the interrelation of disarray, fibrosis, and small vessel disease. Heart 2000;84(5):476-82.

32. Tanaka M, Fujiwara H, Onodera T, Wu DJ, Hamashima Y, Kawai C. Quantitative analysis of myocardial fibrosis in normals, hypertensive hearts, and hypertrophic cardiomyopathy. Br Heart J 1986;55(6):575-81.

33. Varnava AM, Elliott PM, Baboonian C, Davison F, Davies MJ, McKenna WJ. Hypertrophic cardiomyopathy: histopathological features of sudden death in cardiac troponin T disease. Circulation 2001;104(12):1380-1384.

34. Varnava AM, Elliott PM, Mahon N, Davies MJ, McKenna WJ. Relation between myocyte disarray and outcome in hypertrophic cardiomyopathy. Am J Cardiol 2001;88(3):275-9.

35. Maron BJ, Wolfson JK, Epstein SE, Roberts WC. Intramural ("small vessel") coronary artery disease in hypertrophic cardiomyopathy. J Am Coll Cardiol 1986;8(3):545-57.

36. Davies MJ. The current status of myocardial disarray in hypertrophic cardiomyopathy. Br Heart J 1984;51(4):361-3.

37. Maron BJ, Anan TJ, Roberts WC. Quantitative analysis of the distribution of cardiac muscle cell disorganization in the left ventricular wall of patients with hypertrophic cardiomyopathy. Circulation 1981;63(4):882-94.

38. Maron BJ, Wolfson JK, Roberts WC. Relation between extent of cardiac muscle cell disorganization and left ventricular wall thickness in hypertrophic cardiomyopathy. Am J Cardiol 1992;70(7):785-90.

39. Tanaka M, Fujiwara H, Onodera T, Wu DJ, Matsuda M, Hamashima Y, et al. Quantitative analysis of narrowings of intramyocardial small arteries in normal

hearts, hypertensive hearts, and hearts with hypertrophic cardiomyopathy. Circulation 1987;75(6):1130-39.

40. Krams R, Kofflard MJ, Duncker DJ, Von Birgelen C, Carlier S, Kliffen M, et al. Decreased coronary flow reserve in hypertrophic cardiomyopathy is related to remodeling of the coronary microcirculation. Circulation 1998;97(3):230-33.

41. Hagege AA, Dubourg O, Desnos M, Mirochnik R, Isnard G, Bonne G, et al. Familial hypertrophic cardiomyopathy. Cardiac ultrasonic abnormalities in genetically affected subjects without echocardiographic evidence of left ventricular hypertrophy. Eur Heart J 1998;19(3):490-99.

42. Nagueh SF, Bachinski LL, Meyer D, Hill R, Zoghbi WA, Tam JW, et al. Tissue Doppler imaging consistently detects myocardial abnormalities in patients with hypertrophic cardiomyopathy and provides a novel means for an early diagnosis before and independently of hypertrophy. Circulation 2001;104(2):128-30.

43. Maron BJ, Spirito P, Wesley Y, Arce J. Development and progression of left ventricular hypertrophy in children with hypertrophic cardiomyopathy. N Engl J Med 1986;315(10):610-14.

44. Maron BJ, Niimura H, Casey SA, Soper MK, Wright GB, Seidman JG, et al. Development of left ventricular hypertrophy in adults in hypertrophic cardiomyopathy caused by cardiac myosin-binding protein C gene mutations. J Am Coll Cardiol 2001;38(2):315-21.

45. Maron BJ, Casey SA, Poliac LC, Gohman TE, Almquist AK, Aeppli DM. Clinical course of hypertrophic cardiomyopathy in a regional united states cohort. JAMA 1999;281(7):650-55.

46. Roberts R, Sigwart U. New concepts in hypertrophic cardiomyopathies, part I. Circulation 2001;104(17):2113-16.

47. Autore C, Conte MR, Piccininno M, Bernabo P, Bonfiglio G, Bruzzi P, et al. Risk associated with pregnancy in hypertrophic cardiomyopathy. J Am Coll Cardiol 2002;40(10):1864-69.

48. Maron BJ, Olivotto I, Spirito P, Casey SA, Bellone P, Gohman TE, et al. Epidemiology of hypertrophic cardiomyopathy-related death : Revisited in a large non-referral-based patient population. Circulation 2000;102(8):858-64.

49. Elliott PM, Poloniecki J, Dickie S, Sharma S, Monserrat L, Varnava A, et al. Sudden death in hypertrophic cardiomyopathy: identification of high risk patients. J Am Coll Cardiol 2000;36(7):2212-18.

50. Watkins H, McKenna WJ, Thierfelder L, Suk HJ, Anan R, O'Donoghue A, et al. Mutations in the genes for cardiac troponin T and α-tropomyosin in hypertrophic cardiomyopathy. N Engl J Med 1995;332(16):1058-64.

51. Moolman JC, Corfield VA, Posen B, Ngumbela K, Seidman C, Brink PA, et al. Sudden death due to troponin T mutations. J Am Coll Cardiol 1997;29(3):549-55.

52. Yetman AT, Hamilton RM, Benson LN, McCrindle BW. Long-term outcome and prognostic determinants in children with hypertrophic cardiomyopathy. J Am Coll Cardiol 1998;32(7):1943-50.

53. Olivotto I, Cecchi F, Casey SA, Dolara A, Traverse JH, Maron BJ. Impact of atrial fibrillation on the clinical course of hypertrophic cardiomyopathy. Circulation 2001;104(21):2517-24.

54. Maron BJ, Shen WK, Link MS, Epstein AE, Almquist AK, Daubert JP, et al. Efficacy of implantable cardioverter-defibrillators for the prevention of sudden

death in patients with hypertrophic cardiomyopathy. N Engl J Med 2000;342(6):365-73.

55. Östman-Smith I, Wettrell G, Riesenfeld T. A cohort study of childhood hypertrophic cardiomyopathy: improved survival following high-dose β-adrenoceptor antagonist treatment. J Am Coll Cardiol 1999;34(6):1813-22.

56. Roberts R, Sigwart U. New concepts in hypertrophic cardiomyopathies, part II. Circulation 2001;104(18):2249-52.

57. Roberts R, Sigwart U. Current concepts of the pathogenesis and treatment of hypertrophic cardiomyopathy. Circulation 2005;112(2):293-96.

58. Yamada M, Elliott PM, Kaski JC, Prasad K, Gane JN, Lowe CM, et al. Dipyridamole stress thallium-201 perfusion abnormalities in patients with hypertrophic cardiomyopathy. Relationship to clinical presentation and outcome. Eur Heart J 1998;19(3):500-07.

59. Ho H-H, Lee KLF, Lau C-P, Tse H-F. Clinical characteristics of and long-term outcome in chinese patients with hypertrophic cardiomyopathy. The American Journal of Medicine 2004;116(1):19-23.

60. Marian AJ. Modifier genes for hypertrophic cardiomyopathy. Curr Opin Cardiol 2002;17(3):242-52.

61. Marian AJ. Pathogenesis of diverse clinical and pathological phenotypes in hypertrophic cardiomyopathy. Lancet 2000;355(9197):58-60.

62. Lechin M, Quinones MA, Omran A, Hill R, Yu QT, Rakowski H, et al. Angiotensin-I converting enzyme genotypes and left ventricular hypertrophy in patients with hypertrophic cardiomyopathy. Circulation 1995;92(7):1808-12.

63. Tesson F, Dufour C, Moolman JC, Carrier L, al-Mahdawi S, Chojnowska L, et al. The influence of the angiotensin I converting enzyme genotype in familial

hypertrophic cardiomyopathy varies with the disease gene mutation. J Mol Cell Cardiol 1997;29(2):831-38.

64. Ortlepp JR, Vosberg HP, Reith S, Ohme F, Mahon NG, Schroder D, et al. Genetic polymorphisms in the renin-angiotensin-aldosterone system associated with expression of left ventricular hypertrophy in hypertrophic cardiomyopathy: a study of five polymorphic genes in a family with a disease causing mutation in the myosin binding protein C gene. Heart 2002;87(3):270-75.

65. Kaul S, Tei C, Shah PM. Interventricular septal and free wall dynamics in hypertrophic cardiomyopathy. J Am Coll Cardiol 1983;1(4):1024-30.

66. Cohen M, Cooperman L, Rosenblum R. Regional myocardial function in idiopathic hypertrophic subaortic stenosis. An echocardiographic study. Circulation 1975;52(5):842-47.

67. Betocchi S, Hess OM, Losi MA, Nonogi H, Krayenbuehl HP. Regional left ventricular mechanics in hypertrophic cardiomyopathy. Circulation 1993;88:2206-14.

68. Pouleur H, Rousseau MF, van Eyll C, Brasseur LA, Charlier AA. Force-velocity-length relations in hypertrophic cardiomyopathy: evidence of normal or depressed myocardial contractility. Am J Cardiol 1983;52(7):813-17.

69. Hattori M, Aoki T, Sekioka K. Differences in direction-dependent shortening of the left ventricular wall in hypertrophic cardiomyopathy and in systemic hypertension. Am J Cardiol 1992;70(15):1326-32.

70. Gibson DG, Sanderson JE, Traill TA, Brown DJ, Goodwin JF. Regional left ventricular wall movement in hypertrophic cardiomyopathy. Br Heart J 1978;40(12):1327-33.

71. Nagueh SF, Kopelen HA, Lim D-S, Zoghbi WA, Quinones MA, Roberts R, et al. Tissue Doppler imaging consistently detects myocardial contraction and relaxation abnormalities, irrespective of cardiac hypertrophy, in a transgenic rabbit model of human hypertrophic cardiomyopathy. Circulation 2000;102(12):1346-50.

72. Nagueh SF, McFalls J, Meyer D, Hill R, Zoghbi WA, Tam JW, et al. Tissue Doppler imaging predicts the development of hypertrophic cardiomyopathy in subjects with subclinical disease. Circulation 2003;108(4):395-98.

73. McMahon CJ, Nagueh SF, Pignatelli RH, Denfield SW, Dreyer WJ, Price JF, et al. Characterization of left ventricular diastolic function by tissue Doppler imaging and clinical status in children with hypertrophic cardiomyopathy. Circulation 2004;109(14):1756-62.

74. Kuo DC, Oravitz JJ, DeGroat WC. Tracing of afferent and efferent pathways in the left inferior cardiac nerve of the cat using retrograde and transganglionic transport of horseradish peroxidase. Brain Res 1984;321(1):111-18.

75. Taylor EW, Jordan D, Coote JH. Central control of the cardiovascular and respiratory systems and their interactions in vertebrates. Physiol. Rev. 1999;79(3):855-916.

76. Lefroy DC, de Silva R, Choudhury L, Uren NG, Crake T, Rhodes CG, et al. Diffuse reduction of myocardial β-adrenoceptors in hypertrophic cardiomyopathy: a study with positron emission tomography. J Am Coll Cardiol 1993;22(6):1653-60.

77. Li ST, Tack CJ, Fananapazir L, Goldstein DS. Myocardial perfusion and sympathetic innervation in patients with hypertrophic cardiomyopathy. J Am Coll Cardiol 2000;35(7):1867-73.

78. Schäfers M, Dutka D, Rhodes CG, Lammertsma AA, Hermansen F, Schober O, et al. Myocardial presynaptic and postsynaptic autonomic dysfunction in hypertrophic cardiomyopathy. Circ Res 1998;82(1):57-62.

79. Kline RC, Swanson DP, Wieland DM, Thrall JH, Gross MD, Pitt B, et al. Myocardial imaging in man with I-123 meta-iodobenzylguanidine. J Nucl Med 1981;22(2):129-32.

80. Henderson EB, Kahn JK, Corbett JR, Jansen DE, Pippin JJ, Kulkarni P, et al. Abnormal I-123 metaiodobenzylguanidine myocardial washout and distribution may reflect myocardial adrenergic derangement in patients with congestive cardiomyopathy. Circulation 1988;78(5 Pt 1):1192-99.

81. Morimoto S, Terada K, Keira N, Satoda M, Inoue K, Tatsukawa H, et al. Investigation of the relationship between regression of hypertensive cardiac hypertrophy and improvement of cardiac sympathetic nervous dysfunction using iodine-123 metaiodobenzylguanidine myocardial imaging. Eur J Nucl Med 1996;23(7):756-61.

82. Terai H, Shimizu M, Ino H, Yamaguchi M, Uchiyama K, Oe K, et al. Changes in cardiac sympathetic nerve innervation and activity in pathophysiologic transition from typical to end-stage hypertrophic cardiomyopathy. J Nucl Med 2003;44(10):1612-17.

83. Elliott PM, Sharma S, Varnava A, Poloniecki J, Rowland E, McKenna WJ. Survival after cardiac arrest or sustained ventricular tachycardia in patients with hypertrophic cardiomyopathy. Journal of the American College of Cardiology 1999;33(6):1596-1601.

84. Weiss MB, Ellis K, Sciacca RR, Johnson LL, Schmidt DH, Cannon PJ. Myocardial blood flow in congestive and hypertrophic cardiomyopathy:

relationship to peak wall stress and mean velocity of circumferential fiber shortening. Circulation 1976;54(3):484-94.

85. Rubin KA, Morrison J, Padnick MB, Binder AJ, Chiaramida S, Margouleff D, et al. Idiopathic hypertrophic subaortic stenosis: evaluation of anginal symptoms with thallium-201 myocardial imaging. Am J Cardiol 1979;44(6):1040-45.

86. Hanrath P, Mathey D, Montz R, Thiel U, Vorbringer H, Kupper W, et al. Myocardial thallium 201 imaging in hypertrophic obstructive cardiomyopathy. Eur Heart J 1981;2(3):177-85.

87. Yoshida N, Ikeda H, Wada T, Matsumoto A, Maki S, Muro A, et al. Exercise-induced abnormal blood pressure responses are related to subendocardial ischemia in hypertrophic cardiomyopathy. J Am Coll Cardiol 1998;32(7):1938-42.

88. O'Gara PT, Bonow RO, Maron BJ, Damske BA, Van Lingen A, Bacharach SL, et al. Myocardial perfusion abnormalities in patients with hypertrophic cardiomyopathy: assessment with thallium-201 emission computed tomography. Circulation 1987;76(6):1214-23.

89. Cannon RO, Dilsizian V, O'Gara PT, Udelson JE, Schenke WH, Quyyumi A, et al. Myocardial metabolic, hemodynamic, and electrocardiographic significance of reversible thallium-201 abnormalities in hypertrophic cardiomyopathy. Circulation 1991;83(5):1660-67.

90. Udelson JE, Bonow RO, O'Gara PT, Maron BJ, Van Lingen A, Bacharach SL, et al. Verapamil prevents silent myocardial perfusion abnormalities during exercise in asymptomatic patients with hypertrophic cardiomyopathy. Circulation 1989;79(5):1052-60.

91. Takata J, Counihan PJ, Gane JN, Doi Y, Chikamori T, Ozawa T, et al. Regional thallium-201 washout and myocardial hypertrophy in hypertrophic cardiomyopathy and its relation to exertional chest pain. Am J Cardiol 1993;72(2):211-17.

92. von Dohlen TW, Prisant LM, Frank MJ. Significance of positive or negative thallium-201 scintigraphy in hypertrophic cardiomyopathy. Am J Cardiol 1989;64(8):498-503.

93. Dilsizian V, Bonow RO, Epstein SE, Fananapazir L. Myocardial ischemia detected by thallium scintigraphy is frequently related to cardiac arrest and syncope in young patients with hypertrophic cardiomyopathy. J Am Coll Cardiol 1993;22(3):796-804.

94. Cannon RO, Dilsizian V, O'Gara PT, Udelson JE, Tucker E, Panza JA, et al. Impact of surgical relief of outflow obstruction on thallium perfusion abnormalities in hypertrophic cardiomyopathy. Circulation 1992;85(3):1039-45.

95. Tadamura E, Yoshibayashi M, Yonemura T, Kudoh T, Kubo S, Motooka M, et al. Significant regional heterogeneity of coronary flow reserve in paediatric hypertrophic cardiomyopathy. Eur J Nucl Med 2000;27(9):1340-48.

96. Camici P, Chiriatti G, Lorenzoni R, Bellina RC, Gistri R, Italiani G, et al. Coronary vasodilation is impaired in both hypertrophied and nonhypertrophied myocardium of patients with hypertrophic cardiomyopathy: a study with nitrogen-13 ammonia and positron emission tomography. J Am Coll Cardiol 1991;17(4):879-86.

97. Nienaber CA, Gambhir SS, Mody FV, Ratib O, Huang SC, Phelps ME, et al. Regional myocardial blood flow and glucose utilization in symptomatic patients with hypertrophic cardiomyopathy. Circulation 1993;87(5):1580-90.

98. Grover-McKay M, Schwaiger M, Krivokapich J, Perloff JK, Phelps ME, Schelbert HR. Regional myocardial blood flow and metabolism at rest in mildly symptomatic patients with hypertrophic cardiomyopathy. J Am Coll Cardiol 1989;13(2):317-24.

99. Perrone-Filardi P, Bacharach SL, Dilsizian V, Panza JA, Maurea S, Bonow RO. Regional systolic function, myocardial blood flow and glucose uptake at rest in hypertrophic cardiomyopathy. Am J Cardiol 1993;72(2):199-204.

100. Tadamura E, Tamaki N, Matsumori A, Magata Y, Yonekura Y, Nohara R, et al. Myocardial metabolic changes in hypertrophic cardiomyopathy. J Nucl Med 1996;37(4):572-77.

101. Posma JL, Blanksma PK, Van Der Wall EE, Vaalburg W, Crijns HJ, Lie KI. Effects of permanent dual chamber pacing on myocardial perfusion in symptomatic hypertrophic cardiomyopathy. Heart 1996;76(4):358-62.

102. Cecchi F, Olivotto I, Gistri R, Lorenzoni R, Chiriatti G, Camici PG. Coronary microvascular dysfunction and prognosis in hypertrophic cardiomyopathy. N Engl J Med 2003;349(11):1027-35.

103. Memmola C, Iliceto S, Napoli VF, Cavallari D, Santoro G, Rizzon P. Coronary flow dynamics and reserve assessed by transesophageal echocardiography in obstructive hypertrophic cardiomyopathy. Am J Cardiol 1994;74(11):1147-51.

104. Kawada N, Sakuma H, Yamakado T, Takeda K, Isaka N, Nakano T, et al. Hypertrophic cardiomyopathy: MR measurement of coronary blood flow and

vasodilator flow reserve in patients and healthy subjects. Radiology 1999;211(1):129-35.

105. Cannon RO, Rosing DR, Maron BJ, Leon MB, Bonow RO, Watson RM, et al. Myocardial ischemia in patients with hypertrophic cardiomyopathy: contribution of inadequate vasodilator reserve and elevated left ventricular filling pressures. Circulation 1985;71(2):234-43.

106. Dimitrow PP, Krzanowski M, Nizankowski R, Szczeklik A, Dubiel JS. Effect of verapamil on systolic and diastolic coronary blood flow velocity in asymptomatic and mildly symptomatic patients with hypertrophic cardiomyopathy. Heart 2000;83(3):262-66.

107. Pasternac A, Noble J, Streulens Y, Elie R, Henschke C, Bourassa MG. Pathophysiology of chest pain in patients with cardiomyopathies and normal coronary arteries. Circulation 1982;65(4):778-89.

108. Yetman AT, McCrindle BW, MacDonald C, Freedom RM, Gow R. Myocardial bridging in children with hypertrophic cardiomyopathy - a risk factor for sudden death. N Engl J Med 1998;339(17):1201-09.

109. Linzbach AJ. Heart failure from the point of view of quantitative anatomy. Am J Cardiol 1960;5:370-82.

110. Maron BJ, Epstein SE, Roberts WC. Hypertrophic cardiomyopathy and transmural myocardial infarction without significant atherosclerosis of the extramural coronary arteries. Am J Cardiol 1979;43(6):1086-102.

111. Pichard AD, Meller J, Teichholz LE, Lipnik S, Gorlin R, Herman MV. Septal perforator compression (narrowing) in idiopathic hypertrophic subaortic stenosis. Am J Cardiol 1977;40(3):310-14.

112. Wigle ED, Sasson Z, Henderson MA, Ruddy TD, Fulop J, Rakowski H, et al. Hypertrophic cardiomyopathy. The importance of the site and the extent of hypertrophy. A review. Prog Cardiovasc Dis 1985;28(1):1-83.

113. Muthuchamy M, Pieples K, Rethinasamy P, Hoit B, Grupp IL, Boivin GP, et al. Mouse model of a familial hypertrophic cardiomyopathy mutation in a-tropomyosin manifests cardiac dysfunction. Circ Res 1999;85(1):47-56.

114. Yamauchi-Takihara K, Nakajima-Taniguchi C, Matsui H, Fujio Y, Kunisada K, Nagata S, et al. Clinical implications of hypertrophic cardiomyopathy associated with mutations in the α-tropomyosin gene. Heart 1996;76(1):63-65.

115. Thierfelder L, Watkins H, MacRae C, Lamas R, McKenna W, Vosberg HP, et al. α-tropomyosin and cardiac troponin T mutations cause familial hypertrophic cardiomyopathy: a disease of the sarcomere. Cell 1994;77(5):701-12.

116. Coviello DA, Maron BJ, Spirito P, Watkins H, Vosberg HP, Thierfelder L, et al. Clinical features of hypertrophic cardiomyopathy caused by mutation of a "hot spot" in the α-tropomyosin gene. J Am Coll Cardiol 1997;29(3):635-40.

117. Crooks L, Arakawa M, Hoenninger J, Watts J, McRee R, Kaufman L, et al. Nuclear magnetic resonance whole-body imager operating at 3.5 KGauss. Radiology 1982;143(1):169-74.

118. Lanzer P, Botvinick E, Schiller N, Crooks L, Arakawa M, Kaufman L, et al. Cardiac imaging using gated magnetic resonance. Radiology 1984;150(1):121-127.

119. Been M, Kean D, Smith MA, Douglas RH, Best JJ, Muir AL. Nuclear magnetic resonance in hypertrophic cardiomyopathy. Br Heart J 1985;54(1):48-52.

120. Scheffknecht BH, Bonow RO, Dwyer AJ, Maron BJ. Functional assessment of left ventricular ejection dynamics by cine-magnetic resonance imaging in hypertrophic cardiomyopathy. Am J Cardiol 1994;73(13):981-4.

121. Schulz-Menger J, Strohm O, Waigand J, Uhlich F, Dietz R, Friedrich MG. The value of magnetic resonance imaging of the left ventricular outflow tract in patients with hypertrophic obstructive cardiomyopathy after septal artery embolization. Circulation 2000;101(15):1764-1766.

122. Sardanelli F, Molinari G, Petillo A, Ottonello C, Parodi RC, Masperone MA, et al. MRI in hypertrophic cardiomyopathy: a morphofunctional study. J Comput Assist Tomogr 1993;17(6):862-72.

123. Sechtem U, Pflugfelder PW, Gould RG, Cassidy MM, Higgins CB. Measurement of right and left ventricular volumes in healthy individuals with cine MR imaging. Radiology 1987;163(3):697-702.

124. Sakuma H, Fujita N, Foo TK, Caputo GR, Nelson SJ, Hartiala J, et al. Evaluation of left ventricular volume and mass with breath-hold cine MR imaging. Radiology 1993;188(2):377-80.

125. Barkhausen J, Ruehm SG, Goyen M, Buck T, Laub G, Debatin JF. MR Evaluation of ventricular function: True fast imaging with steady-state precession versus fast low-angle shot cine MR Imaging: Feasibility study. Radiology 2001;219(1):264-69.

126. Maier SE, Fischer SE, McKinnon GC, Hess OM, Krayenbuehl HP, Boesiger P. Evaluation of left ventricular segmental wall motion in hypertrophic cardiomyopathy with myocardial tagging. Circulation 1992;86(6):1919-28.

127. Young AA, Kramer CM, Ferrari VA, Axel L, Reichek N. Three-dimensional left ventricular deformation in hypertrophic cardiomyopathy. Circulation 1994;90(2):854-67.

128. Kramer C, Reichek N, Ferrari V, Theobald T, Dawson J, Axel L. Regional heterogeneity of function in hypertrophic cardiomyopathy. Circulation 1994;90(1):186-94.

129. Bergey PD, Axel L. Focal hypertrophic cardiomyopathy simulating a mass: MR tagging for correct diagnosis. AJR Am J Roentgenol 2000;174(1):242-44.

130. Simonetti OP, Kim RJ, Fieno DS, Hillenbrand HB, Wu E, Bundy JM, et al. An improved MR imaging technique for the visualization of myocardial infarction. Radiology 2001;218(1):215-23.

131. Choudhury L, Mahrholdt H, Wagner A, Choi KM, Elliott MD, Klocke FJ, et al. Myocardial scarring in asymptomatic or mildly symptomatic patients with hypertrophic cardiomyopathy. J Am Coll Cardiol 2002;40(12):2156-64.

132. Moon JC, Reed E, Sheppard MN, Elkington AG, Ho S, Burke M, et al. The histologic basis of late gadolinium enhancement cardiovascular magnetic resonance in hypertrophic cardiomyopathy. Journal of the American College of Cardiology 2004;43(12):2260-64.

133. Moon JC, McKenna WJ, McCrohon JA, Elliott PM, Smith GC, Pennell DJ. Toward clinical risk assessment in hypertrophic cardiomyopathy with gadolinium cardiovascular magnetic resonance. J Am Coll Cardiol 2003;41(9):1561-67.

134. Bogaert J, Goldstein M, Tannouri F, Golzarian J, Dymarkowski S. Late myocardial enhancement in hypertrophic cardiomyopathy with contrast-enhanced MR imaging. Am J Roentgenol 2003;180(4):981-85.

135. Teraoka K, Hirano M, Ookubo H, Sasaki K, Katsuyama H, Amino M, et al. Delayed contrast enhancement of MRI in hypertrophic cardiomyopathy. Magn Reson Imaging 2004;22(2):155-61.

136. Amano Y, Takayama M, Amano M, Kumazaki T. MRI of cardiac morphology and function after percutaneous transluminal septal myocardial ablation for hypertrophic obstructive cardiomyopathy. AJR Am J Roentgenol 2004;182(2):523-27.

137. Myerson SG, Bellenger NG, Pennell DJ. Assessment of left ventricular mass by cardiovascular magnetic resonance. Hypertension 2002;39(3):750-55.

138. Katz J, Milliken MC, Stray-Gundersen J, Buja LM, Parkey RW, Mitchell JH, et al. Estimation of human myocardial mass with MR imaging. Radiology 1988;169(2):495-98.

139. Schwammenthal E, Wichter T, Joachimsen K, Auffermann W, Peters PE, Breithardt G. Detection of regional left ventricular asynchrony in obstructive hypertrophic cardiomyopathy by magnetic resonance imaging. Am Heart J 1994;127(3):600-06.

140. Arrive L, Assayag P, Russ G, Najmark D, Brochet E, Nahum H. MRI and cine MRI of asymmetric septal hypertrophic cardiomyopathy. J Comput Assist Tomogr 1994;18(3):376-82.

141. Suzuki J, Watanabe F, Takenaka K, Amano K, Amano W, Igarashi T, et al. New subtype of apical hypertrophic cardiomyopathy identified with nuclear magnetic resonance imaging as an underlying cause of markedly inverted T waves. J Am Coll Cardiol 1993;22(4):1175-81.

142. Soler R, Rodriguez E, Rodriguez JA, Perez ML, Penas M. Magnetic resonance imaging of apical hypertrophic cardiomyopathy. J Thorac Imaging 1997;12(3):221-5.

143. Devlin AM, Moore NR, Östman-Smith I. A comparison of MRI and echocardiography in hypertrophic cardiomyopathy. Br J Radiol 1999;72(855):258-64.

144. Dong SJ, MacGregor JH, Crawley AP, McVeigh E, Belenkie I, Smith ER, et al. Left ventricular wall thickness and regional systolic function in patients with hypertrophic cardiomyopathy. A three-dimensional tagged magnetic resonance imaging study. Circulation 1994;90(3):1200-09.

145. Kramer CM, Rogers WJ, Theobald TM, Power TP, Geskin G, Reichek N. Dissociation between changes in intramyocardial function and left ventricular volumes in the eight weeks after first anterior myocardial infarction. J Am Coll Cardiol 1997;30(7):1625-32.

146. Maier SE, Fischer SE, McKinnon GC, Hess OM, Krayenbuehl HP, Boesiger P. Acquisition and evaluation of tagged magnetic resonance images of the human left ventricle. Comput Med Imaging Graph 1992;16(2):73-80.

147. Hansen D, Daughters G, 2d, Alderman E, Ingels N, Stinson E, Miller D. Effect of volume loading, pressure loading, and inotropic stimulation on left ventricular torsion in humans. Circulation 1991;83(4):1315-26.

148. Aso H, Takeda K, Ito T, Shiraishi T, Matsumura K, Nakagawa T. Assessment of myocardial fibrosis in cardiomyopathic hamsters with gadolinium-DTPA enhanced magnetic resonance imaging. Invest Radiol 1998;33(1):22-32.

149. Prasad SK, Assomull RG, Pennell DJ. Recent developments in non-invasive cardiology. BMJ 2004;329(7479):1386-89.

150. Shan K, Constantine G, Sivananthan M, Flamm SD. Role of cardiac magnetic resonance imaging in the assessment of myocardial viability. Circulation 2004;109(11):1328-34.

151. Edelman RR. Contrast-enhanced MR imaging of the heart: overview of the literature. Radiology 2004;232(3):653-68.

152. Pennell DJ, Sechtem UP, Higgins CB, Manning WJ, Pohost GM, Rademakers FE, et al. Clinical indications for cardiovascular magnetic resonance (CMR): Consensus Panel report. Eur Heart J 2004;25(21):1940-65.

153. Nanjo S, Yamazaki J, Yoshikawa K, Miura M, Seno A. Efficacy of contrast-enhanced MR imaging in cardiomyopathy: an experimental study using Bio14.6 hamsters. Acad Radiol 2002;9(10):1139-47.

154. Amano Y, Kumita S, Takayama M, Kumazaki T. Comparison of contrast-enhanced MRI with iodine-123 BMIPP for detection of myocardial damage in hypertrophic cardiomyopathy. AJR Am J Roentgenol 2005;185(2):312-18.

155. Moon JC, Mogensen J, Elliott PM, Smith GC, Elkington AG, Prasad SK, et al. Myocardial late gadolinium enhancement cardiovascular magnetic resonance in hypertrophic cardiomyopathy caused by mutations in troponin I. Heart 2005;91(8):1036-40.

156. Nishimura T, Yamada N, Haze K, Nagata S. Experience using gadolinium-DTPA in cardiovascular MRI. Magn Reson Med 1991;22(2):354-57.

157. Farmer D, Higgins CB, Yee E, Lipton MJ, Wahr D, Ports T. Tissue characterization by magnetic resonance imaging in hypertrophic cardiomyopathy. Am J Cardiol 1985;55(1):230-32.

158. Fattori R, Rocchi G, Celletti F, Bertaccini P, Rapezzi C, Gavelli G. Contribution of magnetic resonance imaging in the differential diagnosis of cardiac

amyloidosis and symmetric hypertrophic cardiomyopathy. Am Heart J 1998;136(5):824-30.

159. de Roos A, Doornbos J, Luyten PR, Oosterwaal LJ, van der Wall EE, den Hollander JA. Cardiac metabolism in patients with dilated and hypertrophic cardiomyopathy: assessment with proton-decoupled P-31 MR spectroscopy. J Magn Reson Imaging 1992;2(6):711-19.

160. Jung WI, Sieverding L, Breuer J, Hoess T, Widmaier S, Schmidt O, et al. 31P NMR spectroscopy detects metabolic abnormalities in asymptomatic patients with hypertrophic cardiomyopathy. Circulation 1998;97(25):2536-42.

161. Hochachka PW, Clark CM, Holden JE, Stanley C, Ugurbil K, Menon RS. 31P magnetic resonance spectroscopy of the Sherpa heart: A phosphocreatine/adenosine triphosphate signature of metabolic defense against hypobaric hypoxia. PNAS 1996;93(3):1215-20.

162. Lanzer P, Garrett J, Lipton MJ, Gould R, Sievers R, O'Connell W, et al. Quantitation of regional myocardial function by cine computed tomography: pharmacologic changes in wall thickness. J Am Coll Cardiol 1986;8(3):682-92.

163. Pons-Llado G, Carreras F, Borras X, Palmer J, Llauger J, Bayes de Luna A. Comparison of morphologic assessment of hypertrophic cardiomyopathy by magnetic resonance versus echocardiographic imaging. Am J Cardiol 1997;79(12):1651-65.

164. Jääskeläinen P, Miettinen R, Kärkkäinen P, Toivonen L, Laakso M, Kuusisto J. Genetics of hypertrophic cardiomyopathy in eastern Finland: few founder mutations with benign or intermediary phenotypes. Ann Med 2004;36(1):23-32.

165. Hedman A, Hartikainen J, Vanninen E, Laitinen T, Jääskelainen P, Laakso M, et al. Inducibility of life-threatening ventricular arrhythmias is related to maximum left ventricular thickness and clinical markers of sudden cardiac death in patients with hypertrophic cardiomyopathy attributable to the Asp175Asn mutation in the a-tropomyosin gene. J Mol Cell Cardiol 2004;36(1):91-99.

166. Frahm J, Haase A, Matthaei D. Rapid NMR imaging of dynamic processes using the FLASH technique. Magn Reson Med 1986;3(2):321-27.

167. Cerqueira MD, Weissman NJ, Dilsizian V, Jacobs AK, Kaul S, Laskey WK, et al. Standardized myocardial segmentation and nomenclature for tomographic imaging of the heart. A statement for healthcare professionals from the Cardiac Imaging Committee of the Council on Clinical Cardiology of the American Heart Association. Circulation 2002;105(4):539-42.

168. Mosteller RD. Simplified calculation of body-surface area. N Engl J Med 1987;317(17):1098.

169. Götte MJ, van Rossum AC, Twisk JWR, Kuijer JPA, Marcus JT, Visser CA. Quantification of regional contractile function after infarction: strain analysis superior to wall thickening analysis in discriminating infarct from remote myocardium. J Am Coll Cardiol 2001;37(3):808-17.

170. Merlet P, Valette H, Dubois-Rande JL, Moyse D, Duboc D, Dove P, et al. Prognostic value of cardiac metaiodobenzylguanidine imaging in patients with heart failure. J Nucl Med 1992;33(4):471-77.

171. Liebson P, Serry R. Significance of echocardiographic left ventricular mass. Cardiology International 2001;2(2):53-63.

172. Risteli J, Niemi S, Trivedi P, Mäentausta O, Mowat AP, Risteli L. Rapid equilibrium radioimmunoassay for the amino-terminal propeptide of human type III procollagen. Clin Chem 1988;34(4):715-18.

173. Risteli J, Elomaa I, Niemi S, Novamo A, Risteli L. Radioimmunoassay for the pyridinoline cross-linked carboxy-terminal telopeptide of type I collagen: a new serum marker of bone collagen degradation. Clin Chem 1993;39(4):635-40.

174. Risteli J, Risteli L. Analysing connective tissue metabolites in human serum. Biochemical, physiological and methodological aspects. J Hepatol 1995;22(2 Suppl):77-81.

175. Melkko J, Kauppila S, Niemi S, Risteli L, Haukipuro K, Jukkola A, et al. Immunoassay for intact amino-terminal propeptide of human type I procollagen. Clin Chem 1996;42(6 Pt 1):947-54.

176. Brown H, Prescott R. Repeated measures data. In: Applied mixed models in medicine. 1 ed: 1st ed., Chichester, UK, John Wiley & Sons; 1999.

177. Posma JL, van der Wall EE, Blanksma PK, van der Wall E, Lie KI. New diagnostic options in hypertrophic cardiomyopathy. Am Heart J 1996;132(5):1031-41.

178. Grothues F, Smith GC, Moon JC, Bellenger NG, Collins P, Klein HU, et al. Comparison of interstudy reproducibility of cardiovascular magnetic resonance with two-dimensional echocardiography in normal subjects and in patients with heart failure or left ventricular hypertrophy. Am J Cardiol 2002;90(1):29-34.

179. Nagel E, Lehmkuhl HB, Bocksch W, Klein C, Vogel U, Frantz E, et al. Noninvasive diagnosis of ischemia-induced wall motion abnormalities with the use of high-dose dobutamine stress MRI : comparison with dobutamine stress echocardiography. Circulation 1999;99(6):763-70.

180. Plein S, Smith WH, Ridgway JP, Kassner A, Beacock DJ, Bloomer TN, et al. Qualitative and quantitative analysis of regional left ventricular wall dynamics using real-time magnetic resonance imaging: comparison with conventional breath-hold gradient echo acquisition in volunteers and patients. J Magn Reson Imaging 2001;14(1):23-30.

181. Sasayama S, Franklin D, Ross J, Jr, Kemper WS, McKown DU. Dynamic changes in left ventricular wall thickness and their use in analyzing cardiac function in the conscious dog. The American Journal of Cardiology 1976;38(7):870-79.

182. Lieberman AN, Weiss JL, Jugdutt BI, Becker LC, Bulkley BH, Garrison JG, et al. Two-dimensional echocardiography and infarct size: relationship of regional wall motion and thickening to the extent of myocardial infarction in the dog. Circulation 1981;63(4):739-46.

183. Shimizu G, Hirota Y, Kita Y, Kawamura K, Saito T, Gaasch W. Left ventricular midwall mechanics in systemic arterial hypertension. Myocardial function is depressed in pressure-overload hypertrophy. Circulation 1991;83(5):1676-84.

184. de Simone G, Devereux RB, Celentano A, Roman MJ. Left ventricular chamber and wall mechanics in the presence of concentric geometry. J Hypertens 1999;17(7):1001-06.

185. Michele DE, Gomez CA, Hong KE, Westfall MV, Metzger JM. Cardiac dysfunction in hypertrophic cardiomyopathy mutant tropomyosin mice Is transgene-dependent, hypertrophy-independent, and improved by beta - blockade. Circ Res 2002;91(3):255-62.

186. Lauerma K, Niemi P, Hänninen H, Janatuinen T, Voipio-Pulkki LM, Knuuti J, et al. Multimodality MR imaging assessment of myocardial viability: combination

of first-pass and late contrast enhancement to wall motion dynamics and comparison with FDG PET-initial experience. Radiology 2000;217(3):729-36.

187. Weinmann HJ, Laniado M, Mutzel W. Pharmacokinetics of GdDTPA/dimeglumine after intravenous injection into healthy volunteers. Physiol Chem Phys Med NMR 1984;16(2):167-72.

188. Weinmann HJ, Brasch RC, Press WR, Wesbey GE. Characteristics of gadolinium-DTPA complex: a potential NMR contrast agent. AJR Am J Roentgenol 1984;142(3):619-24.

189. Koenig SH, Spiller M, Brown R, Wolf GL. Relaxation of water protons in the intra- and extracellular regions of blood containing Gd(DTPA). Magn Reson Med 1986;3(5):791-95.

190. Jugdutt BI, Amy RW. Healing after myocardial infarction in the dog: changes in infarct hydroxyproline and topography. J Am Coll Cardiol 1986;7(1):91-102.

191. Weber KT. Cardiac interstitium in health and disease: the fibrillar collagen network. J Am Coll Cardiol 1989;13(7):1637-52.

192. Flacke SJ, Fischer SE, Lorenz CH. Measurement of the gadopentetate dimeglumine partition coefficient in human myocardium in vivo: normal distribution and elevation in acute and chronic infarction. Radiology 2001;218(3):703-10.

193. Kim RJ, Chen E-L, Lima JAC, Judd RM. Myocardial Gd-DTPA kinetics determine MRI contrast enhancement and reflect the extent and severity of myocardial injury after acute reperfused infarction. Circulation 1996;94(12):3318-3326.

194. Lombardi R, Betocchi S, Losi MA, Tocchetti CG, Aversa M, Miranda M, et al. Myocardial collagen turnover in hypertrophic cardiomyopathy. Circulation 2003;108(12):1455-60.

195. Trivedi P, Hindmarsh P, Risteli J, Risteli L, Mowat AP, Brook CG. Growth velocity, growth hormone therapy, and serum concentrations of the amino-terminal propeptide of type III procollagen. J Pediatr 1989;114(2):225-30.

196. Sorva R, Anttila R, Siimes MA, Sorva A, Tähtelä R, Turpeinen M. Serum markers of collagen metabolism and serum osteocalcin in relation to pubertal development in 57 boys at 14 years of age. Pediatr Res 1997;42(4):528-32.

197. Crofton PM, Wade JC, Taylor MR, Holland CV. Serum concentrations of carboxyl-terminal propeptide of type I procollagen, amino-terminal propeptide of type III procollagen, cross-linked carboxyl-terminal telopeptide of type I collagen, and their interrelationships in schoolchildren. Clin Chem 1997;43(9):1577-81.

198. Nagueh SF, Chen S, Patel R, Tsybouleva N, Lutucuta S, Kopelen HA, et al. Evolution of expression of cardiac phenotypes over a 4-year period in the β-myosin heavy chain-Q403 transgenic rabbit model of human hypertrophic cardiomyopathy. J Mol Cell Cardiol 2004;36(5):663-73.

199. Kelm M, Schafer S, Mingers S, Heydthausen M, Vogt M, Motz W, et al. Left ventricular mass is linked to cardiac noradrenaline in normotensive and hypertensive patients. J Hypertens 1996;14(11):1357-64.

200. Shimizu M, Ino H, Yamaguchi M, Terai H, Hayashi K, Nakajima K, et al. Heterogeneity of cardiac sympathetic nerve activity and systolic dysfunction in patients with hypertrophic cardiomyopathy. J Nucl Med 2002;43(1):15-20.

201. Arad M, Seidman JG, Seidman CE. Phenotypic diversity in hypertrophic cardiomyopathy. Hum Mol Genet 2002;11(20):2499-506.

202. Ogimoto A, Hamada M, Nakura J, Miki T, Hiwada K. Relation between angiotensin-converting enzyme II genotype and atrial fibrillation in Japanese patients with hypertrophic cardiomyopathy. J Hum Genet 2002;47(4):184-89.

203. Thomson HL, Morris-Thurgood J, Atherton J, Frenneaux M. Reduced cardiopulmonary baroreflex sensitivity in patients with hypertrophic cardiomyopathy. J Am Coll Cardiol 1998;31(6):1377-82.

204. Thaman R, Elliott PM, Shah JS, Mist B, Williams L, Murphy RT, et al. Reversal of inappropriate peripheral vascular responses in hypertrophic cardiomyopathy. J Am Coll Cardiol 2005;46(5):883-892.

205. Järvinen VM, Kupari MM, Poutanen VP, Hekali PE. Right and left atrial phasic volumetric function in mildly symptomatic dilated and hypertrophic cardiomyopathy: cine MR imaging assessment. Radiology 1996;198(2):487-95.

206. Zerhouni EA, Parish DM, Rogers WJ, Yang A, Shapiro EP. Human heart: tagging with MR imaging--a method for noninvasive assessment of myocardial motion. Radiology 1988;169(1):59-63.

207. Axel L, Dougherty L. Heart wall motion: improved method of spatial modulation of magnetization for MR imaging. Radiology 1989;172(2):349-350.

208. Wilke N, Simm C, Zhang J, Ellermann J, Ya X, Merkle H, et al. Contrast-enhanced first pass myocardial perfusion imaging: correlation between myocardial blood flow in dogs at rest and during hyperemia. Magn Reson Med 1993;29(4):485-97.

209. Lauerma K, Virtanen KS, Sipilä LM, Hekali P, Aronen HJ. Multislice MRI in assessment of myocardial perfusion in patients with single-vessel proximal left anterior descending coronary artery disease before and after revascularization. Circulation 1997;96(9):2859-67.

210. Al-Saadi N, Nagel E, Gross M, Bornstedt A, Schnackenburg B, Klein C, et al. Noninvasive detection of myocardial ischemia from perfusion reserve based on cardiovascular magnetic resonance. Circulation 2000;101(12):1379-83.

211. Schmiedl U, Moseley ME, Ogan MD, Chew WM, Brasch RC. Comparison of initial biodistribution patterns of Gd-DTPA and albumin-(Gd-DTPA) using rapid spin echo MR imaging. J Comput Assist Tomogr 1987;11(2):306-13.

212. Van Hecke P, Marchal G, Bosmans H, Johannik K, Jiang Y, Vogler H, et al. NMR imaging study of the pharmacodynamics of polylysine-gadolinium-DTPA in the rabbit and the rat. Magn Reson Imaging 1991;9(3):313-21.

213. Jensen LT. The aminoterminal propeptide of type III procollagen. Studies on physiology and pathophysiology. Dan Med Bull 1997;44(1):70-78.

214. Bishop JE, Laurent GJ. Collagen turnover and its regulation in the normal and hypertrophying heart. Eur Heart J 1995;16 Suppl C:38-44.

215. Kitamura M, Shimizu M, Ino H, Okeie K, Yamaguchi M, Funjno N, et al. Collagen remodeling and cardiac dysfunction in patients with hypertrophic cardiomyopathy: the significance of type III and VI collagens. Clin Cardiol 2001;24(4):325-29.

216. Knuuti J, Sipola P. Is it time for cardiac innervation imaging? Q J Nucl Med Mol Imaging 2005;49(1):97-105.

217. Rapacciuolo A, Esposito G, Caron K, Mao L, Thomas SA, Rockman HA. Important role of endogenous norepinephrine and epinephrine in the

development of in vivo pressure-overload cardiac hypertrophy. J Am Coll Cardiol 2001;38(3):876-82.

218. Wettschureck N, Rutten H, Zywietz A, Gehring D, Wilkie TM, Chen J, et al. Absence of pressure overload induced myocardial hypertrophy after conditional inactivation of Galphaq/Galpha11 in cardiomyocytes. Nat Med 2001;7(11):1236-40.

219. Spirito P, Bellone P, Harris KM, Bernabo P, Bruzzi P, Maron BJ. Magnitude of left ventricular hypertrophy and risk of sudden death in hypertrophic cardiomyopathy. N Engl J Med 2000;342(24):1778-85.

220. Elliott PM, Gimeno Blanes JR, Mahon NG, Poloniecki JD, McKenna WJ. Relation between severity of left-ventricular hypertrophy and prognosis in patients with hypertrophic cardiomyopathy. Lancet 2001;357(9254):420-24.

221. Lim D-S, Lutucuta S, Bachireddy P, Youker K, Evans A, Entman M, et al. Angiotensin II blockade reverses myocardial fibrosis in a transgenic mouse model of human hypertrophic cardiomyopathy. Circulation 2001;103(6):789-91.

222. Oi S, Haneda T, Osaki J, Kashiwagi Y, Nakamura Y, Kawabe J, et al. Lovastatin prevents angiotensin II-induced cardiac hypertrophy in cultured neonatal rat heart cells. Eur J Pharmacol 1999;376(1-2):139-48.

223. Luo JD, Zhang WW, Zhang GP, Guan JX, Chen X. Simvastatin inhibits cardiac hypertrophy and angiotensin-converting enzyme activity in rats with aortic stenosis. Clin Exp Pharmacol Physiol 1999;26(11):903-08.

224. Patel R, Nagueh SF, Tsybouleva N, Abdellatif M, Lutucuta S, Kopelen HA, et al. Simvastatin induces regression of cardiac hypertrophy and fibrosis and

improves cardiac function in a transgenic rabbit model of human hypertrophic cardiomyopathy. Circulation 2001;104(3):317-24.

Kuopio University Publications D. Medical Sciences

D 353. Väisänen, Jussi. Non-competitive NMDA receptor antagonists in rodent modelling of schizophrenia.
2005. 90 p. Acad. Diss.

D 354. Soininvaara, Tarja. Bone mineral density changes after total knee arthroplasty.
2005. 83 p. Acad. Diss.

D 355. Kukkonen, Jarmo. Terveydenhuollon vaikuttavuuden arviointi rutiinisti kerätyn tiedon pohjalta.
2005. 252 p. Acad. Diss.

D 356. Papp, Anthony. Experimental thermal injury: new methods in assessing tissue damage.
2005. 78 p. Acad. Diss.

D 357. Berg, Marja. CT angiography in the assessment of atherosclerotic carotid and renal arteries.
2005. 143 p. Acad. Diss.

D 358. Miettinen, Timo. Whiplash injuries in Finland: incidence, prognosis and predictive factors for the long-term outcome.
2005. 86 p. Acad. Diss.

D 359. Kotaniemi-Syrjänen, Anne. Wheezing requiring hospitalisation in infancy - outcome at early school age: viral aetiology of wheeze and predictive factors for outcome.
2005. 97 p. Acad. Diss.

D 360. Huopio, Jukka. Predicting fractures in middle-aged women.
2005. 86 p. Acad. Diss.

D 361. Gül, Mustafa. Cytotoxic and antifungal acetophenone-derived Mannich bases: effects on redox thiols and heat shock proteins.
2005. 68 p. Acad. Diss.

D 362. Virtanen, Jyrki. Homocysteine, folate and cardiovascular diseases.
2005. 65 p. Acad. Diss.

D 363. Tuomainen, Petri. Physical exercise in clinically healthy men and in patients with angiographically documented coronary artery disease with special referense to cardiac autonomic control and warm-up phenomenon.
2005. 125 p. Acad. Diss.

D 364. Lindgren, Annamarja. Cancer incidence in hypertensive patients.
2005. 94 p. Acad. Diss.

D 365. Töyry, Saara. Burnout and self-reported health among Finnish physicians.
2005. 102 p. Acad. Diss.

D 366. Haapalahti, Mila. Nutrition, gastrointestinal food hypersensitivity and functional gastrointestinal disorders in schoolchildren and adolescents.
2005. 612 p. Acad. Diss.

D 367. Lindi, Virpi. Role of the Human PPAR-γ2 Gene on Obesity, Insulin Resistance and Type 2 Diabetes.
2005. 102 p. Acad. Diss.